UNIVERSITÉ DU QUÉBEC

THÈSE PRÉSENTÉE À

L'UNIVERSITÉ DU QUÉBEC À TROIS-RIVIÈRES

COMME EXIGENCE PARTIELLE

DU DOCTORAT EN BIOPHYSIQUE

PAR

ABDELWAHAB IBRAHIM AHMED

PROTEIN SECONDARY STRUCTURE OF THE ISOLATED PHOTOSYSTEM II (PSII) PARTICLES AND LIGHT-HARVESTING COMPLEX (LHCII) STUDIED BY FOURIER TRANSFORM INFRARED SPECTROSCOPY

1996

RÉSUMÉ

La photosynthèse est l'utilisation de l'énergie solaire par les plantes vertes, les cyanobactéries et les bactéries photosynthétiques pour la synthèse de molécules organiques complexes. Ces molécules sont assemblées à partir de matériaux aussi simple que l'eau, le dioxyde de carbone et les substances inorganiques. Ainsi, la capture de l'énergie lumineuse par les organismes photosynthétiques constitue le premier maillon d'une longue chaîne liant le soleil à une vaste majorité d'organismes vivants (Youvan and Marrs, 1989).

La lumière est absorbée par les pigments des antennes telles les chlorophylles et les caroténoïdes. Les processus de la transformation de l'énergie lumineuse sont initiés par la génération d'états électroniques excités qui donnent par la suite naissance à une séparation des charges positives et négatives dans les centres réactionnel. Ces processus ont lieu dans deux complexes pigments-protéines appelés centre photochimique réactionnel du Photosystème I (PSI) et centre photochimique réactionel du Photosystème II (PSII). Ces centres, en occupant la place du noyau dans les structures membranaires photosynthétiques, jouent le rôle principal dans l'absorption et la conversion de la lumière en énergie chimique stable.

Ces deux photosystèmes ont été isolés et purifiés à partir de membranes chloroplastiques; chacun d'eux contient de 50 à 100 molécules de chlorophylles

et un petit nombre de carotènes. Ces molécules de pigments sont combinées avec des polypeptides (11 dans le photosystème I et 20 dans le photosystème II) qui assurent les fonctions structurelles, enzymatiques et régulatoires du photosystème. Une ou deux chlorophylles de ces photosystèmes forment le centre réactionnel dans lequel l'événement central des réactions lumineuses (le transfert des électrons à l'état excité aux orbitales stables des accepteurs primaires) tient place.

Les photosystèmes I et II contiennent aussi une chaîne de transporteurs impliqués dans le transport des électrons à partir des accepteurs primaires. Ces transporteurs sont formés par diverses protéines qui sont soient des complexes membranaires stables tel le cytochrome b6f, soient des composantes mobiles telles la plastoquinone et la plastocyanine. Le photosystème II contient en outre le mécanisme de l'oxydation de l'eau qui agit comme source d'électrons.

Les membranes internes des chloroplastes contiennent aussi des assemblements de pigments-protéines appelés complexes collecteurs de lumière (CCL) qui forment une partie intégrante des systèmes antennaires. Les pigments de ces CCL sont liés aux protéines dans des complexes sans centres réactionnels ou accepteurs primaires. Aussi, ne sont ils responsables d'aucune conversion de la lumière en énergie chimique à leur niveau, mais ils transfèrent plutôt l'énergie absorbée aux deux photosystèmes. La majorité des organismes photosynthétiques ont deux types de CCL, le CCL-I associé avec le photosystème I et le CCL-II associé avec le photosystème II.

L'élucidation de la relation structure-fonction des protéines membranaires au niveau moléculaire constitue un défi de tous les jours dans

le domaine des les sciences de la vie. Les bactériorhodopsines et les centres réactionnels des bactéries photosynthétiques sont les protéines membranaires les mieux caractérisées (Deisenhofer, et al. 1985; Henderson et al., 1990). La compréhension de leur mécanisme au niveau moléculaire peut aussi donner une image des mécanismes d'autres protéines impliquées dans le gradient de protons et le transfert d'électrons. La connaissance de l'interaction pigment-pigment, qui détermine les propriétés des pigments chlorophylliens, est donc d'une importance particulière dans la compréhension des premières réactions de la photosynthèse.

Durant plusieurs années, la structure des molécules biologiques, a été le sujet de nombreuses recherches visant à determiner leur function. Pour réaliser de telles études, de nouvelles méthodes biophysiques ont été développées à l'insu des résultats obtenus par l'utilisation des techniques conventionnelles comme la biochimie ou la biologie moléculaire. Ces méthodes biophysiques ont permis entre autres de déterminer les dynamiques moléculaires de groupements individuels impliqués directement dans des fonctions spécifiques au sein de la membrane.

Parmi les plus populaires de ces méthodes utilisées et les plus fiables, nous retrouvons la diffraction des rayons -X, la résonance magnétique nucléaire (RMN), le dichroisme circulaire (DC) et la spectroscopie Raman. Ces différentes techniques spectroscopiques ont toutes apporté de très importantes informations sur la structure moléculaire des protéines, toutefois, chacune d'elles comporte des inconvénients majeurs qui la rendent plus limitée à un type déterminé de molécules. Ainsi, la détermination de la structure des protéines par diffraction aux rayons-X nécessite la production de cristaux

relativement grands (200 nm) et assez purs, ce qui est très difficile à obtenir pour la plupart des protéines. Pour la RMN, l'obligation de l'utilisation de protéines de poids moléculaire de moins de 15 kDa la rend très limitée dans ce domaine. Le DC est plutôt incommodé par l'utilisation de protéines en suspension qui présentent des problèmes de diffusion de lumière (Mao and Wallace, 1984), alors que la spectroscopie Raman qui ne semble pas souffrir de cet inconvenient est limitée par un très faible rapport signal sur bruit.

Pour éviter la plupart de ces inconvénients, une nouvelle spectroscopie est de plus en plus utilisée par l'ensemble des chercheurs dans le domaine de la détermination des structures des protéines (Nabedryk et al. 1982; Olinger et al. 1986). L'Infra Rouge par Transformé de Fourier (FTIR) est une méthode assez récente dont la particularité réside dans la haute qualité des spectres obtenus relativement avec aisance. Contrairement aux autres spectroscopies citées précedemment, elle ne necessite généralement qu'une très petite quantité de protéines (1 mM) qui peuvent être dans une grande variété d'environnements tels en solution aqueuse, dans des lipides, en cristaux ou dans les solvants organiques. Elle est en outre généralisée à tous les types de molécules, pigments, protéines ou produits synthétiques (Dong et al. 1989), du moment qu'elle est basée uniquement sur l'absorption par des liaisons moléculaires. De plus cette spectroscopie ne nécessite pas de sondes supplémentaires ce qui facilite relativement l'interpretation des résultats (Potter et al. 1985; Gorga et al. 1989).

Notre objectif dans ce projet était étudier quelques points qui restent très débatus dans le domaine de la photosynthèse. Dans cette étude, la

spectroscopie FTIR a occupé une place de choix et a été utilisée pour analyser les points suivants:

1-L'interaction des CCLII avec les ions métalliques divalents toxiques.

2-La structure de la Chlorophylle $P680^{+}$.

3-L'effet de la chaleur sur les membranes enrichies en PSII en présence de betaine et sucrose.

4-La structure secondaire de la protéine extrinsèque de 33 kDa.

Au cours de cette étude, nous avons pu dégager les conclusions suivantes:

La spectroscopie infrarouge transformée de Fourier est une méthode très efficace dans l'étude de la conformation des protéines en solution, principalement à cause de sa forte sensibilité à la conformation de la bande amide I (1700-1620 cm^{-1}) qui émerge des vibrations d'élongation de la chaîne principale C=O. Combinée avec les techniques d'accrossiment de la résolution, telles la spectroscopie de dérivation secondaire et de déconvolution, en plus de l'application des techniques de curve-fitting iteratives, cette méthode fournit de riches informations sur la structure secondaire des protéines. En outre, les informations sur la conformation tirées de la bande amide I mènent à discerner les corrélations qui existent entre les types conformationnels spécifiques et les composantes des bandes dans la région amide.

L'interaction des ions divalents des métaux lourds avec les protéines du complexe collecteur de lumière (CCL-II) des membranes chloroplatiques des

thylacoïdes a été étudiée en solution aqueuse à différentes concentrations des ions métalliques (0,01 à 20 mM) en utilisant la spectroscopie FTIR. Les résultats obtenus par cette méthode dans les régions amide I (1700-1620 cm^{-1}) et amide II (1800-1500 cm^{-1}) ont montré qu'il existe une forte interaction entre les protéines et le métal à haute concentration de ce dernier, alors qu'à très faible concentration, la liaison avec le cation est négligeable. La liaison avec les ions métalliques se fait principalement *via* le groupement carbonyl des protéines à faible concentration cationique, alors que la coordination ionique aux groupements C=O et C=N des protéines a été observée pour les hautes concentrations cationiques. La liaison tyrosine-métal a été aussi observée pour quelques ions métalliques à haute concentration. Des changements conformationnels majeurs des hélices-α aux feuillets-β et aux structures coudées ont été observés en présence de ces cations métalliques à haute concentration.

La structure du donneur primaire des électrons du photosystème II, $P680^+$ a été étudiée pour examiner s'il est composé d'une chlorphylle (Chl) monomérique ou dimérique. Dans cette étude, la spectroscopie FTIR a été utilisée pour analyser les changements dans les modes vibrationnels se produisant par l'effet de la photooxydation du $P680^+$ dans les PSII dépourvus d'ions manganèse (Mn). Nous avons pu montré que l'illumination de ces derniers en présence d'accepteurs artificiels d'électrons résulte en des changements dans le spectre de différence d'absorbance (en présence et en absence de lumière) qui sont typiques de la formation du $P680^+$.

Le spectre de différence FTIR obtenu sous des conditions similaires est caractérisé par deux pics négatifs, localisés à 1694 et 1652 ou 1626 cm^{-1}, et qui

peuvent être assignés au groupement 9-ceto de la chlorophylle du P680; cette dernière bande est un bon indicateur de groupements fortement associés. Ces vibrations sont déplacées respectivement à 1714 et 1626 cm^{-1} dans les caractéristiques positives du spectre de différence attribué à $P680^{+}$. La présence de deux paires de bandes attribuées au groupement 9-ceto est discutée dans le cadre d'un P680 formé d'un dimère de chlorophylles.

La structure des membranes du Photosystème II, isolées des thylacoïdes du chloroplaste, est profondément affectée par les solutés présents dans leur environnements. En utilisant la spectroscopie FTIR, nous avons étudié l'effet de la chaleur sur les membranes du PSII en présence de glycinebétaine et de sucrose. Il a été conclu qu'à des températures élevées, la glycinebétaine et le sucrose agissent comme agents protecteurs des protéines membranaires du PSII. La quasi totalité des structures hélices-α ont été protégées et aucun changement majeur dans leur conformation n'a été observé. Ce résultat peut s'accorder avec le concept développé par Timasheff et ces coéquipiers qui postule que le comportement des protéines en présence de soluté est une conséquence d'interactions préférentielles entre les constituants du système soluté-protéine-solvant.

La protéine extrinsèque de 33 kDa du PSII est un important élément de l'appareil de dégagement d'oxygène dont le rôle est de stabiliser le groupement de manganèse à des concentrations physiologiques de chlorure et de minimiser la quantité du calcium nécessaire au dégagement d'oxygène.

L'analyse de la séquence d'acides aminés de cette protéine, basée sur la méthode de Chou-Fasman, suggère que cette protéine contient une grande

proportion de structures hélice-α. Une étude estimative utilisant des techniques plus sophistiquées a conclu que ce polypeptide ne contient en général qu'un petit nombre périodique de structures secondaires ordonnées. Dans la présente étude, en utilisant la spectroscopie FTIR, nous avons mesuré les proportions des structures secondaires présentes dans la protéine de 33 kDa. Notre résultat indique que la protéine stabilisant le manganèse (33 kDa) contient une large proportion de structures en feuillets-β (36%), une quantité relativement plus faible de structure en hélices-α (27%), de structures coudées (24%) et des structures non-ordonnées (13%).

Finalement, ces études démontrent que le pouvoir réel de la spectroscopie FTIR réside dans sa capacité de confirmer la structure secondaire des protéines ou de suivre les changements relatifs dans ces mêmes structures en fonction de variables sélectives. Cette capacité d'augmentation de résolution de l'FTIR à fournir une caractérisation structurale rapide et fiable est d'une grande importance quand l'information structurale à partir de la cristallographie aux rayons X est difficile à obtenir.

SUMMARY

The effect of different factors on the protein secondary structure of Photosystem II membranes and its surrounding was studied using Fourier-transform-Infrared spectroscopy with its enhancement techniques such as deconvolution, second derivatives and curve-fitting.

The interaction of divalent metal ions with the light-harvesting (LHC-II) proteins of chloroplast thylakoids membranes was investigated in aqueous solution at different metal ion concentrations (0.01 to 20 mM), using Fourier transform infrared (FTIR) difference spectroscopy. The infrared difference spectroscopic results for the amide I and amide II regions (1800-1500 cm^{-1}) have shown a strong metal-protein interaction at high metal ion concentrations, whereas at a very low concentration the metal cation binding is negligible. The metal ion binding is mainly *via* the protein carbonyl group at low cation concentration, whereas metal ion coordination to the protein C=O and C-N groups were observed at higher cation concentrations. The metal-tyrosine binding was also observed for some ions at high metal ion concentrations. Major conformational changes from α-helix to those of the β-sheet and turn structures were observed, in the presence of these metal cations at high concentrations.

The structure of the primary electron donor of PSII, P680, is still under debate. It is not decided if it is composed of chlorophyll (Chl) monomer or dimer. In this study, FTIR spectroscopy was used to analyze the changes in the vibration modes occurring upon photooxidation of $P680^+$ in a Mn-depleted PSII. It is demonstrated that illumination of the above in the presence of artificial electron acceptors results in a light-minus-dark absorbance change typical of the formation of $P680^+$. The light-minus dark FTIR spectrum obtained under similar conditions is characterized by two negative peaks located at 1694 and 1652 or 1626 cm^{-1} that can be assigned to the 9-keto groups of the P680 Chl, the latter band being indicative of a strongly associated group. These vibrations are shifted to 1714 and 1626 cm^{-1}, respectively, in the positive features of the difference spectrum attributed to $P680^+$. The occurrence of two pairs of bands attributed to 9-keto groups is discussed in terms of P680 being formed of a Chl dimer.

The integrity of Photosystem II membranes isolated from chloroplast thylakoids is profoundly affected by the solute environment. Using FTIR spectroscopy we studied the effect of heat treatment on PSII-membranes in the presence of glycinebetaine and sucrose. It is concluded that glycinebetaine and sucrose act as protecting agents for the PSII-membrane protein under elevated temperature. The integrity of α-helical structure was about to be protected and no major conformation changes were observed. These results can be accommodated readily in a concept developed by Timasheff and his coworkers according to which the responses of proteins to their solute environment are consequences of interaction preferences among the constituents of the solvent -protein-solute systems.

The 33 kDa extrinsic protein of PSII is an important component of the oxygen-evolving apparatus which functions to stabilize the manganese cluster at physiological chloride concentrations and to lower the calcium requirement for oxygen evolution. Chou-Fasman analysis of the amino acid sequence of this protein suggests that this component contains a high proportion of α-helical structure. A computational study using more sophisticated techniques concluded that the protein contained little periodically ordered secondary structure. In this study, we have measured the relative proportions of secondary structure present in 33 kDa protein using FTIR spectroscopy. Our results indicate that this protein contains a large proportion of β-structure (36%) and relatively small amount of α-helical structure (27%), turn (24%) and other structures (13%)

TABLE OF CONTENTS

LIST OF ABBREVIATIONS

A	: absorbance
ATP	: adenosine tri-phosphate
CD	: circular dichroism
Chl	: chlorophyll
CP	: chlorophyll protein complex
Cyt	: cytochrome
D1/D2	: polypeptides of the PSII reaction center
DCBQ	: 2, 5-dichloro-p-benzoquinone
DCCD	: dicyclohexylcarbodiimide
DCMU	: 3-(3,4-dichlorophenyl)-1,1-dimethyl urea
DCPIP	: 1,6-dichlorophenolindophenol
EDTA	: ethylenediamenetetraacetic acids.
EMR	: electro magnetic radiation
FTIR	: Fourier transform infrared
G	: free energy
G^o	: standard free energy
H	: enthalpy
HEPS	: 4-(2-hydroxyethyl)-piperazinesulfonic acid;
IR	: infrared
kDa	: kilodalton
LHCI	: light harvesting complex specifically associated with PSI
LHCII	: light harvesting complex specifically associated with PSII

$NADP^+$: nicotinamide adenine dinucleotide phosphate oxidized

NADPH : nicotinamide adenine dinucleotide phosphate reduced

MES : 2--(N-morpholino)ethane sulfonic acid

MSP : manganese stabilizing protein

n : refractive index

NMR : nuclear magnetic resonance

$P680^+$: primary electron donor of photosystem II

P700 : the reaction center of PSI

Pheo : pheophytin

PMSF : phenymethylsulphonyfluoride

PQ : plastoquinone

PQH_2 : plastoquinol

PSI : Photosystem I

PSII : photosystem II

Q_A : primary quinone acceptor

Q_B : secondary quinone acceptor

S : entropy

S_o-S_4 : charge storage states of the water -oxidizing complex.

SDS-PAGE : sodium dodecylsulfate-polyacrilamide gel electrophoresis

TES : acide N-Tris (hydroxymethyl) methyl-2-aminoethane sulfonique

TRIS : tris-(hydroxymethyl)aminomethane;

Tricine : N-tris(hydroxymethyl)-mnethylglycine

Tyr : tyrosine

μ : reduced mass

UV : ultraviolet

LIST OF FIGURES

LIST OF TABLES

CHAPTER I

INTRODUCTION

PHOTOSYNTHESIS

In general terms photosynthesis could be defined as a series of chemical reactions in a plant, using sun light as energy, that converts carbon dioxide and water into molecules such as glucose that the plant can use as an energy source.

1.1 ENERGY AND THE BIOLOGICAL SYSTEM

A continuing input of energy is necessary to maintain life. The living system represents a highly organized state, thus a very low-entropy state. As we know from thermodynamics that for any reaction or process to proceed spontaneously, it must have a negative free-energy change associated with it. The free energy change, ΔG, is related to the change in enthalpy (ΔH) and entropy (ΔS) that occurs in the process:

$$\Delta G = \Delta H - T\Delta S$$

If a process yields a more highly organized state, as do most processes in the formation and maintenance of biological systems, the entropy change will be negative and ($-T\Delta S$) will be a positive number. Unless the ΔH term is sufficiently large and negative to override the entropy term (which is not usually the case) the ΔG will be positive, and the reaction or process will not occur spontaneously unless energy is made available to it.

Say, for example, a cell needs to synthesize a quantity of protein, making low-entropy complex molecules out of high-entropy simpler molecules. The

process requires not only raw materials (the simpler molecules), but also a source of energy. This energy can be supplied through the coupling of chemical reactions. If a reaction requiring free energy, such as protein synthesis, and a reaction releasing free energy are coupled, the overall free-energy change for the two coupled reactions is the sum of their ΔG's and the unfavorable reaction can occur.

What is the source of energy that powers cell metabolism, the mechanical work of muscle contraction, and the electrical work of nerve-impulse transmission? The original source of energy for all purposes is the sun. However, most cells are unable to directly use solar energy. Only photosynthetic cells can absorb radiant energy and transform it into the chemical energy of biological molecules.

Photosynthesis, carried out by green plants, eukaryotic algae, cyanobacteria, and photosynthetic bacteria, constantly replenishes the organic molecules oxidized by all organisms as a source of cellular energy (Youvan and Marrs, 1989). The reactions of photosynthesis use the energy of sunlight to convert inorganic substances into organic molecules. In most photosynthetic organisms organic molecules are assembled from raw materials no more complex than water, carbon dioxide, and a supply of inorganic materials.

Photosynthetic organisms typically synthesize much greater quantities of organic substances than they require for their own activities. Much of the remainder is used as a fuel source by animals and other organisms that live by eating plants. These plant-eating forms are consumed in turn by other organisms, and so on down the line until the last of the organic matter assembled by photosynthesis is completely oxidized to carbon dioxide and water.

Because the reactions capturing light energy provide the first step in this extended pathway of energy flow, photosynthesis is the vital link between the energy of sunlight and the vast majority of living organisms. Without the activity of photosynthetic prokaryotes and eukaryotes in capturing light and converting it to chemical energy, most of the earth's creatures, including the human population, would soon cease to exist.

1. 1. 1 Reducing Power for Biosynthesis

The reducing power of a compound is dependent upon its affinity for electrons and the concentration of its reduced and oxidized forms. This affinity can be defined by its redox potential. For convenience, all redox potentials are compared to that of hydrogen gas at 1 atmosphere of pressure bubbling over a platinum electrode in a solution at pH = 0

$$H_2 \longrightarrow 2H^+ + 2e^-$$

This reaction is arbitrarily given a redox potential of zero volts. At pH 7.0 the reaction is pulled to the right because $[H^+]$ is low, and the redox potential therefore drops to - 4.2 V. At equilibrium the difference in redox potential, between two couples is related by the equation:

$$E = Eo\ (pH\ 7) + \frac{RT}{nF} \ln \frac{oxidant}{reductant}$$

in which E is the potential in volts, the standard term, Eo(pH 7) is called the standard oxidation-reduction potential, the concentration term here includes the number of electrons that are transferred in the oxidation-reduction reaction, n and the Faraday F is a constant which is equal to 23,062 $calV^{-1}$ or 96,486JV^{-1} at 25 °C. In practice, if each redox couple initially has equal concentrations of oxidized and reduced forms, then electrons will move from the couple with the more negative potential to that with the more positive potential.

There are two particularly important molecules in oxidation/reduction reactions within cells. These are the cofactors nicotinamide adenine dinuclueotide (NAD^+) and nicotinamide adenine dinucleotide phosphate ($NADP^+$). The redox potential at pH 7.0 of both $NAD^+/NADPH + H^+$ and $NADP^+/NADPH + H^+$ is -0.32 V. It is believed that in cells NAD^+ is approximately 90% oxidized and $NADP^+$ 90% reduced. These values will, of course vary with the particular metabolic state of cells but would mean that their redox potentials were respectively -0.29 V and -0.35 V. The redox potential of $1/2\ O_2 + 2H^+/H_2O$ is 0.82 V. Photosynthesis couples the oxidation of water to the reduction of $NADP^+$ using the electron transport components in

the thylakoid membrane of chloroplasts. This is a redox potential difference of 1.15 V. The energy for this reduction comes from the absorption of light (Nicholls, 1982; Bryce and Hill, 1993).

1.2 LIGHT ABSORPTION IN PHOTOSYNTHESIS

The quantitative characteristics of light in relation to photochemistry have been described (Giese, A. 1964; Calvert and Pittse, 1967; Clayton, 1980).

In order for plants to grow they must be able to convert the energy from the sun into a useful form. Humans produce pigments in their skin that protect them from harmful effects of solar radiation; in contrast, exposure of plants to light stimulate them to produce pigments that absorb and utilize light energy.

Visible light is a form of radiant energy with wavelengths ranging from about 400 nm, seen as blue light, to 680 nm, seen as red. Although radiated in apparently continuous beams, the energy of light actually flows in discrete units called photons. The photons of a beam of light contain an amount of energy that is inversely proportional to the wavelength of the light. The shorter the wavelength, the greater the energy of a photon.

The energy content of photons at various wavelengths is given in Table 1 in cal/Einstein. The Einstein relates light energy to a gram molecular weight and is equivalent to a "mole" of light, 6.023×10^{23} photons. From the Table it can be seen that one mole of Chl, containing 6.023×10^{23} molecules and absorbing one Einstein of red light at 650 nm, absorbs 43,480 cal of energy (Walker, 1979).

Molecules such as Chl appear colored or pigmented because they absorb light at certain wavelengths and transmit light at other wavelengths. The color of a pigment is produced by the transmitted light. Chlorophyll, for example absorbs blue and red light and transmits intermediate wavelengths that are seen in combination as green.

Table 1 : Energy Content of Light at Various Wavelengths.

Wavelength (nm)	Color	cal/ Einstein
395	Violet	71,800
490	Blue	57,880
590	Yellow	48,060
650	Red	43,480
750	Far red	37,800

Light is absorbed by antenna pigments such as Chl by electrons occupying certain orbitals in a pigments molecule. In darkness or exposed to light at wavelengths not absorbed by the molecule, these electrons occupy orbitals at a relatively low energy level (Figure 1) known as the **ground state**. If an electron absorbs the energy of a photon, it moves to a new orbital at higher energy level. In the new orbital the electron is said to be in an **exited state.** Typically, exited orbitals are farther than ground-state orbitals from the atomic nuclei, associated with light sensitive electrons. The difference in energy levels between the ground-state and excited-state orbitals is exactly equivalent to the energy contained in the photon of light absorbed.

Figure 1 shows the concept of absorption of photons (hv) by Chl molecule, energizing an electron to an excited state (a) and its subsequent decay with release of energy. Capture of a more energetic photon (b) results in a higher energy level orbital being filled and then a decay by radiationless transition. Heat may also raise an electron to a higher energy level and the energy is emitted when the electron drops back to the ground state. The main energy-dissipating processes are by radiationless transitions, prompt fluorescence, delayed light emission, phosphorescence, by chemical reactions in photosynthesis and energy transfer, for example of triplet energy to oxygen or carotenoids or of excitation energy to other chlorophyll and pigment molecules.

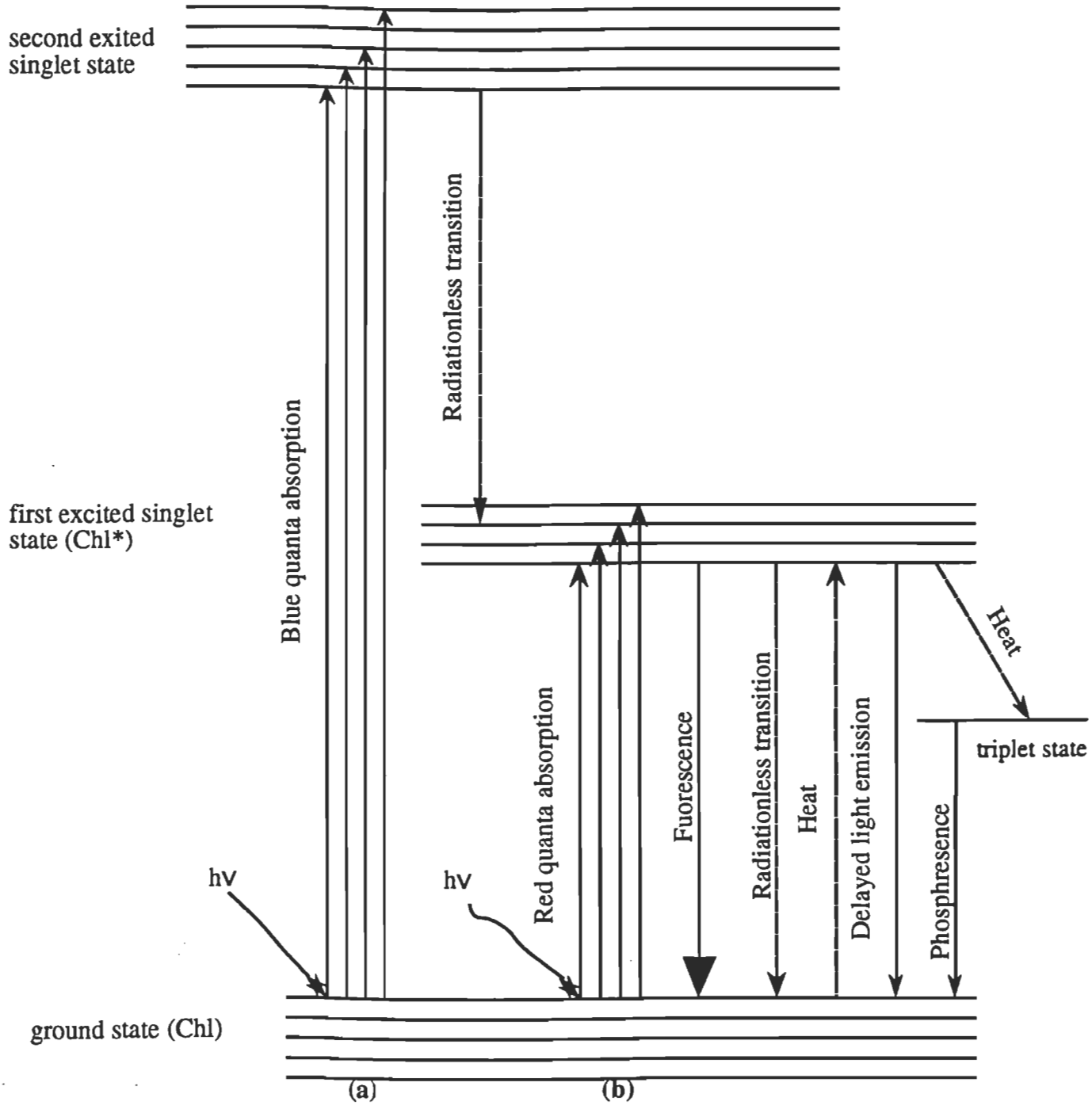

Figure 1. Diagram of energy states in the chlorophyll molecule. The ground, first, and second excited states of the molecule posses a series of energy sublevels. Heat loss occurs when the excited molecule reverts to the lowest sublevel energy of the excited state. The fluorescence emission is shifted to the red end of the spectrum relative to the excitation spectrum because the light emitted in fluorescence is less than that observed during excitation (Stoke's shift).

Electrons in the higher levels of the first excited singlet, S, state, (energy Es) decay by radiationless transition (R) to the lower levels and, if the excitation energy is not used in photochemistry or transferred to other molecules, decay to singlet state, S_o, by emission of "prompt" fluorescence of lower energy (E_f) than the exciting light, as Ef= Es-R. Thus a solution of chlorophyll irradiated with blue light emits red fluorescence. **Phosphorescence** is light emission occurring many seconds or minutes after illumination due to the transfer of triplet (T) to singlet (S) ground state transition. **Delayed fluorescence** involves the $T \rightarrow S \rightarrow S_o$ transition(with small $T \rightarrow S$, energy gap) and has the phosphorescence decay time but the fluorescence spectrum, or triplet annihilation or $T_1+T_1 \rightarrow S_i \rightarrow S_o$ transition with different relationship to the energy absorbed. In Chl a of the thylakoids prompt fluorescence is emitted at a peak of 685 nm. It shows the accumulation of excitation energy in the antenna and is inversely related to the use of electrons; it indicates the state of electron transport and biochemical processes relative to energy capture. Delayed fluorescence, also called delayed light emission, was first observed by Strehler and Arnold (Lawlor, 1987) and occurs in all photosynthetic organisms; it is from excited singlet states of Chl and is of similar wavelength to fluorescence, but shorter wavelength than phosphorescence. Fluorescence and delayed light emission have similar action and emission spectra and saturation characteristics to photosynthesis. Delayed light is emitted from Chl re-excited over a long period from a store of energy produced in the light, so that the time course is long compared to prompt fluorescence.

1.2.1 Light Absorbing Molecules

Although chlorophylls are the molecules directly involved in light absorption and the transfer of electrons to primary acceptors in photosynthesis, other pigments called carotenoids, also absorb light energy and pass it on to the Chls. Both chlorophylls and carotenoids are lipid molecules bound to thylakoid membranes and stromal lamellae in chloroplasts.

1.2.1.1 Chlorophyll

The chlorophylls are a family of closely related molecules based on tetrapyrrole ring (Figure 2). The ring structure of chlorophylls (Katz et al., 1979)

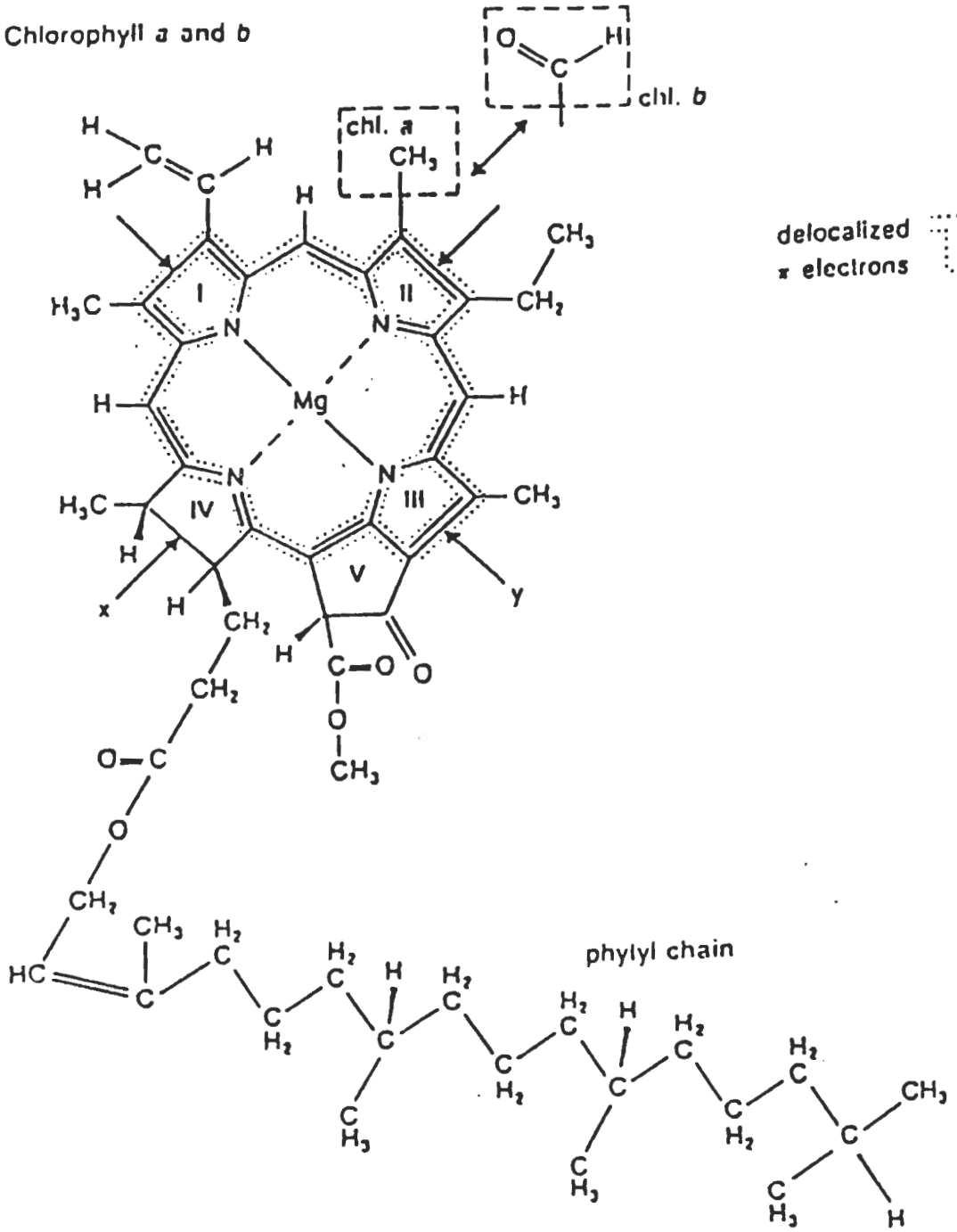

Figure 2. The structure of chlorophylls a and b.

is similar to those of cytochromes and hemoglobin except for the presence of an extra subunits. A magnesium atom is bound at the center of the Chl ring. Attached to the ring is a long, hydrophobic side chain that gives to the two major chlorophylls found in higher plants, Chl a and Chl b, their lipid like solubility characteristic. Chl a and b differ only in the side groups attached to one carbon of the tetrapyrrole ring. Of the two types Chl a plays the central role in the conversion of light to chemical energy in all photosynthetic eukaryotes and also in cyanobacteria; Chl b is one of several pigments that pass the energy of absorbed light to Chl a. The closely related Chl c occurs in an accessory pigment with Chl a in brown algae, diatoms, and dinoflagellates.

Chlorophyll contains many electrons capable of moving to excited orbitals by absorbing light. These electrons can simultaneously occupied many vibrational and rotational levels, and because the incident radiation that is used in most spectrophotometers contains a large number of photons, many vibrational and rotational levels that are associated with the higher electron state can be simultaneously populated in different molecules. As the wavelength of the incident radiation is altered (scanned) a molecule can be excited from the same electron, vibrational and rotational levels to a single excited electron level, but to different vibrational and rotational levels. Because the energetic differences between the vibrational and rotational levels, that are associated with a particular electron levels are small, the many possible changes in energy between the vibrational and rotational levels of the two electron levels overlap, causing broad absorptive band in the ultraviolet-visible region of Chl, rather than a single, sharp peak. The broad curve is called an absorption spectrum (Figure 3). Each Chl type has a distinct absorption spectrum.

Absorption spectra are modified by association of chlorophylls with other molecules in chloroplast membranes, particularly with proteins. For example purified Chl a absorbs red light most strongly at 665 nm when dissolved in acetone. In chloroplast membranes in which the pigments are closely associated with other molecules, individual Chl a molecules may absorb light strongly at other wavelengths such as 660, 670, 680 and 700 nm. Although their absorption spectra are altered, the chemical structure of the chlorophylls is not

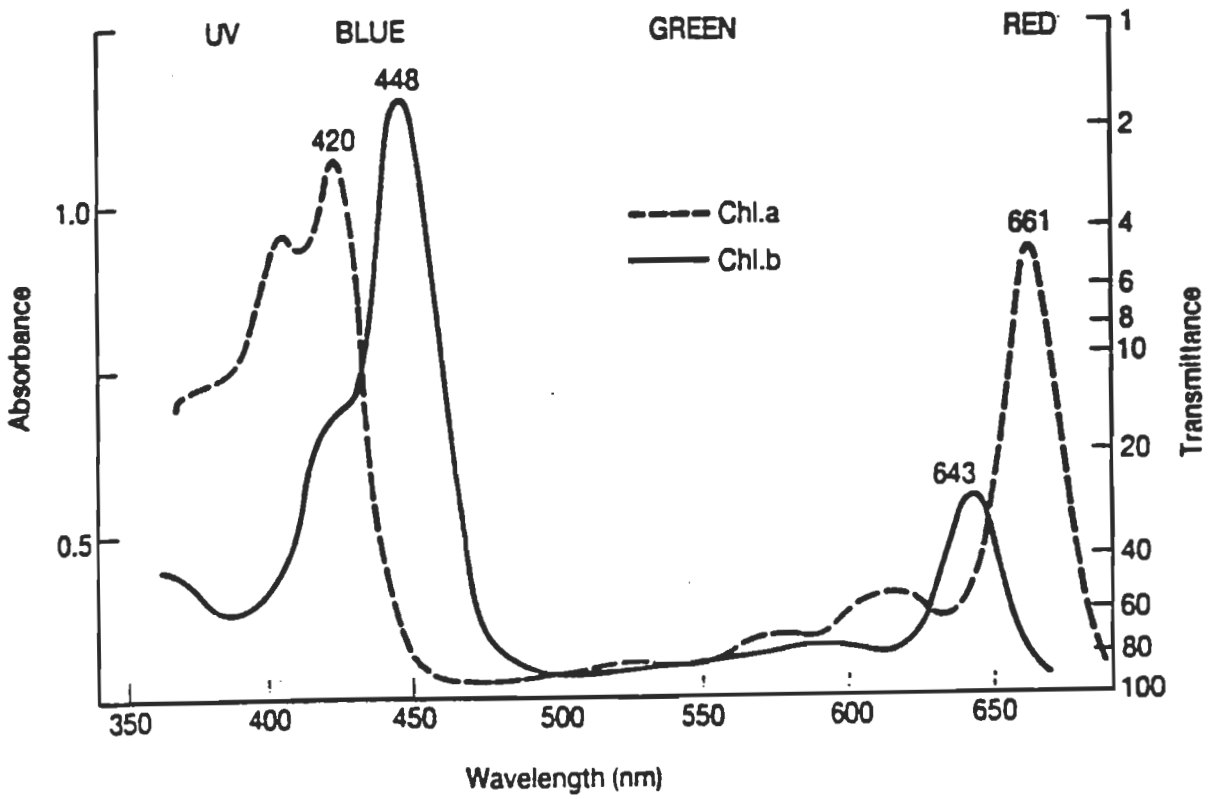

Figure 3: The absorption spectra of chlorophylls a and b in 80% acetone showing absorption in the red and blue and transmission in the green.

changed by association. Some of the associations responsible for modifying light absorption, particularly these producing absorption peaks in Chl a at 680 and 700 nm, figure importantly in the light reactions of photosynthesis.

Although chlorophylls absorb light in the blue end of the spectrum as well as in the red, the energy level of an excited electron passed from Chl a to a primary electron acceptor is equivalent to that of photons in the red wavelengths between 680 and 700 nm. The difference in energy between any shorter light wavelength absorbed and the energy of excited electrons released by Chl is lost as heat. This characteristic makes all wavelengths absorbed by chlorophylls equally effective in photosynthesis, even though photons at the shorter wavelengths contain more energy.

1.2.1.2 Carotenoids

The carotenoids (figure 4) constitute a separate family of light-absorbing lipids built upon a single, long carbon chain containing 40 carbon atoms. Various substitutions in side groups attached to the 40-carbon backbone give rise to different carotenoid pigments. Two types of carotenoids occur in all green plants. The carotenes are pure hydrocarbons that contain no oxygen atoms; chief in abundance among these pigments in the higher plants is B-carotene (Figure 4). The second major carotenoid type, the xanthophylls (also called carotenol), are closely similar except for the presence of oxygen atoms in their terminal structures (Siefermann, 1985).

Carotenoids of both types have multiple light-absorbing electrons associated with the alternating single and double bonds of the backbone chain. These electron absorbs at blue-green wavelengths from 400 to 550 nm and transmit other wavelengths in combination that appear yellow, orange, red, or brown

The carotenoids in their role as accessory pigments, absorb light at wavelengths weakly absorbed by chlorophylls in the blue end of the spectrum. The light energy absorbed by carotenoids, and by Chl b, is eventually transferred by inductive resonance to the Chl a molecules involved in transforming light into chemical energy. The net effect of the entire combination of chlorophylls

and carotenoids is to broaden the spectrum of wavelengths used efficiently as energy sources for photosynthesis.

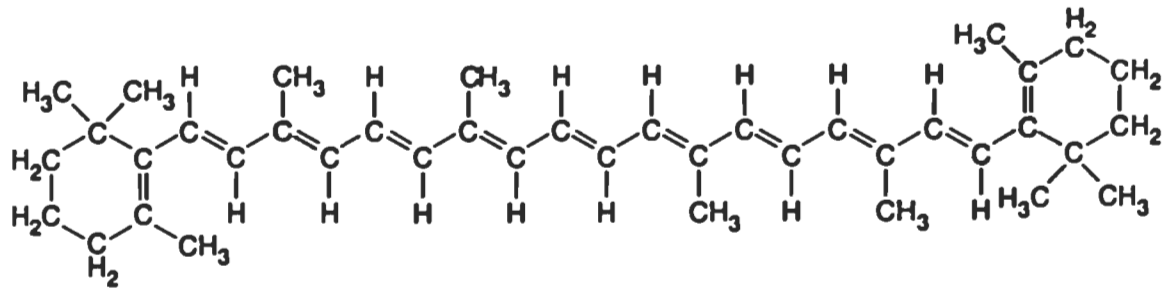

a β-carotene

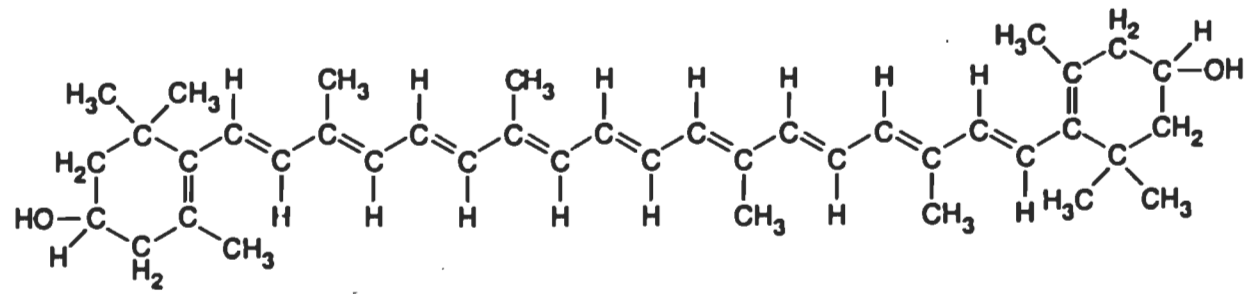

b lutein (a xanthophyll)

Figure 4 : B-carotene and lutein (a-xanthophyll).

1.3 THE ORGANIZATION OF PHOTOSYNTHETIC PIGMENTS IN CHLOROPLASTS

Carotenoids and Chl molecules are organized with proteins and other molecules into large complexes that play central roles in light reactions. Two of these complexes, called photosystems I and II, act directly in the absorption of light and the conversion of light to chemical energy in eukaryotic plants. The two photosystems have been isolated and purified from chloroplast membranes; work with the isolated photosystems has revealed that each

contains from about 50 to 100 Chl a molecules and a smaller number of carotenes. These pigment molecules are combined with polypeptides (as many as 11 in photosystem I and 20 in photosystem II) that carry out structural, enzymatic, regulatory, and other functions in the photosystems. One or two Chl a molecules within the photosystems form a reaction center in which the central event of the light reactions (the transfer of excited state electrons to stable orbitals in a primary acceptors) takes place. The photosystems also contain a sequence of carriers involved in the transport of electrons away from the primary acceptor. Photosystem II, in addition, uses the mechanism of water-splitting as an electron source

The internal membranes of chloroplasts also contain pigment-protein assemblies called light-harvesting complexes (LHCs), which act as accessory light-gathering "antennas". The pigments of the accessory antennas are linked with proteins in complexes without reaction centers or primary acceptors. Because LHCs have no reaction centers or primary acceptors, no conversion of light to chemical energy takes place within them. Instead, the energy of absorbed light is passed on to the two photosystems. Most eukaryotes have two types of LHCs; LHC-I is associated with photosystem I and LHC-II with photosystem II.

1.3.1 Photosystem I

Photosystem I (Figure 5) contains a light-absorbing group of about 130 Chl a molecules and 16 β-carotenes combined with 10 to 11 polypeptides into a structure known as the core antenna (Andersson and Styring, 1991; Golbeck and Bryant, 1991). Individual pigment molecules absorbing light energy in the core antenna pass the absorbed energy to the reaction center, which in photosystem I consists of a specialized form of Chl a called P700 (pigment). P700 is given this name because its light absorption spectrum changes sharply at a wavelength of 700 nm as electrons are passed to the primary acceptor of the photosystem. The photosystem I reaction center is believed to contain a pair of P700 molecules associated with a pair of large 80 kDa polypeptides. Photosystem I also contains a series of built-in electron carriers, including several iron-sulfur (Fe/S) centers.

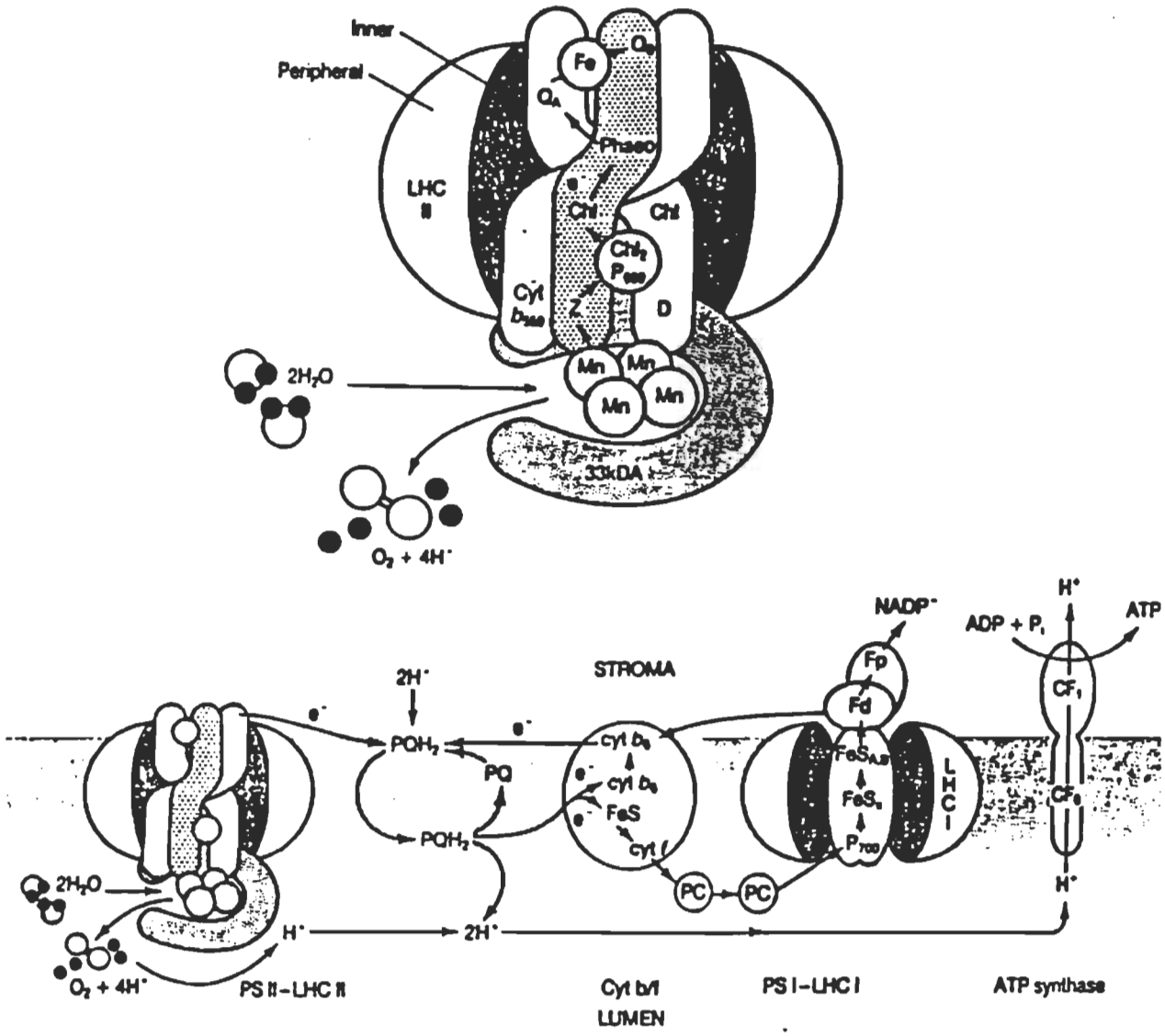

Figure 5 : The locations of the photosystems and electron transport carriers in thylakoid membranes.

These carriers conduct electrons away from the reaction center within the system (Glazer and Melis, 1987).

1. 3 . 2 Photosystem II.

The core antenna of photosystem II (Figure 5) contains about 50 Chl a molecules and a much smaller number of β-carotenes (Hansson and Wydrzynski 1990; Ghanotkis and Yocum, 1990). The reaction center of this photosystem contain a specialized form of Chl a, P680, which undergoes a conspicuous change in light absorption at 680 nm as electrons are passed to the primary acceptor. A pair of P680 chlorophylls is probably located at the reaction center of photosystem II, along with two other Chl a molecules acting in an accessory role. A pair of Chl molecules lacking Mg^{2+} (pheophytins) (Nanba and Satoh 1987) participate in the transfer of electrons from the reaction center to the primary acceptor. These pigments are bound to two related proteins (Hearst, 1987) of 32, and 34 kDa (D1 and D2 respectively), which provide the environment necessary for many of the PSII redox reactions to function properly, and to form the reaction center. A short series of carriers based on quinones is also associated with the D1 and D2 polypeptides. PSII contains the chlorophyll-binding proteins CP47 and CP43, which function as light-harvesting antenna proteins (Green 1988). Another major polypeptide of Photosystem II is cytochrome b559 (Cramer et al., 1986). The function of this Cyt in the photosystem remains unknown. In addition to these integral PSII proteins, there are several peripheral proteins, the most important of which perhaps is the "33 kDa" which is known to shield the manganese center and has also been called the manganese-stabilizing protein (Kuwabara et al., 1987; Tyagi et al., 1987; Philbrick and Zilinkas, 1988).

Our current conceptions about the many aspects of PSII activity involving protein and cofactors interactions is largely obtained from the crystallization and X-ray diffraction analysis of the reaction centers from two species of photosynthetic purple bacteria (Allen et al., 1987a, 1988, Chang et al 1986; Deisenhofer et al., 1985; Michel et al., 1986) along with the realization that there are significant functional and structural homologies between the D1 and D2 proteins in PSII and the L and M subunits of the reaction center complexes

from these purple bacteria (Barber, 1987; Michel and Deisenhofer, 1986; Rochaix et al., 1984, Rutherford, 1986, 1987). Even though this homology is limited to the acceptor side of the photosystem (spanning the region between and including the primary acceptor (and possibly the primary donor) and the secondary quinone [Q_B], it provides a basis for many hypothesis in regard to the functionally and structurally important residues in D1 and D2 (Michel and Deisenhofer, 1987), and the membrane topology of these proteins (Syare et al., 1986, Trebst., 1986). In spite of the presumable structural resemblance between PSII and bacterial reaction centers, our present understanding of PSII protein arrangement, complex assembly, and prosthetic group binding is still very incomplete.

The water-splitting mechanism is also associated with photosystem II. This system includes three soluble polypeptides and four manganese atoms (Dismukes, 1981) that form a manganese center linked to the surface of the photosystem II complex. By a process that is still incompletely known, these elements promote the oxidation of water as the first step in the light reactions. The total protein complement of photosystem II, including the water-splitting complex, may have as many as 22 different polypeptides (Masojdik et al., 1987).

1. 3. 2. 1 The Extrinsic Polypeptides of 16, 23, and 33 kDa

In plants and algae, three extrinsic polypeptides located at the luminal side of PSII of about 33, 23 and 16 kDa, respectively are implicated in the binding of the inorganic cofactors of water oxidation. However, in vitro experiments with isolated PSII complexes from plants have shown that all 3 polypeptides can be removed without loss of water oxidation. The fact that the 16 and 23 kDa peptides are not present in cyanobacteria clearly assigns a non-catalytic function to these peptides. Presumably the 16 and 23 kDa peptides modulate the binding of Ca^{2+} and Cl^- at the water oxidizing side in plants and algae (Murata and Miyao, 1985).

The extrinsic 33 kDa (Camm et al., 1987; Isoagai et al., 1983; Enami et al., 1989; Milner et al., 1987) polypeptide is present in all oxygenic organisms and is much more tightly associated with the intrinsic PSII peptides (Figure 5) than the 16 and 23 kDa peptides (Camm et al., 1987). The non catalytic role for the

33, 23, and 16 kDa proteins was observed quite early (Henry et al., 1982) and became widely recognized when it was found that the electron-transport activity lost by removal of the three proteins could be restored by the addition of Ca^{2+} and /or Cl^- ions (Andersson et al., 1984; Ghanatakis et al., 1984; Miyao and Murata, 1984a; Nakatani, 1984; Ono and Inoue, 1984). The restoration of oxygen evolution could only be observed with high, unphysiological levels of Ca^{2+} and Cl^-. Thus, it was suggested that the extrinsic proteins were essential for the high affinity binding of Ca^{2+} and Cl^- to the catalytic site of water oxidation (Murata and Miyao, 1985; Andersson and Akerland, 1987). The binding of the Ca^{2+} and Cl^- ions are usually related to the presence of the 23 and 16 kDa subunits. However, such a function must also be considered for the 33-kDa protein since its removal further increases the requirement for Cl^- ions for optimal oxygen evolution (Imaoka et al., 1986). Interestingly, it has recently been shown that the 33 kDa protein displays strong sequence homology to the calcium-binding site of mammalian intestinal calcium-binding proteins, and it has been shown through ligand-blotting studies to bind Ca^{2+} ions (Gray et al., 1989).

1.3.3 Light-Harvesting Complexes (LHCS)

LHC antennas are large particles that completely span the photosynthetic membranes. The LHC-II antenna, however dissociates from photosystem II complexes under certain conditions, so that the accessory antenna and the photosystem may occur as either a tight complex or separately in chloroplast membranes. The energy of photons absorbed within the LHCs is presumably passed to the photosystems by the same inductive resonance walk taking place in the core antennas of the photosystems (Mullet et al., 1980).

The two LHC antennas contain about 80 to 120 Chl molecules in a ratio of about 3 to 4 Chl a molecules to each Chl b. The LHC-I antennas forms more ore less permanent complex with photosystem I. The Chl a and b molecules are combined with three or four polypeptides to form the LHC-I complex (Golbeck and Bryant, 1991).

1.4 ABSORPTION AND MIGRATION OF LIGHT ENERGY WITHIN THE PHOTOSYSTEMS.

After a photon of light is absorbed by a pigment molecule associated with either photosystem, the absorbed energy is passed to the Chl a molecules at the reaction center. Although the mechanism transferring the energy is not completely understood, the energy of an absorbed photon is considered to "walk" by inductive resonance from one pigment to another in a core antenna until it reaches the reaction center. The entire walk typically occurs within less than a billionth of a second, without significant loss of the absorbed energy as heat (Andreaesson and Vanngard, 1988). Once absorbed light energy reaches the Chl a molecules at the reaction center, it is apparently trapped in this location and does not migrate back to other pigment molecules of the assembly. One factor in the trapping is the rapid transfer of electrons from the chlorophylls to a primary acceptor. Another may depend on slightly lower energy level associated with the excited orbital in P680 or P700 (Hanson and Wydrzynski, 1990). After dropping into these orbitals, the excited electrons may not contain enough energy to move back from P680 or P700 to other pigment molecules in the photosystems (Renger, 1992).

The two photosystems (PSII and PSI) are linked in chloroplasts by an electron transport system that conducts electrons from one photosystem to the next, and delivers electrons to $NADP^+$ at the end of the pathway. Most molecules oxidized and reduced in the photosynthetic system, consist of nonprotein prosthetic groups organized with proteins into large complexes. The use of various herbicides to block specific steps in the photosynthesis pathway have revealed that the photosynthetic carriers are arranged in a Z pathway (Figure 6) first advanced as a possibility by R. Hill and F. Bendall. The first leg of the Z is the pathway of electron flow from water through PSII.

The electron then flows through a long series of carriers that connect PSII and PSI; this series forms the diagonal of the Z. As they pass through this series, electrons lose energy; some of the released energy is used to pump H^+ across the membrane housing the carriers. The electrons then pass through PSI and are transferred to a short transport chain leading to the final acceptor of the

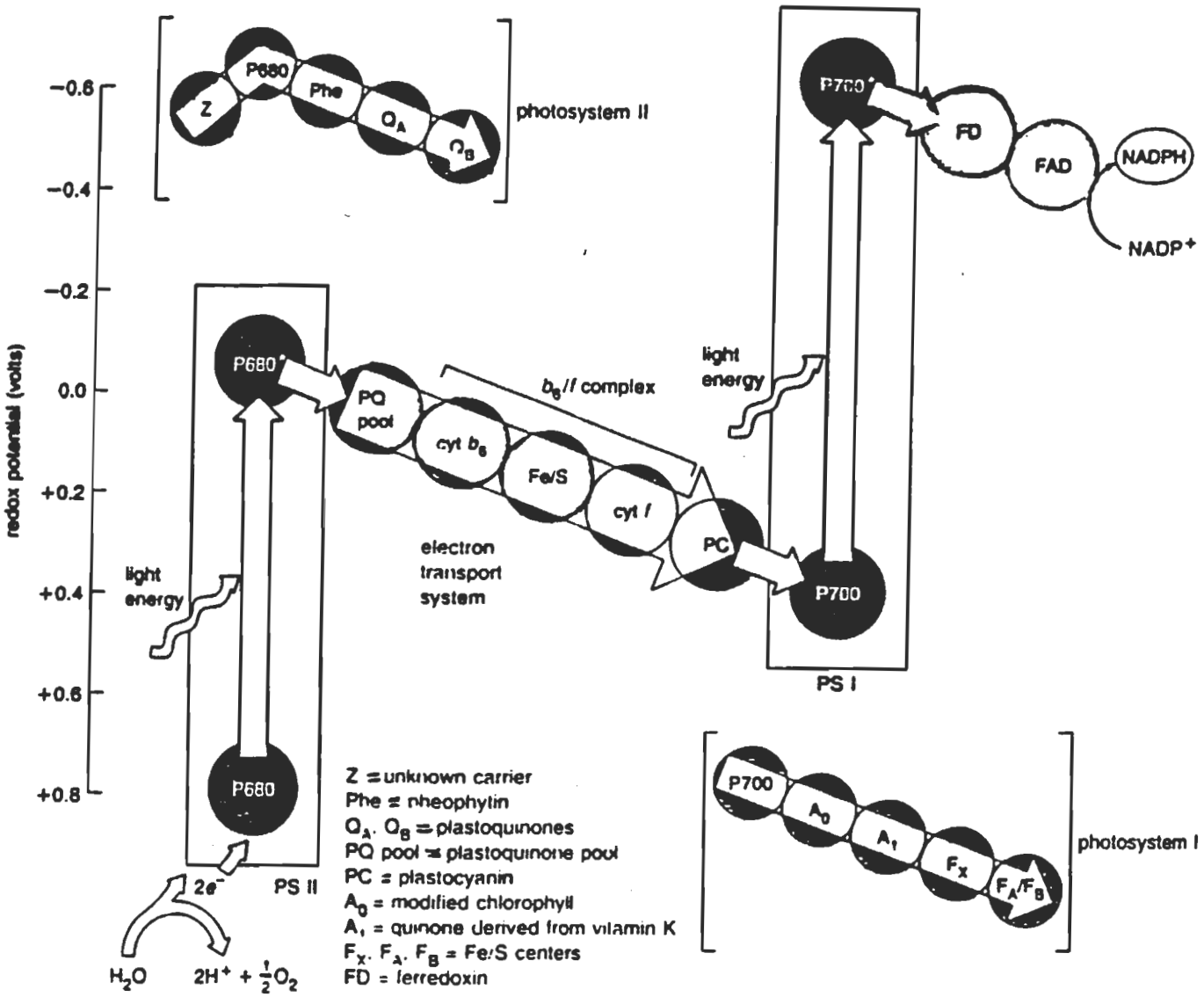

Figure 6 : The prosthetic groups acting as electron carriers and their tentative sequence in the Z pathway. The asterisks indicate the excited forms of P680 and P700.

chloroplast system, $NADPH^+$. The tentative positions of individual prosthetic groups acting as carriers within the Z pathway are shown in Figure 6 (Ort and Good, 1988).

Electrons entering the Z pathway are removed from water at low energy levels by the water-splitting complex in photosystem II. The electrons removed from water are delivered to the reaction center of PSII by an electron carrier identified as Z a tyrosine residue denoted Y_Z. This side chain picks up electrons from the water-splitting reaction and releases them to the Chl P680 at the reaction center. P680 accepts single electrons and raises them to excited orbitals through the absorption of light energy.

After excitation electrons are released to the primary acceptor of PSII, identified as a plastoquinone, a quinone type typical of chloroplasts (Figure 7). The plastoquinone forming the primary acceptor of PSII (Schatz and Holzwarth, 1987; Nuijs et al., 1986; Eckert et al., 1988) is identified as Q_A which is defined as a specially bound PQ molecule which undergoes a two-step reduction process (Vethuys, 1981). Delivery of electrons from P680 to Q_A occurs via pheophytin (Kimov et al., 1987). Pheophytin evidently acts as an intermediary in the transfer by housing electrons in unstable orbitals for a fraction of a second. From Q_A (Gorkon, 1974) electrons flow to a second plastoquinone, Q_B which is considered as the final electron carrier in the PSII complex. The entire pathway of electron flow within the photosystem II complex thus includes:

$$2H_2O \longrightarrow (Mn)_4 \longrightarrow Yz \longrightarrow P680 \longrightarrow Pheophytin \longrightarrow Q_A \longrightarrow Q_B$$

The H^+ removed from water by PSII is released to add to the H^+ gradient produced by electron transport in the chloroplasts.

Electrons are transferred from the Q_B carrier of PSII to a pool of plastoquinone molecules that forms the first carrier of the transport system linking the two photosystems (Figure 6). In the pool, individual plastoquinone molecules are unassociated with proteins and free to diffuse within the membrane interior. Electron transfer to the pool probably occurs simply by detachment and entry into the pool of the reduced Q_B molecule from PSII. The

reduced plastoquinone diffusing into the pool is replaced in PSII by an oxidized plastoquinone from the pool. Electrons from the plastoquinone pool flow through three carriers, cytochrome b_6, a Fe/S protein, and Cyt f (Amou, 1991). The complex containing these carriers is known as the Cyt b_6/f complex. Then from the Cyt b_6/f complex electrons pass to the final carrier linking the photosystems, plastocyanin. This carrier, a protein containing a copper atom that varies between the Cu^+ an Cu^{2+} states during alternate cycles of oxidation and reduction, shuttles electrons from the Cyt b_6/f complex to PSI.

From plastocyanin electrons flow to the P700 Chl molecules at the reaction center of PSI. After excitation by light absorption electrons are transferred from P700 to the primary acceptor of this photosystem, a modified form of Chl known as A_o. From A_o electrons flow to A_1, a quinone derived from Vitamin K. The electron then flow through a chain of three Fe/S centers, designated F_X, F_A, and A_B. The sequence of electron flow within the three Fe/S centers remains uncertain but may proceed from F_X to either of the other two (Paschorn et al., 1988). The pathway of electron flow within PSI is therefore :

$$P700 \longrightarrow A_o \longrightarrow A_1 \longrightarrow F_X \longrightarrow (F_A/F_B)$$

Electrons are next transferred to the first carrier outside PSI, ferredoxin, an Fe/S protein that acts as a separate, highly mobile electron carrier in the chloroplast system. From ferredoxin electrons flow along the short final chain from FNR (ferrodoxin 'NADP' reductase) to $NADP^+$ to complete the Z pathway.

Electrons receive two boosts in energy as they move through the Z pathway, one in PSII and one in PSI (Figure 6). The two consecutive boosts raise the electrons to energy levels high enough to reduce $NADP^+$. Along the way some energy is trapped from the electrons and used to produce an H^+ gradient. The gradient is established primarily through the activity of the Cyt b_6/f complex, which acts as an electron-driven pump actively transporting H^+. In the chloroplasts H^+ is pumped from the stroma into thylakoid compartments.

The pattern of electron flow in a Z pathway from H_2O to $NADP^+$ is frequently called noncyclic photosynthesis because electrons are removed from water and travel in a one way direction to $NADP^+$. Figure 6 summarizes the organization of the individual electron carriers within the photosystems and carrier complexes of the chloroplast system. All the components of the Z pathway are located on or within the thylakoid membranes or stromal lamellae of chloroplasts.

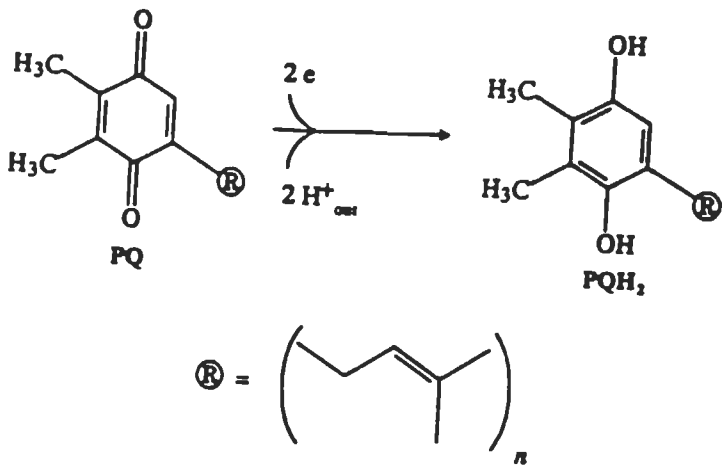

Figure 7 : Plastoquinone, a carrier that transport electrons within the photosystem II complex and in the electron transport system linking the photosystems in the Z pathway.

1.5 THE WATER-SPLITTING SYSTEM

The water-splitting reaction carried out by PSII, developed in cyanobacteria some 2, to 3 billion years ago, is one of the most significant and fundamentally important of all biological interactions. The reaction enabled photosynthetic organisms to use one of the most abundant substances on earth (water) as an electron source. The reaction is also responsible for the oxygen present in the atmosphere which paved the way for the evolution of aerobic organisms, in which oxygen serves as the final acceptor for electrons removed in cellular oxidation. The reaction oxidizing water into $2H^+$ and $1/2\ O_2$, carried out by the group of three peripheral membrane polypeptides attached the surface of PSII and the manganese center, is believed to involve two molecules of water and to proceed in a four-step pathway first proposed by Kok and his coworkers 1970 (Figure 8). One of the major lines of evidence used to develop the model is the fact that if PSII is illuminated by light with very brief flashes, four sequential flashes are required to complete the water-splitting reaction, and O_2 is released at only one of the flashes. Movement from one step to the next in the pathway is intimately linked to the excitation of electrons in PSII.

On this basis Kok proposed that at the beginning of the pathway (Figure 8), two molecules of water are split

$$2H_2O \longrightarrow 4H^+ + 4e^- + O_2$$

The four electrons and four H^+ are picked up by the manganese center, which may consist of four manganese atoms (Yocum et al., 1981; Berthold et al., 1981) (Figure 8-b shows one of several possibilities for the lattice). The electrons and protons are then removed one at a time from the manganese center in a series of steps

As the first of the four electrons is removed (step 1), it is picked up by the Yz carrier and delivered to Chl a P680 at the reaction center. Transfer to P680 reoxidizes Yz, and readies it for acceptance of the electron to be released in step 2.

The system is limited by excitation, however, so that the reaction sequence cannot progress to step 2 until the electron delivered from step I is excited by light absorption in the reaction center. Once excitation has occurred, and the electron has passed to the primary acceptor, the mechanism is ready to progress to step 2. Step 2, 3, and 4 take place similarly, with an excitation completing each step. Protons are removed from the manganese center at some but not all of the steps; current indications are that one H^+ is released at step 1 and 3, and the remaining two H^+ at step 4, as shown in (Figure 8-a). The two oxygen atoms removed in the preliminary reaction of the pathway are released as O_2 at the last step.

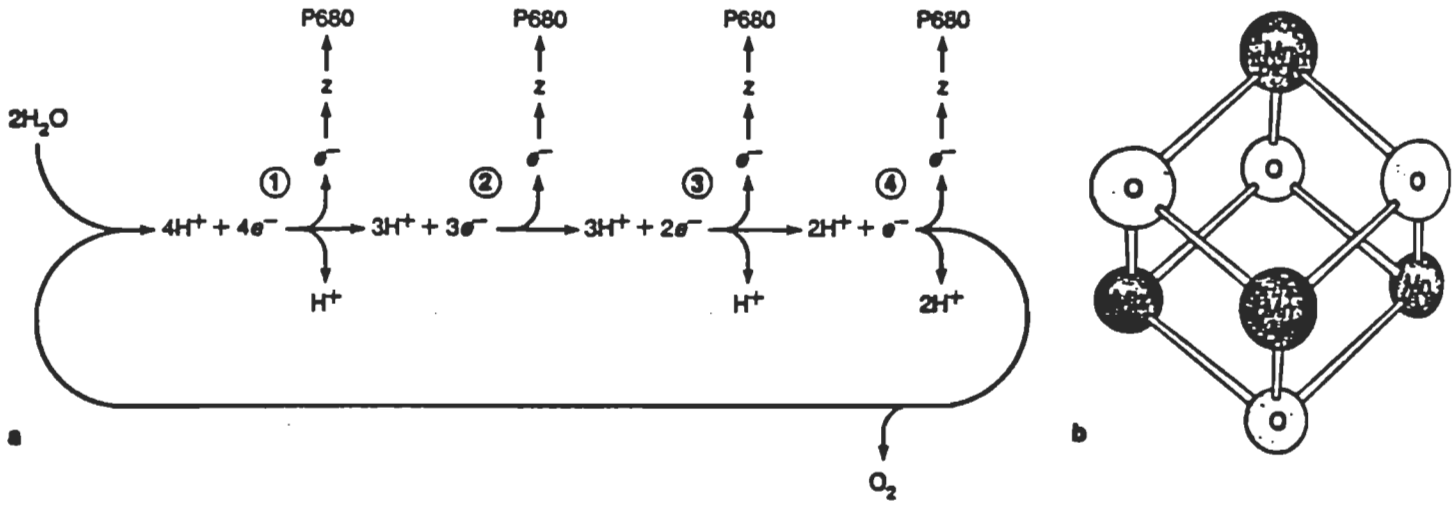

Figure 8 : The reaction pathway splitting water to generate electrons for the Z pathway. (a) The series of stepwise reactions removing electrons from water and delivering them one at a time to the P680 reaction center of photosystem II. (b) A possible arrangement of manganese and oxygen atoms in the manganese center.

Many features of the pathway are still not understood. Both Ca^{2+} (Boussac and Rutherford,1988a; Yocum, 1991) and Cl^- (Critchely, 1985, Murata and Miyao, 1985) are required for the reaction to proceed, at a level of about two or three Ca^{2+} and four to five Cl^- per manganese center. The role of these ions is unknown. They may play structural or regulatory roles, or may contribute to catalysis of the reaction. The precise structure of the manganese center and its linkage to PSII are also unknown (Rutherford, 1989, Brudvig et al., 1989; Vincent and Christou 1987, Pecoraro, 1988). It is considered likely that the binding site is located in a pocket on the surface of either of the D1 or D2 polypeptides or in the interface between the two polypeptides. Valence changes of the manganese ions of the center between 2+, 3+, and 4+ states undoubtedly contribute to the uptake and release of electrons. However, the combinations and sequence of these changes remain unknown. The function of the three soluble polypeptides (17, 24 and 33 kDa) is also uncertain. Curiously, the water-splitting system reaction can proceed without the polypeptides if Ca^{2+} and Cl^- concentrations are raised to abnormally high levels. This may indicate that the polypeptides simply promote Ca^{2+} and Cl^- binding so that the reaction can proceed at physiological concentrations of these ions (Homann, 1987).

Elucidation of the structure function relationship in membrane-protein on a molecular level challenges life-science today. Bacteriorhodopsin and the bacterial photosynthetic reaction-center are the structurally and functionally best characterized membrane proteins (Deisenhofer, et al., 1985; Henderson et al., 1990). Understanding their mechanism on the molecular level might also give insight into the mechanism of other vectorial proton and electron transfer proteins. Knowledge of the pigment-pigment interaction which tune the properties of the Chl pigments is, thus, of particular importance in the understanding of the primary events in photosynthesis.

Over the last few years, the understanding of the interactions between the proteins and the cofactors involved in various aspects of PS II activity has readily advanced. One of the major driving forces towards a better insight into these interactions has been the crystallization and X-ray diffraction analysis of reaction centers from photosynthetic purple bacteria (Michel et al., 1986, Allen et al., 1987; El-Kabbani et al., 1991), along with the realization that there is an

extensive functional and structural homology between parts of PSII and of the reaction center complex from purple bacteria (Trebst, 1986; Michel and Deisenhofer, 1986). It has become clear how much the PSII proteins contribute to the particular properties and orientation of the PSII cofactors needed to optimally function in energy transfer and electron transport through the photosystem. For this reason, protein structure and cofactor function need to be considered in conjunction, even though generally biochemical and biophysical aspects of PSII have been treated separately. A simultaneous and integrated understanding of structural and functional aspects is expected to be critical to the design of further experimentation geared towards an elucidation of the mechanism by which PSII can successfully utilize light energy to initiate a well-orchestred series of redox reactions that is one of the corner stones of photosynthesis process.

Although there have been many significant advances in photosynthesis research in the last few years which have led to our current perceptions of PSII structure and functions, combined with all recent major efforts, there remain several important questions which will need to be addressed in the future.

Therfore the objective of this project is to investigate some of these questions which are still under a great debate between many researchers in photosynthesis. In this study we will use Fourier-Transform Infrared (FTIR) spectroscopy in the first place to test the following:

1-Interaction of LHC-II with toxic divalent metal ions

2-The structure of Chl $P680^{+}$

3-Heat treatment of PSII membrane in the presence of betaine and sucrose.

4-The secondary structure of the 33 kDa extrinsic protein

1.6 COMPLEXATION OF DIVALENT METAL IONS WITH LHC-II

1.6.1 Metal Ions and Photosynthesis

Metal toxicity in relation to photosynthesis has attracted much attention in view of increasing industrialization and pollution. In most of the studies, elevated levels of heavy metals were used which were toxic for the system under study. However, the availability of any metal in the soil is determined by various factors namely absorption by organic matter, clays, soil pH, formation of low molecular weight chelates etc.

The problem of heavy metal pollution is on the increase through out the world. Although any heavy metal ion can be toxic to the plant at elevated levels; Hg, Cd, Pb, Cu, Zn, have been generally observed to cause phyto-toxicity in soils.

Hg, Cd, Pb, are the major environmental contaminants which are present in air, water, and soils, especially in areas of heavy automobile traffic, near smelters and in the area where oil is burnt for heating purposes. These heavy metals when released into the environment settle down with dust and contaminate both foliage and soil. Reduction in corn and barley growth has been reported at a very low concentration. These heavy metals have been shown to inhibit net photosynthesis in green alga, and reduce oxygen evolution by affecting electron transport (Krupa et al., 1992).

Copper and zinc are known to be essential micronutrients in both alga and higher plant, these ions at concentration above 1 μM are increasingly toxic, inhibitors for electron transport (Baszynski et al., 1986, Krupa et al., 1987b, Rashid and Carpentier, 1991). Studies on PSI found that copper inhibits electron transport due to the direct interaction of copper with ferredoxin on the reducing side of PSI. The Hill reaction in PSII was also sensitive to copper. On the other hand Cu deficiency results in a high degree of saturation of thylakoid lipid, which affects the function of the PSII acceptor side, in addition, the pigment composition of LHCII appears disturbed (Droppa et al., 1987).

Heavy metals are known to interfere with a variety of photosynthetic functions. Hg has been shown to interrupt the flow of electrons at multiple sites, such as plastocyanin and the reaction center of PSI and with the activity of enzymes, such as ferrdoxin-$NADP^+$-oxidoreductase (Oettmeier, 1992). In general the effect of metal ions can be summarized as follow:

1)-Toxic ions as environmental contaminants 2)- Inhibit O_2 evolution, 3)- Inhibit electron transport, 4)- Inhibit enzymes activity (Hg^{2+}), 5)- Micronutrients are required for activation of many enzymes at low level (Zn^{2+}, Cu^{2+}). 6)- Participation in O_2 evolution mechanism (Ca^{2+}, Mn^{2+}), 7)- Inhibit net photosynthesis.

1. 6. 2 Light-Harvesting Complex II

The efficiency of photosynthesis is greatly enhanced by antenna or light-harvesting complexes which collect light energy and transfer it to the photosynthetic reaction centers. The most prominent antenna in higher plants is the major light-harvesting complex of photosystem II (LHCII).

According to a recent crystallographic study (Kuhlbrandt and Wang, 1991; Evans and Nugent 1991) LHCII contains three closely similar or identical polypeptides, with each binding 8 Chl a and 7 Chl b molecules. About 50% of the Chl a content and 75% of the Chl b of higher plant chloroplasts is concentrated in LHC-II antennas. LHC-II antennas also contain a few carotenoid molecules, including both β-carotene and xanthophylls. Although the proportion of xanthophylls in LHC-II is relatively small, the total collection of LHC-II antennas contains almost all the xanthophylls of higher plant chloroplasts (Thornber et al., 1988).

Apart from its function as an antenna that collects radiant energy, this complex, regulates the transfer of excitation energy to the reaction centers of PSII and PSI, depending on the phosphorylation of its apoprotien (Bennet et al., 1984; Staehelin, 1986). The complex also mediates the interaction of thylakoid membranes, which leads to the formation of stacks of membrane vesicles, the chloroplast grana. LHCII is a highly asymmetric transmembrane protein composed of three structurally equivalent monomers. The ability of LHCII

from widely different plant species to form such oligomeric supramolecular arrays suggests that this structure is of general significance. The importance of the oligomeric structure of LHCII in radiant energy collection and energy transfer and the molecular mechanisms of this oligomerization are studied by experiments with different in vivo and in vitro factors modifying the composition and structure of LHCII (Qlumely and Schmidt, 1987).

Among the in *vivo* factors affecting the composition and structure of LHCII, the effects of radiant energy, herbicides, low temperature, mineral deficiency, heavy metal ion pollution and specific mutations have been investigated (Lemoine et al., 1982; Leech and Walton, 1983; Huner et al., 1987; Krupa et al., 1987a, b; Maroc et al., 1987; Abadia et al., 1988; Krol et al., 1988; Krupa 1988b)

Previous investigations have demonstrated a strong influence of monovalent and divalent cations on the conformation, activity and stability of LHCII-protein. Several studies have demonstrated that this protein has a strong metal ion binding affinity (Krupa, 1988; Baron et al., 1993)

Thus in this work we will investigate the binding of Cd^{2+}, Hg^{2+}, Cu^{2+}, Pb^{2+}, Zn^{2+}, Ca^{2+}, Mg^{2+}, and Mn^{2+} on the secondary structure of LHC-II protein using FTIR spectroscopy.

1.7 STRUCTURE OF $P680^+$

As we previously described the oxidation of water is most easily and safely accomplished by a concerted 4-electron event, oxidizing two water molecules to one O_2 molecule. Nevertheless, the midpoint potential of + 0.8 V and the waste product, O_2, entail considerable risks of damage to the photosynthetic apparatus. PSII needs not only a special device to accumulate the four oxidizing equivalents and ensure their concerted action, but also an oxidant strong enough to make it happen. The oxidation potential of the primarily photooxidant in PSII, $P680^+$, cannot be measured directly but has been estimated at + 1.0 to + 1.3 V (Jursinic and Govindjee, 1977), at + 1.1 V (Klimov et al., 1979) and at + 1.2 by independent approaches. It is much higher than in all other photosystems and suggests an essentially different structure or

environment. It is so high that $P680^+$ will oxidize not only the tyrosine which normally acts as the secondary electron donor Y_Z but also other amino acid residues and pigments in its vicinity (Van Gorkom, 1985).

The structure of P680 and its molecular environment must be responsible for the high potential of $P680^+$ / P680. P680 consists of Chl a and the midpoint potential of monomeric Chl a in solution is about +0.8 V (Davis et al., 1979). It has often been proposed that P680 is a monomer, not a special pair like in other photosystems. That may explain why its redox potential is not lower than that of Chl a in vitro, but something special in its environment must still be postulated to explain why its redox potential is higher by 0.3-0.4 V. P680 has many properties that may be taken as evidence for a monomeric structure. The Q_y absorption band is hardly red-shifted relative to that of the antenna Chl a; the oxidized state and the triplet state appear to be localized on a single Chl a molecule (reviewed by Hoff 1987). Stark effect (Losche et al., 1988) and hole-burning measurements (Tang et al., 1990) do not show the features characteristic of the special pair in purple bacteria, and most recently LD-ADMR (linear dichroic absorbance-detected magnetic resonance) measurements showed that the angles between the Q_y transition moment and the triplet x- and y-axis are the same as for Chl a in ethanol (Van der Vos te al. 1992). On the other hand, the oxidized-minus-reduced absorbance difference spectrum of P680 is significantly different from that of monomeric Chl a in vitro and the other properties are found in P700 as well (Brog et al., 1970).

Arguments suggesting a dimer structure of P680 are the following. The histidines which in the purple bacterial L and M proteins form ligands to the Mg atoms of the special pair, but not those which ligate the accessory BChls, are conserved in D1 and D2 proteins (Michel and Deisenhofer, 1988). At low temperature a conservative CD doublet is observed at the position of the Qy absorption band of P680 (Otte et al., 1992). Van Kan et al.,(1990) found that 4 pigments, presumably 2 Chl and 2 Pheo, contribute to the 680 nm absorption band of the isolated reaction center and Schelvis et al.,(1993) found that their selective excitation leads to homogeneous 3 ps kinetics. The initial bleaching upon selective excitation of the long wavelength pigments has at least twice the amplitude expected for excitation of one molecule (Schelvis et al., 1993) and

is halved with a time constant of 0.1 ps (Durant et al., 1992). Schelvis et al.,(1993) concluded that P680 is a special pair like in other photosystems, but disguised as a monomer by two features: the Q_y transition moments are nearly (anti) parallel and placed approximately at the magic angle with their connecting axis. This geometry results in a very small exciton splitting with nearly all transition probability in one of the two exciton bands.

Difference FTIR has already proven to be useful in elucidating structure/function in membrane proteins (Braiman and Rothschild,1988). FTIR difference studies of photosynthetic reaction centers from purple bacteria, non-sulfur bacteria have also been reported (Mantele, 1992). However, there are relatively few difference infrared studies of light-induced electron transfer mechanism in PSII, perhaps because of the structural complexity of this large protein complex (Tavitian et al., 1986; Nabedryk 1990a; Berthomieu et al., 1990a,b).

We will use here FTIR difference (light-minus-dark) spectroscopy to obtain the first vibrational difference spectrum that reflects contributions from the oxidation of P680. From the vibration spectra of $P680^+$ we will try to draw a conclusion about the structure of this cation, is it monomer or dimer?

1.8 EFFECT OF BETAINE AND SUCROSE ON PSII

Excessive swelling of thylakoids isolated from chloroplasts can be prevented by adjusting the osmotic potential of the medium they are suspended in. Sucrose is the most frequently chosen osmolyte, but other solutes like NaCl or sorbitol have been used as well. The habit of including sucrose in the preparation and assay media has been maintained by most investigators even when they work with preparations of photosynthetic membranes which no longer are vesicular, e.g., the PSII membranes isolated by a Triton-X-100 treatment of thylakoids according to (Berthold et al., 1981). However, beyond a general realization that these solutes acts as stabilizers of PSII preparations and as cryoprotectants during their storage, other implications of their presence are rarely considered.

During the past decade, various reports on solute-modified properties of PSII membranes have appeared in the literature (Brudvig et al., 1983, Satoh and Katoh, 1985; Boussac and Rutherford, 1988; Wydrznski, et al. 1990, Papageorgiou et al., 1991). In one of these publications, (Wydrznski, et al., 1990) reported how, in media lacking any solutes other than MES-buffer, PSII membranes would lose 75% of their water oxidizing activity in the course of 10 hours. The authors identify the absence of Cl^- ions in the medium as a critical factor contributing to the activity loss and, on the basis of the complexities of the observed Cl^- effects, raise the question whether the well established cofactor role of Cl^- in photosynthetic water oxidation is perhaps not a mechanistic one, but a structural one instead. In another article, Papageorgiou et al.,(1991) report that the treatment of PSII membranes with 1.2 M NaCl to dissociate the extrinsic 17 and 23 kDa polypeptides was unsuccessful when 1.2 M betaine had been added to the incubation medium.

The non-toxic osmolite glycinebetaine is accumulated to relatively high concentrations by several species of plants and bacteria exposed to salt stress or water deficit (Wyn jones and Storey, 1981; Cosnka et al., 1989; Wydrznski et al., 1989). Plants grown in high-salt medium contain a higher amount of the osmolite and therefore, the synthesis of this quaternary ammonium compound may be considered as a protective mechanism against elevated osmolarity (Gnard et al., 1991). Various compatible solutes such as polyhydric alcohols, sugars sand amino acids are also accumulated in vascular plants in response to seasonal acclimation to cold stress (Yancey et al., 1982; Alberdi and Corcuea, 1991). It was postulated that the formation of ice-crystals at membrane surfaces produces a dehydrating effect analogous to the action of deficit (Guy, 1990) and that the accumulation of glycinebetaine during cold acclimation may improve freezing tolerance in leaves (Kishitani et al., 1994).

Various polyhydric alcohols and sugars were also known to stabilize protein structure and function and to increase the transition temperature of some polypeptides in aqueous solutions (Gerlsma, 1970; Gerlsma and Stuurs, 1972, 1974). Glycinebetaine has been shown to stabilize complex enzymes such as ribulose-1,5-biphosphate carboxylase/oxygenase and glucose-6-phosphate

dehydrogenase maintaining their subunit structure even at high concentrations of NaCl (Incharoensakdi et al., 1986; Gabby-Azaria et al., 1988).

Glycinebetaine is synthesized in the chloroplast from the oxidation of choline by specific enzymes (Hanson et al., 1985) and can be found in this organelle at concentrations up to 0.3 M when leaves are grown in saline environments (Robinson and Jones, 1985). In the chloroplast, glycinebetaine has been postulated to act on membrane permeability (Homann, 1992). However, compatible co-solutes at high concentrations where shown to decrease freezing damage to thylakoid membranes and to prevent the heat-induced dissociation of membrane-bound polypeptides such as the CF1 subunit of the chloroplast ATP synthase (Volger et al., 1978; Volger and Santarius, 1981).

More recently, it was demonstrated that glycinebetaine greatly stabilizes the oxygen evolving function of PSII during incubation of isolated cyanobacterial thylakoid membranes or spinach PSII submembrane fractions at room temperature (Mamedov et al., 1993).

It was shown that glycinebetaine exerts a stabilizing effect on the oxygen evolving complex and prevents the release of the extrinsic polypeptides from PSII submembrane preparations in the presence of salts (Papageorgiou et al., 1991; Homann, 1992; Murata et al., 1992).

Glycinebetaine also protected the oxygen evolving activity against heat stress in thylakoid membranes preparations (Williams et al., 1992; Mamedov et al., 1993). In PSII particles isolated from Phormidium laminosum, this co-solute retarded the heat-induced release of an extrinsic polypeptides of 9 kDa required for oxygen evolution in these preparations (Stamatakis and Papageorgiou, 1993). The oxygen evolving activity of PSII core preparations isolated from pea was also greatly protected against heat stress in the presence of co-solutes due to the more stable binding of the 33 kDa extrinsic polypeptide to the complex (Williams and Gounaris, 1992). However, PSII-mediated dichlorophenolindophenol (DCPIP) photoreduction activity was not further stabilized by sucrose in $CaCl_2$-washed PSII core preparations already lacking this polypeptides and it was concluded that the protective action of co-solutes was

restricted to the oxygen evolving complex, more precisely at the level of the extrinsic polypeptides of 33 kDa (Williams and Gounaris, 1992).

In the present work, we will investigate the effect of glycinebetaine and sucrose on PSII membrane under heat treatment. FTIR spectroscopy with resolution-enhancement techniques will be used for this purpose.

1.9 SECONDARY STRUCTURE OF 33 kDa EXTRINSIC PROTEIN

PSII-membranes consists of both intrinsic and extrinsic proteins subunits. Intrinsic polypeptides with apparent molecular masses of 49 (CPa-1), 45 (CPa-2), 34 (D1), 32 (D2), 9 and 4.5 (α and β subunits of Cyt b_{559}), and 4 kDa (psb1 gene product) in association with an extrinsic 33-kDa polypeptides have been assumed to form the minimal complex of photosynthetic oxygen evolution (Ghanotakis et al., 1987).

In higher plants, two additional extrinsic protein components with apparent molecular masses of 24 and 17 kDa are associated with the oxygen-evolving complex.

The extrinsic 33-kDa protein is much more tightly associated with intrinsic PSII proteins than are the 24 and 17 kDa proteins. Removal of this proteins requires treatment with high concentrations of alkaline-Tris (Yamamoto et al., 1981), $CaCl_2$ (Ono et al., 1983), or NaCl-urea (Miyao and Murata, 1984). Treatment with alkaline-Tris also leads to the loss of the manganese cluster associated with the active site of PSII (Kuwabara and Murata, 1982). This was taken as evidence that the manganese cluster was associated with this extrinsic protein. $CaCl_2$ and NaCl-urea washes, however, efficiently remove the 33 kDa protein without the concomitant loss of the manganese cluster if the protein-depleted PSII preparation is maintained at a high chloride concentration (> 100 mM). At chloride concentrations below 100 mM, two of the four manganese associated with PSII rapidly become paramagnetically uncoupled and then dissociate from PSII membranes (Mavankal et al., 1987). These studies indicate that the extrinsic 33 KDa proteins act as a manganese-stabilizing protein for PSII. Additionally, mutants in the cyanobacterium Synechocystis 6803 which lack the 33 kDa protein cannot

grow autotrophically at reduced calcium concentrations (Phibrick et al., 1991). Biochemical removal of the 33 kDa protein from PSII membranes increases the calcium requirement for oxygen evolution (Bricker, 1992; Boussac and Rutherford, 1988a). These results suggest that the 33 kDa protein also modulates the calcium requirement of PSII. Recent studies have confirmed and extended previous studies (Ono and Inoue 1983; Miayo and Murata, 1984; Kuwabara, 1983; Miyao et al., 1987) which demonstrated that significant rates of oxygen evolution can occur in the absence of manganese-stabilizing protein. The presence of this protein is, however, required for the high rates of oxygen evolution observed in vitro and in isolated PSII preparations. (Bricker, 1992; Burnap and Sherman, 1991).

While this protein obviously is an important component of the oxygen-evolving complex, relatively little is known of its structural organization. Previous studies have demonstrated that the 33 kDa extrinsic protein is associated with CP 47 (Enami et al., 1987, Bricker et al., 1988; Odom and Bricker, 1992) and perhaps other intrinsic components of PSII. Studies examining the stoichiometry of this protein indicate that there are either one (Murata et al., 1983,; Enami et al., 1991; Xu and Bricker, 1992), or two copies present per PSII reaction center. Additionally, the presence of an intramolecular disulfide bridge has been demonstrated (Tanaka and Wada, 1988; Camm et al., 1987).

Because the importance of the 33 kDa protein for PSII efficiency is generally recognized, bacterial expression systems have been designed to allow easy purification, investigation and engineering of this protein (Selder and Michel, 1990). However, the potential of this powerful approach is limited by the absence of a model for 33 kDa protein that would include structure and active sites. Today, not much is known about the 33 kDa protein at the molecular level and few insights provided so far regarding its structure do not allow construction of a testable model. The main elements that have been reported about the 33 kDa protein structure are: its amino acid sequence (about 250 residues) (Borthakur and Haselkorn, 1989) its approximate dimensions, proposed to be similar to a disk of 7 nm diameter and 1.5-3.3 nm thickness; (Haag et al., 1990) and the presence of a disulfur bridge between C28 and C51,

which appears necessary for the binding of the 33 kDa protein to PSII. (Tanaka and Wada, 1988).

An important step towards the establishment of a testable model that will allow identification of the sensitive sites in the 33 kDa protein is an analysis of its amino acid sequence. Previous proposals for 33 kDa protein active sites (Colman and Govinndjee, 1977; Philbrick and Zilinskkas, 1988)) did not take advantage of this source of information. Conserved properties, such as segments hydrophylicity, chain flexibility, and residue exposure propensity, help in locating the potentially active sites. Also, the sequence itself contains structural identification that can be revealed by applying recently developed structure prediction methods. It is now generally recognized that the amino acid sequence holds all the information required for most proteins to achieve proper folding (Fasman, 1991). Although long range interactions cannot be predicted and used to draw tertiary folding, short-range interactions between neighboring residues have allowed successful prediction or matching of the secondary structures of many proteins (Chou and Fasman, 1978; Biou et al., 1988; Kyte and Doolittle, 1982). Successes in modeling natural protein (Crawford et al., 1987) and in *de novo* protein design further supports the potential of secondary structure prediction methods (Beauregard et al., 1991).

Most attempts to predict protein structure have concentrated on predicting the elements of secondary structure, because 90% of the residues in most proteins are involved either in α–helices (38%), β-strands (20%), or reverse turns (32%). If the secondary-structure elements could be predicted accurately, it might be feasible to pack them together to generate the correct folded conformation (Ptitsyn and Finklestein, 1983)

The various amino acid residues do demonstrate conformational preferences. The relative tendencies of the various residues to be involved in α–helices, β-strands, and reverse turns are given by conformational preferences Pα, Pβ and Pτ, respectively. These preferences, however, are only marginal. For example, the most helix-preferring amino acids, Glu, occurs in α–helices only 59% more frequently than random, and even Gly and Pro residues are found in

helices about 40% as often as random, even though they are not stereochemically compatible with the helical conformation.

Fortunately, helices, β-sheets, and reverse turns are not determined by a single residue but by a number of them adjacent in the sequence. A segment of a particular secondary structure is much more probable when several adjacent residues prefer that structure. A number of prediction schemes based on such empirical observations have been proposed. The easiest to use, and the best known, is that of P. Y. Chou and G. D. Fasman(1987), which classifies the amino acids as favoring, breaking, or being indifferent to each type of conformation. An α–helix is predicted if four out of six adjacent residues are helix-favoring and if the average value of P_α is greater than 1.0 and greater than P_β; the helix is extended along the sequence until either Pro or a run of four sequential residues with average value of $P_\alpha < 1.0$ is reached. A β-strand is predicted if three out of five residues are sheet-favoring and if the average value of P_β is greater than 1.04 and greater than P_α; the strand is extended along the sequence until a run of four residues with an average value of $P_\beta<1.0$ is reached. A reverse turn is the likely conformation when sequences of four residues characteristic of reverse turns are found.

A more a priori theory, based on stereochemical considerations of the hydrophobic, hydrophilic, and electrostatic properties of the side chains in terms of the structural rules of folded proteins, was proposed by Lim(1974). Interactions between side chains separated by up to three residues in the sequence are considered in term of their packing in either the helical or β-sheet conformations. For example, a sequence with alternating hydrophobic and hydrophilic side chains is likely to be a strand in β-sheet, in which the orientations of the side chains alternate, with the hydrophilic side exposed to the solvent and hydrophobic side buried in the interior of the protein. A helical segment must have hydrophobic residues every three or four residues to give at least one side of the helix a hydrophobic surface with which to interact with the rest of the protein structure.

Recently the secondary structure of the 33 kDa protein has been investigated by predictions algorithm (Teeter and Whitlow, 1988), far UV-

circular dichroism spectroscopy (Xu et al., 1994), and unconstrained Chou-Fasman analysis. Such studies can reveal some useful results about the substructures of this protein. However the relative insensitivity of these studies to certain 33 kDa protein conformations, such as β-sheet, results in essentially qualitative and quantitative limitations.

Thus we felt that it was necessary to critically re-examine the secondary structure conformation of the 33 kDa protein, due to its importance in the stabilization of the manganese cluster. As an alternative we decided to used FTIR spectroscopy with its resolution-enhancement techniques which has more advantages over the methods that have been used before.

CHAPTER II

INFRARED SPECTROSCOPY

2.1 INTRODUCTION

For many years the structure of biological molecules and the relationship between their structure and their functions have been the subject of intense research.

Progress in understanding how biological membranes function depends to a large extent not only on advances in molecular biology, microbiology, and biochemistry, but also on the development of new biophysical methods. Ideally, such methods should allow the visualization of structures at atomic resolution and the determination of the molecular dynamics of individual groups, especially those involved directly in function. While recent progress in crystallography has demonstrated that high-resolution structures of even complex membrane protein systems can be obtained, the problem of determining the dynamics of membrane proteins at the level of chemical groups remains largely unsolved.

Numerous physical techniques exist for the structural analysis of lipids, peptides and proteins. Of those, X-ray diffraction, nuclear magnetic resonance (NMR) and circular dichroism (CD) spectroscopy have been among the most popular. Each of these techniques provides important information concerning molecular structure, with each technique however having its own particular problems.

When we consider studies of protein structure we know that X-ray diffraction requires the production of relatively large (200 nm) crystals which

are sometimes difficult to obtain. Owing to line broadening effects NMR spectroscopy is limited to the investigation of proteins of molecular weight less than 15 kDa. CD spectroscopy is unable to distinguish between β-sheet and turn structures, and the spectra often contain overlapping contributions from the amino acid side chains (Chang et al., 1978). Problems with light scattering in membrane suspension (Mao and Wallace, 1984) can limit the usefulness of CD spectroscopy. For the study of membrane proteins infrared and Raman spectroscopy do not suffer from problems related to light scattering, molecular size or crystallization. Raman spectroscopy is limited by the poor signal-to noise ratio generally obtained (this problem may be overcome by the recent development of Fourier transform Raman spectroscopy).

FTIR is becoming increasingly popular with experimentalists studying the structure and function of biomolecules (Nabedryk et al., 1982; Olinger et al., 1986), a particular feature of the FTIR for the study of proteins is that high quality spectra can be obtained with relative ease with very small amount, of protein (1 mM) in a variety of environments, such as aqueous solution, lipids, crystals and organic solvents. There are no problems associated with background fluorescence, light scattering or the size of the molecule.

FTIR spectroscopy, unlike fluorescence and Resonance Raman Spectroscopy is not limited to providing information on the chromophores, as it can monitor absorption from all bonds of the biomolecule. Furthermore, FTIR spectroscopy does not rely on the use of additional probe molecules, as is required with some spectroscopic methods.

The ability to measure the infrared spectrum of crystals as well as solutions, intact tissues, or even a single cell (Dong et al., 1989) makes infrared methods particularly well-suited for comparing the structure of a protien in aqueous solution with its structure in a crystal (Potter et al., 1985; Gorga et al., 1989).

2.2 CLASSIFICATION OF INFRARED SPECTRA

Several excellent reviews and book chapters have appeared that include discussion of vibrational spectroscopy of biological membranes (Wallach et al., 1979; Fringeli and Gunthard, 1980; Parker, 1983; Mantsch, 1984; Mendelsohn and Mantsch, 1986). Here we are somewhat narrower in our focus, concentrating mainly on recent IR work aimed at elucidating the structure and dynamics of membrane proteins. We emphasize in particular studies and techniques that can be used to probe changes in the covalent bonded structures and in the local environments of individual groups in membrane proteins. We believe that continued development of these IR-based methods along with high-resolution structural methods will go far toward bridging the gap between the structure and the function of membrane proteins.

The energy of a molecule consists partly of translational energy, partly of rotational energy, partly of vibrational energy, and partly of electronic energy. For a first approximation these contributions can be considered separately. Electronic energy transitions normally give rise to absorption or emission in the ultraviolet and visible regions of electromagnetic spectrum. Pure rotation gives rise to absorption in the microwave region or the far infrared. Molecular vibrations give rise to absorption bands throughout most of the infrared region of the spectrum. In our study we shall mainly be concerned with the interaction of electromagnetic radiation with molecular vibrations. Many chemists refer to the radiation in the vibrational infrared region of the electromagnetic spectrum in terms of a unit called wavenumbers (ν). Wavenumbers are expressed as cm^{-1}, and are easily computed by taking the reciprocal of the wavelength (λ) expressed in centimeters. The relation between the frequency (ν) and wavenumbers are given by the equation :

$$\nu = \frac{1}{\lambda} = \frac{n\nu}{c}$$

where c is the velocity of light in vacuum (2.997925×10^{10} cm/sec), and (c/n) is the velocity of light in medium whose refractive index is n, in which the wave is measured. The refractive index of air is 1.0003. The frequency ν is

independent of the medium and is expressed in cycles per second (sec^{-1}) or Hertz (Hz), and λ is the wave length in cm.

Infrared (IR) radiation is EMR in the wavelength range that is adjacent to and of less energy than visible radiation. The name of the region is derived from the fact that radiation in the region is less (infra) energetic than that of visible red radiation. Almost any compound having covalent bonds, whether organic or inorganic, will be found to absorb various frequencies of electromagnetic radiation in the IR region of the spectrum. The IR spectrum provides a rich array of absorption bands. Many of the absorption bands cannot be assigned accurately; those that can, however, provide a wealth of structural information about a molecule.

IR absorption generally corresponds to change in vibrational and rotational levels in molecules, i. e. to changes in the rate or direction of vibration of a portion of a molecule in relation to the remainder of the molecule or of rotation of the molecule about its center of gravity. In most cases changes in vibrational levels require more energy than changes in rotational levels. The infrared region is divided into three smaller regions according to energetic proximity to the visible spectral region:

1- Near-infrared region extends from the edge of the visible region (0.7 μm or 1400 cm^{-1}) to about 2.8 μm (3600 cm^{-1}). The spectrophotometric apparatus that is used in the near-infrared region most closely resembles that used in the visible region. Some low-energy electron transitions as well as changes in vibrational and rotational levels can occur in near-infrared region. The near-infrared region is generally restricted to the study of compounds that contain OH, NH, and CH groups.

2- Mid-infrared region extends from about 2.8 μm (3600 cm^{-1}) to about 50 μm (200 cm^{-1}). Because changes in vibrational levels of most molecules occur in the mid-infrared region, it is of most use for analysis.

3- Far-infrared region covers the range from 50- μm (200 cm^{-1}) to about 500 μm (20 cm^{-1}). Many purely rotational changes are superimposed upon vibrational

changes. Radiation of less energy than 20 cm^{-1} is classified in the microwave or radiowave region of the spectrum.

2. 3 THEORY OF INFRARED SPECTROSCOPY

A molecule is not a rigid assemblage of atoms. A molecule can be said to resemble a system of balls of varying masses, corresponding to the atoms of a molecule, and springs of varying strengths, corresponding to the chemical bonds of a molecule.

Because most analytical samples are in the liquid or solid state, the analyst is primarily concerned with changes in the vibrational levels. There are two main types of spectroscopic methods based on the vibration of the atoms of the molecule, namely IR and Raman spectroscopy. Raman spectroscopy is sensitive to vibration that modulate bond polarizability. Vibrations that leads to change in the dipole moment of a molecule can be detected and measured using IR spectroscopy. Although Raman scattering is generally weak, its intensity is greatly increased when there is a chromatophoric group within a larger molecule. Resonance Raman spectroscopy is, however, unsuitable for studying the role of the non-chromatophoric components proteins, e. g. most of the amino acid side chains. For studying vibrations of these groups, IR spectroscopy is generally the most sensitive technique.

There are two kinds of fundamental vibrations for molecules: **1-Stretching**, in which the distance between two atoms increases or decreases, but the atoms remain in the same bond axis, Stretching vibrations can be either symmetric or asymmetric. **2-Bending** (or deformation), in which the position of the atom changes relative to the original bond axis., bending vibrations are nuclear motions that cause change in the angle between two vibrating bands, and consequently require a molecule that contains at least three atoms. Bending vibrations are classified as rocking, scissoring, twisting, or wagging depending upon the motion of the two outer nuclei in comparison to the central nucleus.

Infrared absorption occurs when the frequency of the alternating field that is associated with the incident radiation matches a possible change in vibrational frequency of the absorbing molecule. When a match occurs, EMR can be absorbed by molecule causing a change in the amplitude of vibration or a change in the rate of rotation.

The possible number of modes of vibration is 3N-6 for a molecule consisting of N atoms (3N-5 if the molecule is linear). Thus for a biomolecule such as protein there are many vibrations which can result in a complex spectrum. Fortunately, however, many of the vibrations can be localized to specific bonds or groupings, such as the C=O and O-H groups. This has led to the concept of characteristic group frequencies. Typical group frequencies of interest to biochemists include C=O, -COOH, COO-, O-H and S-H. There are many vibrational modes that do not represent a single type of bond oscillation but are strongly coupled to neighboring bonds. For example, the IR spectrum of a protein is characterized by a set of absorption regions known as the amide modes.

In order for electromagnetic radiation to be absorbed by a molecule, it is necessary for the molecule to undergo a change of dipole moment during the absorption. If no change in the distribution of charge in the molecule occurs, the varying charge in the electric component of the radiation has nothing with which to interact and cannot transfer energy to the molecule. Molecules that have a completely symmetrical charge distribution and in which no charge in dipole moment occurs when the molecule vibrates with a different amplitude or rotates at a different rate do not absorb infrared radiation. Substances that are transparent to infrared radiation are primarily monoatomic and homonuclear diatomic gases such as He, Ne, Cl_2, N_2 and O_2. Nearly all other substances absorb radiation in the infrared region.

Additional (nonfundamental) absorption bands may occur because of the presence of overtones (or harmonics) that occur with greatly reduce intensity, as 1/2, 1/3,..... of the wavelength (twice, three times,.... the wave numbers), and difference bands (the difference of two or more different wave numbers).

Some of the various stretching and bending vibrations that can exist within a molecule are shown schematically in Figure 9. Bending vibrations generally require less energy and occur at longer wavelength (lower wavenumber) than stretching vibrations. Stretching vibrations are found to occur in order of bond strengths. The triple bond (absorption at 4.4-5.0 μ, 2300-2000 cm^{-1}) is stronger than the double (absorption at 5.3-6.7 μ, 1900-1500 cm^{-1}), which in turn is stronger than the single bond (C-C, C-N and C-O absorption at 7.7-12.5 μ, 1300-800 cm^{-1}). When a single bond involves the very small proton (C-H, O-H, or N-H), stretching vibrations occur at much higher frequency (2.7-3.8 μ, 3700-2630 cm^{-1}). The O-H bond absorbs near 2.8 μ (3570 cm^{-1}) and the O-D bond absorbs near 3.8 μ (2630 cm^{-1}); in this case the strengths of the bonds are nearly the same but the mass of one atom is doubled. The way these are spread out over the vibrational infrared is illustrated schematically in Figure 10.

An approximate value for the stretching frequency (ν), in cm^{-1} of a bond is related to the masses of the two atoms (m_1 and m_2, in grams), the velocity of light (c), and the force constant of the bond (k, in dyne/cm) :

$$\nu = \frac{1}{2\pi c}\sqrt{\frac{k}{\mu}}$$

which is derived from Hooke's law for vibrating springs. The term μ, or reduced mass of the system, is given by

$$\mu = \frac{m_1 m_2}{m_1 + m_2}$$

single, double, and triple bonds have force constants (k) that are approximately 5, 10, and 15 x 10^5 dynes/cm, respectively.

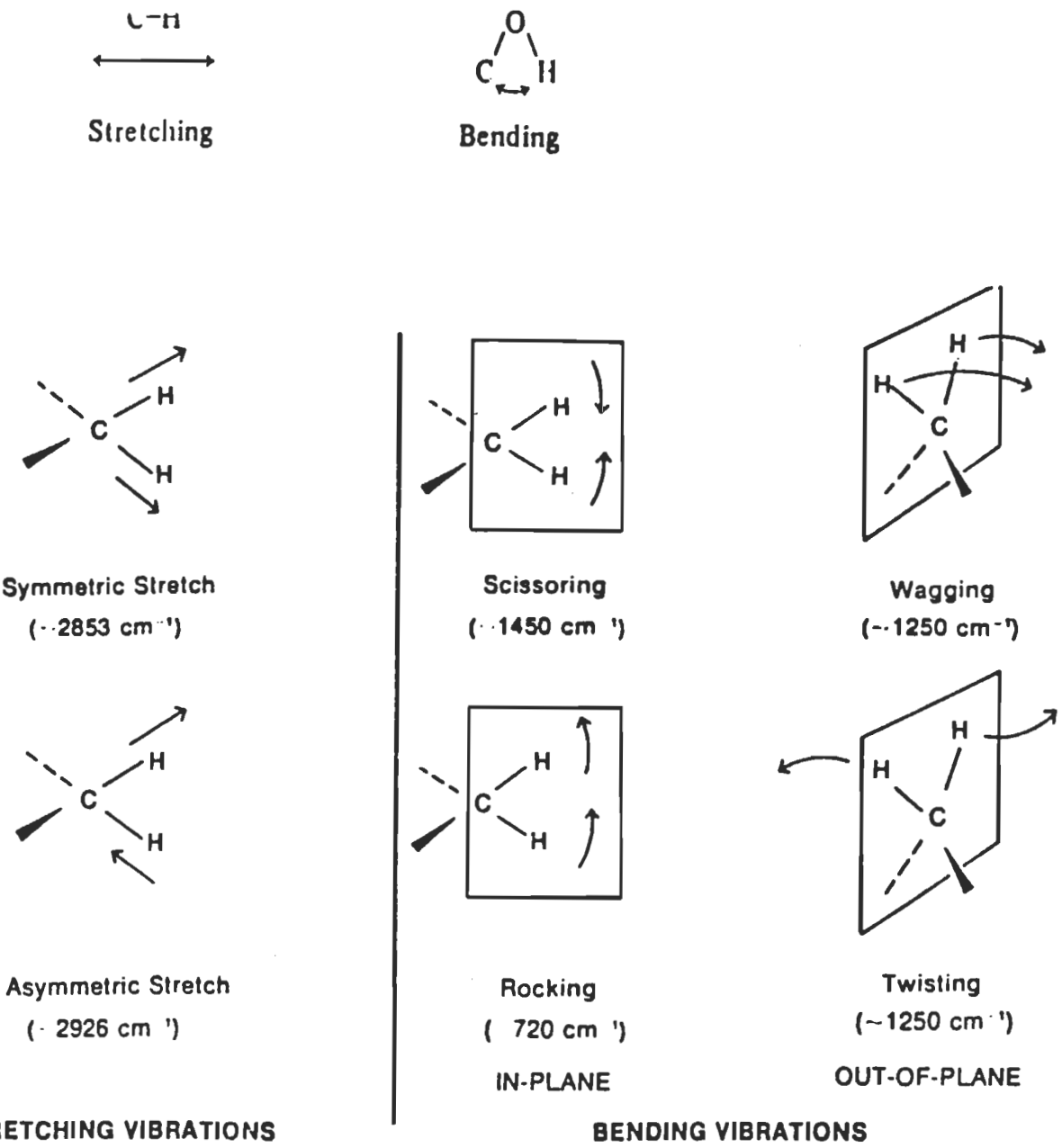

Figure 9. Various stretching and bending vibrations that can exist within a molecule.

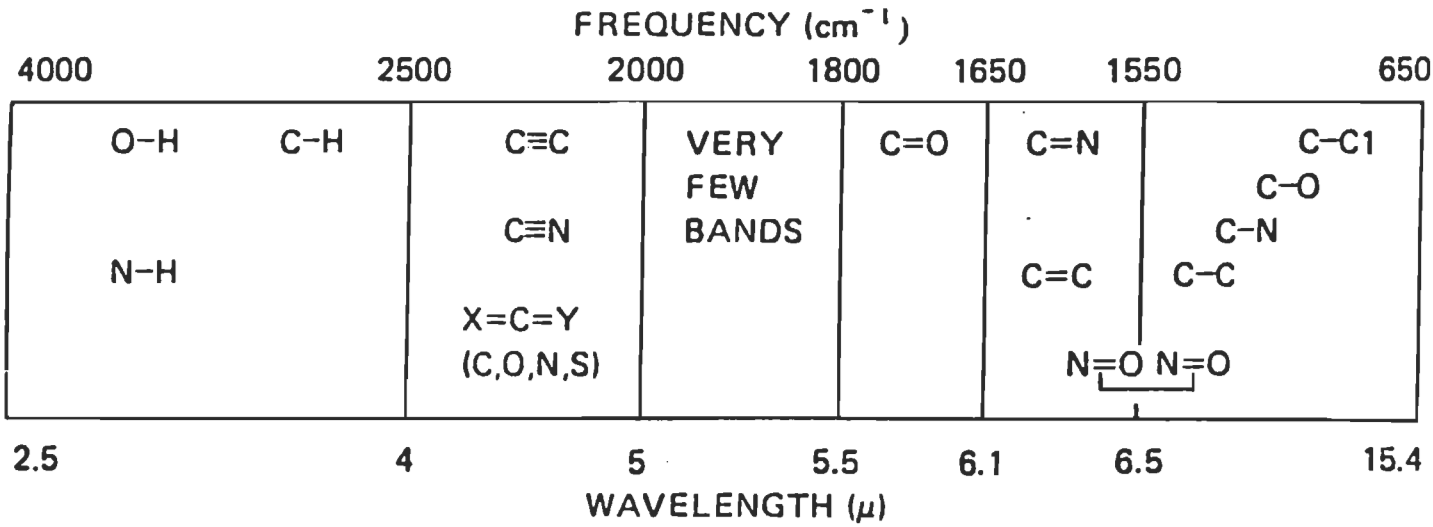

Figure 10 : The approximate regions where various common types of bonds absorb (stretching vibrations only; twisting, and other types of bond vibrations have been omitted for clarity).

2. 4 FTIR INSTRUMENTATION AND COMPUTATION METHODS

All IR spectrometers include a broad band source (usually an incandescent ceramic material), optic for collimating the IR light and directing it through a sample, an IR detector, and some means for analyzing the wavelength dependence of the transmitted light. In conventional dispersive spectrometers, this last function is accomplished by spreading the light spatially with a diffraction grating and selecting individual spectral elements with a narrow slit; thus only a narrow range of wavelengths reaches the sample and detector at any time. Collection of a spectrum covering a broad wavelength range requires sequential scanning over different spectral elements.

In general, a more efficient approach is to detect the signals from different wavelengths simultaneously. In the case of visible and near-UV dispersive spectrometers, this can be accomplished by using multichannel area detectors. However, such detectors are not available with useful sensitivity through the IR region of general interest for vibrational spectroscopy (400-4000 cm^{-1}). This has been overcome by using (Fourier transform infrared) FTIR techniques.

The alternative approach employed in FTIR spectrometers is to pass the broad band IR beam through an interferometer such as the Michleson interferometer before sending it through the sample and then to a single very sensitive detector. This is achieved by directing a polychromatic beam onto a beam splitter which directs the beam onto two mirrors, at right angle to each other. One of these mirrors moves in direction perpendicular to its axis, such that when the beams recombine at the beam splitter, a path length difference is introduced which results in interference. The recombined beam is directed through the sample and onto the detector. The detector output as a function of mirror retardation produces on interferogram which is the sum of the sine waves for all frequencies present, Fourier transformation of the interferogram produces the spectrum.

The Michelson interferometer (Figure 11) functions in the following manner. Radiation from the source is emitted and directed toward a beam splitter. Half of the radiation is reflected by the beam splitter to a mirror that

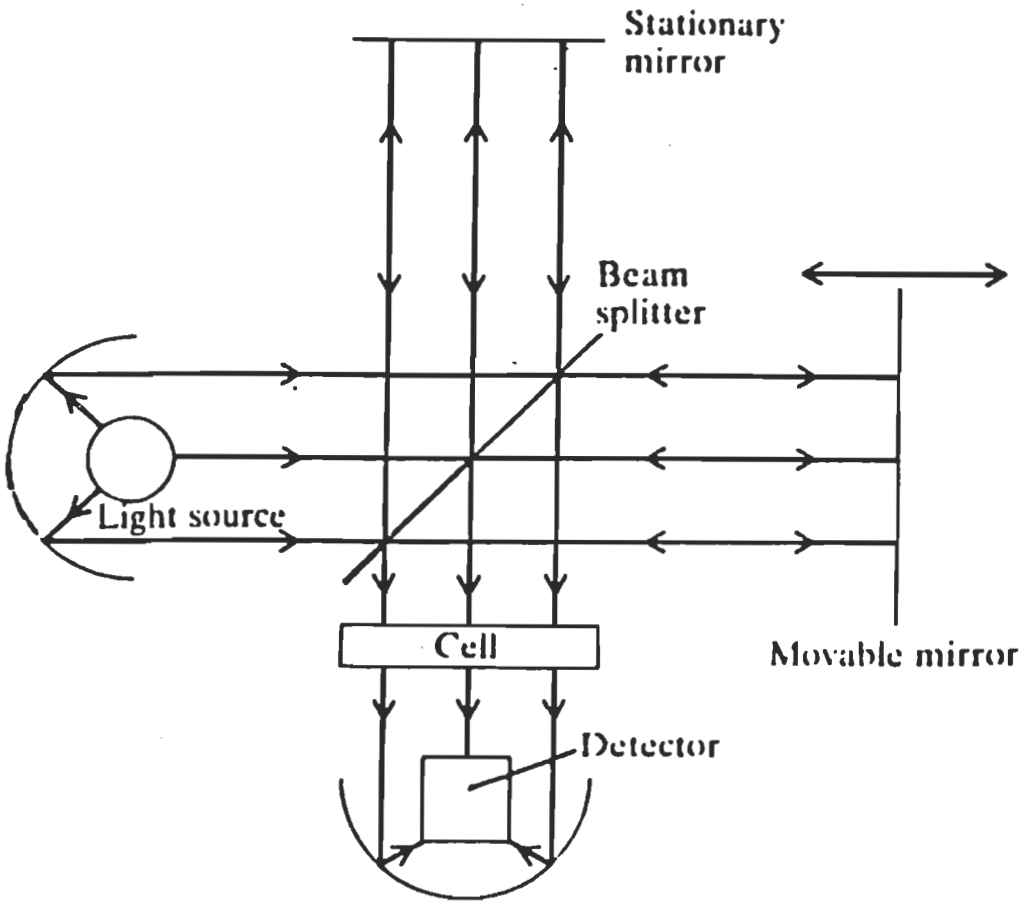

Figure 11 : An optical diagram of a Michelson interferometer as used for Fourier transform spectrophotometry. The arrows indicate the direction of radiative travel and the direction of mirror motion.

reflects the radiation back toward the beam splitter. The remaining portion of the radiation passes through the beam splitter and strikes a mirror that is continuously moved back and forth over a distance of as much as 21 cm. After striking the movable mirror, the radiation is reflected back to the beam splitter. A portion of the radiation that was reflected from the stationary mirror and a portion of the radiation from the movable mirror combine at the beam splitter and pass through the cell. After passage through the cell the radiation is focused on the detector.

If the round-trip distance through which the radiation travels between the beam splitter and the stationary mirror is identical to the round-trip distance between the beam splitter and the movable mirror, the radiation from the two mirrors arrives in-phase at the beam splitter, the cell, and the detector As the movable mirror changes positions, however, the distances between the mirrors and the beam splitter are no longer identical and radiation of a fixed wavelength will only arrive in-phase at the cell and detector when the round-trip distance between the movable mirror and the beam splitter is equal to the round-trip distance between the stationary mirrors and the beam splitter plus or minus a whole-number multiple of the wavelength of the radiation. If the movable mirror moves away from the equidistant point by a factor of $\lambda/4$, the round-trip distance is altered by $\lambda/2$ and the reflected radiation is out-of-phase with that from the stationary mirror and destructively interferes. If the movable mirror is $\lambda/2$ from the equidistant point, the radiation is in-phase with that from the stationary mirror and constructively interferes. As the distance changes, different wavelengths of radiation become in-phase and out-of-phase at a frequency that is dependent upon both the wavelength of the incident radiation and the rate at which the mirror moves. By controlling the rate of mirror motion, a series of simultaneous signals that oscillate at frequencies that are directly proportional to the frequencies of the electromagnetic radiation arrive at the detector, and oscillate sufficiently slowly for the detector to measure. The detector simultaneously measured all of the frequencies that pass through the cell and routes the information to the computer which decodes the information using a mathematical method called Fourier transform. The decoded spectrum is directed to the readout device.

Fourier transform infrared spectrophotometery is particularly useful in those circumstances where spectra of low-concentration sample are required and in those cases where a spectrum must be obtained rapidly. FTIR spectrophotometers can be used as detectors for chromatography.

The advent of micro-computer controlled spectrometry and the development of the Fourier transform data collection and manipulation methods associated with FTIR spectroscopy have greatly increased the areas of application of the technique. Mathematical procedures are now available that can separate individual sub-components that strongly overlap in the spectra of biomolecules. The most commonly used methods for this purpose are Fourier self-deconvolution and derivative spectroscopy. These procedures are sometimes referred to as resolution-enhancement techniques. These techniques do not increase the instrumental resolution, but increase the extent to which the individual component bands can be separated. Both the derivative and deconvolution procedures involve a band-narrowing process that results in the separation of the overlapping components. They provide a means for observing changes in the frequency and intensity of bands in the spectra of proteins.

2. 6. RESOLUTION ENHANCEMENT OF FTIR SPECTRA.

In the past, practical usefulness of the IR method was, however, severely limited by such factors as low sensitivity of the infrared measurements, interfering absorption from the surrounding media or solvents and, most importantly, by difficulties in extracting the structural information contained in the conformation-sensitive infrared bands. The first two obstacles have been largely overcome by the development of computerized FTIR instrumentation; this has improved the signal-to-noise ratio and also allows extensive data manipulation. The third difficulty appears to be of a more fundamental nature. It reflects the fact that the conformation-sensitive amide bands of proteins are composites which consist of overlapping component-bands originating from different structures, such as α–helices, β-strands, turns and non-ordered polypeptide fragments (Miyazawa and Blout, 1961; Byler and Susi, 1986). Due to the inherently large widths of these overlapping

component bands (greater than the separation between peak maxima), they cannot be resolved and/or identified in the broad contours of experimentally measured spectra. Thus, until recently the infrared estimates of protein secondary structure were deduced from global shape of the composite bands; the information, thus, obtained was only qualitative and often of questionable value. Various attempts to obtain semi-quantitative estimates of protein conformation from infrared spectra were based on different types of optimization analysis of the overlapping bands (Chiragadze et al., 1973), however, such an approach is limited and not fully reliable as it requires numerous input parameters which are generally not available.

A significant step forward in the infrared spectroscopic analysis of proteins was made recently by developing computational procedures for the resolution enhancement of broad infrared bands. These band-narrowing methods allow the decomposition of the complex amide bands into their underlying components. This new methodology not only enriches the qualitative interpretation of infrared spectra, but also provides a basis for the quantitative estimation of protein secondary structure. The most practically used methods for this purpose are Second-derivative and Fourier-self deconvolution (Susi and Byler, 1986; Braiman and Rothschild, 1988; Jachson and Chapman, 1989). The combination of resolution enhancement methods with the judicious application of curve-fitting techniques can reveal a wealth of information concerning the secondary structure of proteins (Byler and Susi, 1981; Lee and Chapman, 1986; Surewicz and Mantsch, 1986).

2. 6. 1 Second-Derivative

This method involves calculating (Susi and Byler, 1983; Lee et al., 1985; Dong et al., 1990) the second derivative S(**v**) of the absorbance spectrum A (**v**), i.e. $S(\mathbf{v}) = A^n(\mathbf{v})$. Taking the second derivative of overlapping lorentzian bands produces sharpened peaks that have half-widths only 37% as large as those of the parent bands. In addition, the intensity of each second-derivative band is increased in inverse proportion to the half-width of the original band. Thus, narrower bands are highlighted in the second-derivative spectrum.

Recently developed techniques permit the determination of the relative amounts of different types of secondary structure.

2. 6. 2 Fourier-Self-Deconvolution

This method was introduced several years ago (Kauppinen et al., 1981) and several reports on its application to protein and biomembrane IR spectra have now appeared. It can generally be implemented quite easily on an FTIR spectrometer, since it can make use of the Fourier transform programs that are employed to compute the spectrum from an interferogram (Earnest et al., 1987; Olinger et al., 1986; Susi and Byler, 1986).

The basis for Fourier self-deconvolution is that the Fourier transform of a pure Lorentzian function

$$E(\underline{\nu}) = \sigma/\pi \ [\sigma^2 + (\underline{\nu} - \underline{\nu}_o)]$$

is a damped cosine function

$$I(x) = [\exp(-2\pi\sigma 1 x 1 2\cos(2\pi\underline{\nu}_o x)]$$

in these equations σ represents the Lorentzian half-width at half-maximum and ν_o is the center frequency of the peak. If the damped cosine function in the second equation above is multiplied by exp ($2\pi\sigma|x|$) and an inverse Fourier transformation is then carried out, a Lorentzian function with zero half-width (i.e. a σ-function) results. In practice, such a perfect deconvolution is not achievable owing to several factors, including the finite resolution of the spectrometer, the deviation of real band shapes from the assumed Lorentzian shape, and the inequality of damping factors (intrinsic linewidths) for subcomponent bands.

2. 6, 3 Difference Spectroscopy

Another useful technique for detection of small and subtle changes in protein structure is difference spectroscopy. This technique has been the first and the most widespread application, and has been used from the early 1980s for probing structural differences between a protein's various conformational states (Rothschild et al., 1981; Bagley et al., 1982; Engelhard et al., 1985), photoreactive proteins like the visual pigments rhodopsin and bacterial retinal proteins (Siebert et al., 1981; Rothschild et al., 1981; Siebert et al., 1983; Siebert et

al., 1983) and the photosynthetic reaction centers (RC) from plants and bacteria (Mantele, 1993)

The principle of difference spectroscopy involves the subtraction of a protein absorbance spectrum in state A from that of the protein in state B. Thus for example, the spectrum of sample is obtained before and after being triggered by a particular agent, such as light, and then the two spectra are subtracted. This reduces the complexity of interpreting the conformational change that is induced by the trigger. The difference spectrum reflects those groups that undergo a specific change in their structure or their environment. Assignment of the peaks in the difference spectra has been achieved by use of chemical and isotopic modifications. This approach is a powerful one, as the background absorbance due to functional groups that are not involved in the change are subtracted out.

2. 7 ASSIGNMENT OF PROTEIN IR SPECTRA

In infrared spectra the amide bands that arise from the vibration of the peptide groups provide information on the secondary structure of polypeptides and proteins. Analysis of the peptide group vibration in model compounds and in polypeptide systems allows assignments of these characteristic bands. Changes in the hydrogen bonding involved in the peptide linkages results in changes in the vibrational frequency of the different amide modes.

The amide groups of polypeptides and proteins possess nine characteristic vibrational modes or group frequencies. Of these, the one most useful for an infrared spectroscopic analysis of the secondary structure of proteins in aqueous media is the so-called amide I band. Amide I bands are sensitive to the nature of the secondary structure as this involves specific hydrogen bonding of the C=O and N-H groups (Susi et al., 1967, Susi, 1969, Parker 1983). Attempts were also made to utilize other vibrational modes, particularly the amide II and amide III bands. However, the sensitivity of the amide III mode to the polypeptide backbone conformation is still not well established. The amide II mode, on the other hand, although sensitive to the

secondary structure, gives rise only to a very weak infrared band. Due to different selection rules, the amide III band is much stronger in the corresponding Raman spectra, and it is the latter technique that seems better suited for the analysis of this vibrational mode. The amide I band arises principally from C=O stretching vibration of the peptide group. The amide II band is primarily N-H binding with a contribution from C-N stretching vibrations. The amide III absorption is normally very weak in the IR, arising primarily from N-H binding and C-N stretching vibrations. Most infrared studies of protein conformation focus on absorption in the amide I region 1700-1600 cm^{-1} (Table 2) which arises primarily from stretching vibrations of the backbone C=O groups.

Table 2 Band Assignments For Various Protein Secondary Structure In Amide I Region (1700-1600 Cm^{-1}).

Band position (cm^{-1})	Assignments
1630-1640	β-sheet
1644	random
1650-1655	α-helix
1670-1680	turns
1680-1690	β-sheet

CHAPTER III

MATERIALS AND METHODS

3. 1 FTIR-INSTRUMENTATION

The infrared spectra were recorded at ambient temperature using a Bomem DA3-0.02 Fourier-transform spectrometer instrument equipped, with a liquid-nitrogen-cooled mercury/cadmium/telluride (HgCdTe) detector, KBr beam splitter, and Globar source (Ste. Foy, Quebec, Canada). The spectra were taken with resolution 2 to 4 cm^{-1} on suspended aqueous solution and thin films, using BaF_2 windows.

Spectra were digitized on and then transferred on a 386-based personal computer equipped with Spectra Calc. Algorithm (Galstic Industries Corp., Salem, NH) Software.

3. 2 EXTRACTION OF PSII MEMBRANES

PSII Particles (BBY) were isolated according to (Berthold et al., 1981) with some modifications (Rashid and Carpentier, 1989). Spinach leaves were obtained from local market. Washed leaves (100 g) were ground quickly in a blender for 10 s in 300 ml of an ice cooled buffer medium comprising 50 mM Tricine/NaOH (pH 7.6), 10 mM NaCl, 5 mM $MgCl_2$, O.4 M sorbitol, 6 mM ascorbate and 1 mM PMSF. The slurry was squeezed through four layers of gauze and then filtered through eight layers of gauze containing two layers of cotton wool. The chloroplasts were isolated by centrifugation of the filtrate at 4000 rpm for 7-8 min.

The chloroplast pellet was suspended in 200 ml buffer containing 50 mM Tricine/NaOH (pH 7.6), 10 mM NaCl, 5 mM $MgCl_2$ and 0.1% ascorbate, using a Wheaton homogenizer. The suspension was allowed to stand for 1 min and then centrifuged at 4000 rpm for 7-8 min and the resulting pellet is the broken chloroplast (thylakoid membranes).

The thylakoid membranes were incubated in 20 mM Mes-NaOH (pH 6.2), 15 mM NaCl, 10 mM $MgCl_2$ and 4% Triton X-100 with a Chl concentration of 1 mg/ml. After an incubation of 20 min in the dark on ice. The unsolubilized membranes were precipitated by centrifugation at 5000 rpm for 10 min. The supernatant was carefully removed and centrifuged at 17500 rpm for 30 min. The PSII enriched fraction (PSII membranes) obtained as a pellet were finally suspended in a solution containing 20 mM Mes-NaOH (pH 6.2), 15 mM NaCl, and 10 mM $MgCl_2$ at a Chl concentration of 1 mg/ml. The PSII membranes were stored in liquid nitrogen and slowly thawed just before experiments.

3.3 CHLOROPHYLL CONCENTRATION MEASUREMENT

The concentration of Chl were determined in 80% acetone using the procedure of Arnon (1949) as follow:
In a tube containing 5 ml of acetone 80%, an amount of PSII membranes extract (10 µl) was added, the mixture was stirred for 1 min, followed by centrifugation for 2 min at 6000 rpm. The absorbance was measured at 663 nm and 645 nm using a spectrophotometer. The calculation of the total amount of chlorophyll was carried out using the following equations:

$$\text{Chl } \underline{a} = 12.7 \times A_{663} - 2.9 \times A_{645} = \text{mg/l}$$

$$\text{Chl } \underline{b} = 22.9 \times A_{645} - 4.68 \times A_{663} = \text{mg/l}$$

$$\text{Chl total} = \text{Chl } \underline{a} + \text{Chl } \underline{b}$$

this procedure was repeated three times, and the amount of Chl was calculated by taking the average of the three measurements .

3.4 MEASUREMENT OF OXYGEN EVOLUTION

The rate of oxygen evolution was measured using a Clark-type electrode in a 3 ml cell kept at 20 °C by a circulating water bath (Allakhverdiev et al., 1993). The sample was illuminated by red light (KC 11 filter) passing through a heat filter consisting of 5% $CuSO_4$ solution, the light intensity at the cell surface was 100 W m^{-2}. The reaction mixture contained 50 mM HEPES-NaOH (pH 6.5), 10 mM NaCl, 5 mM $CaCl_2$, 0.2 mM phenyl-p-benzoquinone, 0.3 mM potassium ferricyanide as electron acceptor, and Chl at a concentration of 20µg/ml.

3.5 Mn-EXTRACTION

The complete (>95%) extraction of Mn from PSII membranes was reached as described in Klimov et al., (1982). PSII membranes particles at 50µg Chl/ml were incubated for 1 h at 2 °C in a medium containing 1 M Tris-HCl (pH 8.0) and 0.5 M $MgCl_2$. Then the PSII membranes particles were precipitated at 2000 xg. The pellet was washed twice by resuspention at 10 mg Chl/ml followed by centrifugation, first in 0.8 M Tris-HCl (pH 8.0) and then in 20 mM Tris-HCl (pH 8.0), 35 mM NaCl, and 1 mM EDTA. The depleted PSII particles were finally suspended in medium consisting of 20 mM Mes-NaOH (pH 6.2), 15 mM NaCl, and 10 mM $MgCl_2$ at a Chl concentration of 1 mg/ml. Finally the Mn-depleted PSII preparations were stored in liquid nitrogen and slowly thawed just before experiments.

3.6 PREPARATION OF LHCII

The LHC-II was purified from PSII membrane as reported in Burke et al., (1978). PSII-enriched membranes were washed in 100 mM sucrose, 5 mM EDTA, 20 mM Tricine-NaOH buffer pH 8.0, recovered by centrifugation at 100,000 X g for 1 h at 4 °C and resuspended in distilled water to a Chl concentration of 0.5 mg/ml. Triton X-100 was added to 0.1:5.0 w/v and the mixture incubated at room temperature for 30 min. Unsolubilized material was removed by centrifugation at 40,000 X g for 30 min and the supernatant cooled on ice prior to loading onto 0.05-0.5 M continuous sucrose gradients.

The gradients were centrifuged at 100,000 X g for 15 h at 4 °C in a Beckman Sw28 rotor. The highly fluorescent band containing LHCII was subsequently purified from this fraction by precipitation in the presence of 100 mM KCl and 10 mM $MgCl_2$, the pellet was suspended in a solution containing 20 mM Mes-NaOH (pH 6.2), 15 mM NaCl, and 10 mM $MgCl_2$ at Chl concentration 1 mg/ml, then were stored in liquid nitrogen and slowly thawed just before experiments.

Metal ion stock solutions : a metal chloride stock solutions of all metals used for this study, were prepared at a concentration of 25 mM in water, then the desire concentrations were prepared by consecutive dilutions.

3.7 FTIR SPECTRA OF LHC II

Samples for FTIR measurements were prepared from LHCII, by drying, the equivalent of 50 µg Chl (for each sample) on BaF_2 windows for 20-30 min under light stream of dry nitrogen. The samples contained different concentrations of metal ions. Five different concentrations 0.01, 0.1, 1.0, 10.0 and 20 mM for all metal ions were used in this study. A standard sample was prepared by drying an amount of LHCII which is equivalent to 50 µg Chl on a BaF_2 window under a light stream of dry nitrogen for 20-30 min, no metal ion was added in this measurement. This sample was used as standard for calculating difference spectra. The difference was taken by subtraction of spectra of LHCII (standard) from that of LHCII + Metal.

A good subtraction was obtained by a flat baseline around 2200 cm^{-1} caused by the cancellation of the water combination mode (1600 + 600 cm^{-1}) (Dousseau et al., 1989). The difference spectra ((LHC + metal ion)-(LHC)) were reproduced, using the CH stretching bands at 2900 cm^{-1} as internal and the Triton-X100 band at 1280 cm^{-1} as external references. These vibrations exhibited no spectral changes on protein complex formation under the treatment of LHC II with metal ion, and they were canceled upon subtraction.

The subtraction of water was carried out as reported (Dousseau et al., 1989). Proper subtraction of water was judged to yield an approximately flat baseline from 1900 to 1720 cm^{-1} avoiding negative wide lobes. A good

subtraction was obtained by a flat baseline around 2200 cm^{-1} caused by the cancellation of the water combination mode (1600 + 600 cm^{-1}).

3. 8 LIGHT-MINUS DARK FTIR SPECTRA OF P680$^+$

Mn-depleted PSII particles were treated with 500 µM potassium ferricyanide and 10 µM silicomolybdate at a Chl concentration of 1 mg/ml. From this reaction mixture, 50 µl (which is equal to 50 µg of chlorophyll) were deposited on a BaF_2 window. The sample was dried under a light stream of dry nitrogen for 20-30 min.

The FTIR spectra were recorded at 20 °C before and during illumination (100 W m^{-2}) by a fiber optic guide connected to an Oriel model 77501 Fiber Optic Illuminator equipped with a heat filter and a red filter (600 nm). The resulting spectra were analyzed using difference spectra technique. The difference was determined by subtracting the spectra before illumination from that during illumination (Light-minus-dark spectra).

The difference light-minus-dark spectra were calculated using the C-H stretching bands around 2900 cm^{-1} as internal standard. The precision of the method of subtraction was tested using different Mn-depleted samples before and during illumination under the same experimental conditions. The difference spectra obtained showed a flat baseline for the C-H stretching vibrations around 2900 cm^{-1}.

3.9 PSII INCUBATION WITH BETAINE AND SUCROSE

3. 9 . 1 Heat Treatment

For heat treatment, a set of three samples (1 ml total volume each sample) that contained PSII-membranes at Chl concentration 1mg/ml were prepared. 1 M glycinebetaine and 1 M sucrose were added to the first and second sample respectively. Each set of three samples were incubated simultaneously for 5 min at the temperature under investigation (20, 40, 60 or 70 °C) using a water bath. After incubation the treated sample were dialysed for 3 h against several changes of 5 mM Mes-NaOH (pH 6.0). The treated samples were collected after dialysis and kept at 4 °C for FTIR measurement.

3. 9. 2 FTIR Measurements

Aliquots from the heat incubated PSII-betaine and PSII-sucrose samples equivalent to 50 μg Chl, after heat treatment (as described previously) at different temperatures were deposited on BaF_2 windows, then dried under a light stream of dry nitrogen for about 30 min. FTIR spectra were recorded for each sample. These experiments were repeated three times and the average of three measurements along with the standard deviation were calculated.

The protein secondary structure was analyzed from the shape of the amide I band (Byler and Susi, 1986). Fourier self-deconvolution and second derivative resolution enhancement as well as curve-fitting procedures were applied, so as to increase the spectral resolution in the region of 1700-1800 cm^{-1}. The self-deconvolution was performed by using a Lorentzian line shape for the deconvolution and a Gaussian line shape for apodization (Kauppinen et al., 1987). In order to quantify the area of the different components of the amide I band revealed by self-deconvolution, a least-square iterative curve-fitting was used to fit the Lorentzian line shapes to the spectrum between 1700-1600 cm^{-1}. Before curve-fitting was done, a straight baseline passing through the ordinates at 1700 and 1600 cm^{-1} was subtracted. The baseline was modified by the least-square curve-fitting, which allowed the horizontal baseline to be adjusted as an additional parameter to obtain the best fit. It is known that no meaningful curve-fitting can be performed by simple examination of the original infrared spectra, that is why the self-deconvolution procedure has to be carried out first. The resolution enhancement that results from the self-deconvolution is such that the number and the position of the bands to be fitted is determined (Byler and Susi, 1986; Kauppinen et al., 1987; Surewicz et al., 1987; He et al., 1991). A first curve-fitting was done on a spectra deconvoluted with K= 1.5-2.5. The initial input parameters of the curve-fitting were set as follow: (a) the frequency was adjusted manually by moving the cursor on the monitor screen of the computer; (b) the intensity were calculated to be two-thirds of the spectrum intensity at the frequency chosen and the full width at half-height was used to the extent of deconvolution applied. None of the input parameters were kept constant during the curve-fitting procedure.

In the second stage, the same set of initial input parameters, but with widened full width at half-height were used to fit the undeconvoluted original spectrum for a new curve-fitting, in order to obtain results free of any possible artifact introduced by the deconvolution procedure, in the integrated intensities. This is very important for dichroic ratio measurement. The resulting curve-fitted was analyzed as follows: Each Lorentzian band was assigned to a secondary structure according to the frequency of its maximum: α-helix (1647-1660 cm^{-1}); β-sheet (1615-1640 cm^{-1}); turn (1660-1680 cm^{-1}); random (1641-1646 cm^{-1}) an β-antiparallel (1681-1692 cm^{-1}). The area of all the component bands assigned to a given conformation were then summed and divided by the total area. The number obtained was taken as the proportion of the polypeptides chain in that conformation. These assignments are according to previous values determined theoretically (Krimm and Bandeker, 1986) and experimentally (Byler and Susi, 1986). The accuracy of this method was tested on several proteins of known secondary structures, such as Cyt c (α-helix 49%) and bacteriorhodopsin (α-helix 63%), which resulted in error of ± 3-5 % (Goormaghtigh et al., 1990).

The intrinsically overlapped amide I band contour was subjected to resolution enhancement using a second-derivative calculation. The secondary structure composition was determined by second derivative/curve-fitting analysis using Spectra Calc Software (Galactic, Industries Co., Salem, NH, U. S. A) on a 386-based personal computer. The inverted second-derivative spectra were obtained by factoring by -1 and were fitted with Gaussian band profiles.

Initial band positions were taken directly from the second derivative spectra, and no additional band was added unless clearly resolved. During the curve-fitting process, the heights, widths, and positions of all bands were varied simultaneously. After this iterative process was completed, the relative integrated intensity of each band was then calculated from the final fitted band heights and widths; areas of the peaks from 1700 to 1600 cm^{-1} were determined and expressed as a percentage of the total peak area in this range.

3.10 PURIFICATION OF 33 kDa MANGANESE-STABILIZING PROTEIN.

Fresh preparation of PSII membranes were washed three times in a buffer containing 10 mM NaCl, 300 mM sucrose and 25 mM Mes-NaOH (pH 6.5) by centrifugation at 36 000 x g at 4 °C for 10 min, and resuspended in the same medium. The 33 kDa was isolated according to (Xu and Bricker, 1992) with some modifications. To remove the extrinsic 16 and 24 kDa polypeptides, PSII membranes were incubated in 1.0 M NaCl, 50 mM Mes-NaOH (pH 6.0), 10 mM $MgCl_2$, and 300 mM sucrose at a Chl concentration of 1 mg/ml for 1 h on ice and in the dark. The suspension was then centrifuged at 36 000 x g for 30 min. The pellet was resuspended in the same solution and centrifuged at 36 000 x g for 20 min to remove any remaining loosely bound 16 and 24 kDa proteins.

The NaCl-treated PSII membranes was incubated with 1.0 M $CaCl_2$, 50 mM Mes-NaOH (pH 6.0), 15 mM NaCl, 10 mM $MgCl_2$ and 300 mM sucrose at a Chl concentration of 1 mg/ml for 30 min, on ice, and in the dark. The suspension was centrifuged at 36 000 x g for 30 min. The supernatant which contained the 33 kDa extrinsic protein was concentrated using an ultrafiltration device (Amicon PM10 Diaflo membrane). The solution of 33 kDa protein was then dialyzed for 3 h against several changes of 5 mM Mes-NaOH (pH 6.0) at 4 °C and centrifuged to remove a pale green precipitate. The total period of dialysis was as short as 16 h in order to minimize proteolytic breakdown of protein. The 33 kDa protein solution was collected and kept at 4 °C for the other measurements.

3.10.1 DETERMINATION OF PROTEIN CONCENTRATION

The Bradford Assay, a rapid and reliable dye-based assay for determining protein content in solution, was used here to determine the concentration of 33 kDa protein. This assay is sometimes referred to as the Bio-Rad assay after the company which sells the widely used protein determination kit. (Bradford, 1976).

3.10.2 SDS-PAGE ELECTROPHORESIS OF THE 33 kDa PROTEIN

Protein composition was analyzed by SDS-polyacrylamide gel electrophoresis (SDS-PAGE) using the buffer system of (Laemmli, 1970). Electrophoresis was performed in miniature slab gels (Hoefer Scientific Instrument) containing 15% acrylamide in the linear slab gel mode at room temperature. The gels were stained with coomassie brilliant blue R-250 and scanned with an LKB Ultro Scan XL laser densitometer. The following solution were used when performing SDS-PAGE:

a)-Resolving solution

For resolving the gel we used 50 ml of solution containing : 25 ml acrylamide 30%, 11.7 ml distilled water, 12.5 ml Tris, 500 µl SDS 10%, 300 µl ammonium persulphate, and 25 µl TEMED.

b)-Stacking solution

5 ml of the staking gel consists of: 0.670 ml acrylamide 30%, 3.0 ml distilled water, 1.25 ml Tris, 50 µl SDS 10%, 25 µl ammonium persulphate (100 mg/ml water) and 4 µl TEMED.

c)-Sample buffer:

Before depositing on the gel the sample was treated in a solution containing: 2.5 ml Tris (pH 6.8), 4.0 ml SDS 10%, 2.0 ml glycerol, 1.0 ml 2-mercapethanol, and 0.5 ml distilled water

d)-Electrophoresis buffer

The running buffer solution consists of 25 mM Tris, 192 mM glycine and 0.1% SDS.

e)-Staining buffer

Gels were stained with a buffer consisting of 0.04% (w/v) coomassie brilliant blue R-250 (Bio-Rad) in 50% (v/v) methanol and 10% (v/v) acetic acid for 3h.

f)-Destaining buffer

Gels were destained first in a solution of 50 (v/v) methanol and 10 % (v/v) acetic acid for 1 h. The second, destain was in a solution of 0.05% methanol and 0.07 glacial acetic acid for 12 h.

The amount of the 33 kDa protein deposited on the gel was about 15 µg and 10 µg in two different wells. For PSII-membranes it was the amount equal to 7 µg Chl. A protein kit (phosphorylase b, 94 kDa; albumin, 67 kDa; ovalbumin, 43 kDa; carbonic anhydrase, 30 kDa; a-lactoalbumin, 14 kDa) purchased from Sigma Chemical Co. was used as a standard.

Quantification of the amount of 33 kDa protein on the gel was accomplished by scanning the stained 33 kDa protein band on the polyacrylamide gel and the relative abundance of proteins was estimated from the peak area of the densitogram.

3. 10. 3 FTIR SPECTRA ANALYSIS OF 33 kDa PROTEIN

50 µl aliquots of 33-KDa solution (equivalent to 385 µg protein/ml) were deposited on BaF_2 windows, then dried under a light stream of dry nitrogen for about 20 min. FTIR spectra were recorded with a resolution of 2 to 1 cm^{-1} and 100 to 500 scans and treated as in section 3. 9. 2. These experiments were repeated three times and the amount of 33 kDa secondary structures along with the standard deviation were calculated.

CHAPTER IV

RESULTS AND DISCUSSION

4.1 BINDING OF METAL IONS WITH LHCII

In the course of interacting Cd, Hg, Pb, Cu, Zn, Mg, Ca and Mn with LHCII, we obtained the FTIR spectrum of LHCII without and with metal ion for each metal.

The infrared spectrum of uncomplexed LHCII-proteins (without metal ion) showed a broad and unresolved absorption band centered at 3300 cm^{-1} related to the amide A (N-H stretching vibrations) and three other absorption bands with medium intensities at 2946, 2927, and 2870 cm^{-1} (Figure 12), which are assigned to the protein symmetric and antisymmetric C-H stretching frequencies (Nabedryk et al., 1984). The protein amide I (C=O stretching) was observed as a strong band at 1656 cm^{-1}, while amide II (N-H bending and C-N stretching) appeared at 1549 cm^{-1}. A shoulder band at 1514 cm^{-1} is related to the tyrosine vibration (Nabedryk et al., 1984). The presence of the amide I band at 1656 cm^{-1} as a strong feature of the spectra is indicative of proteins being mainly in the α-helix conformation and the shoulder and weak components appearing at 1675 and 1628 cm^{-1} (Figure 12) were attributed either to the Chl vibrational modes or to the presence of some minor β-sheet and turn structures associated with the proteins (Nabedryk et al., 1984; Chapados et al., 1991). A weak band at 1736 cm^{-1} is assigned to the ester carbonyl stretching vibration of the lipid with some contribution from Chl. The weak bands at about 1400 cm^{-1} are related to the C-H bending modes (Nabedryk et al., 1984).

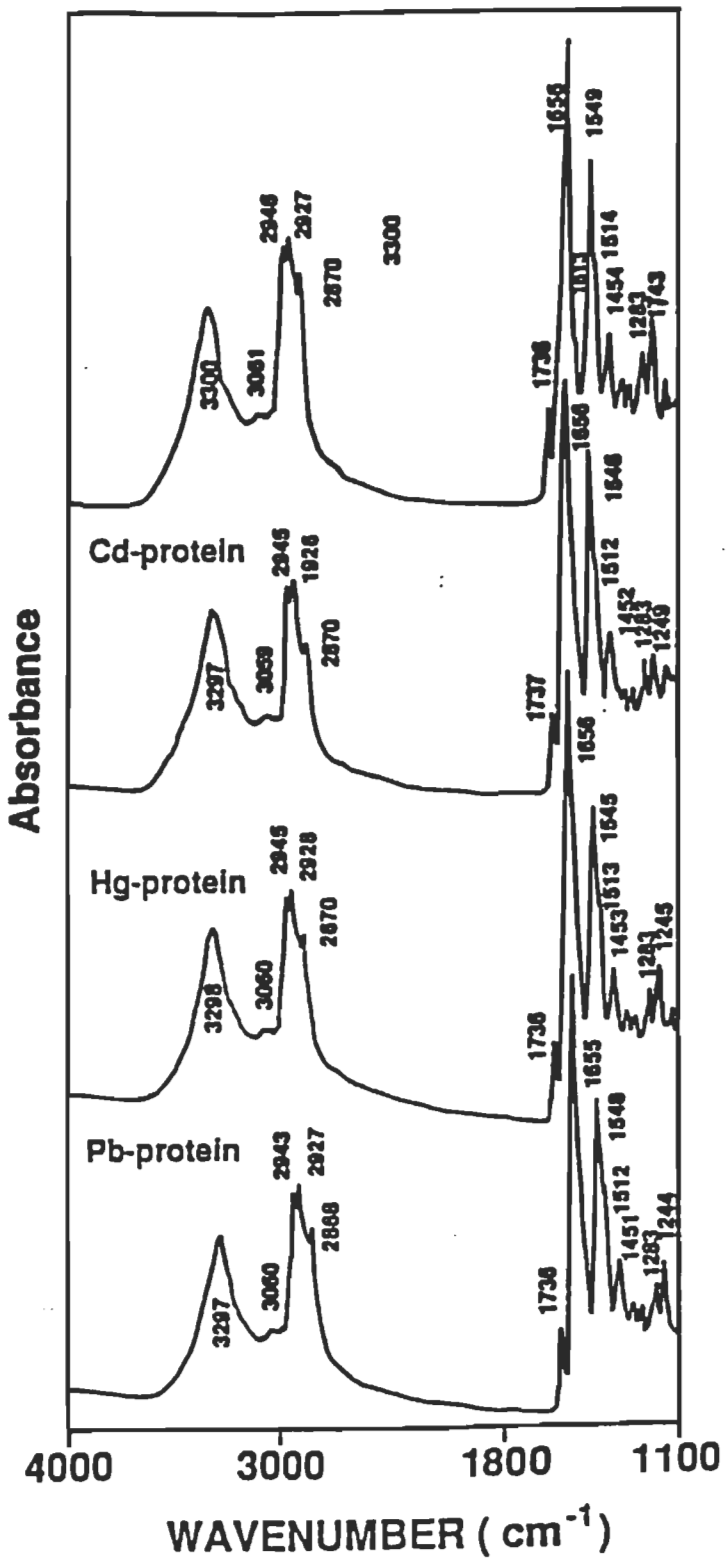

Figure 12 : FTIR spectra of the LHCII proteins in the presence of Cd, Hg and Pb (1 mM) in aqueous solution in the region of 4000-1100 cm^{-1}.

Interpretation of the difference spectra:

If no interaction occurs between metal cation and protein, the difference spectrum shows no spectral features and looks like a base line. If there is interaction between protein and cation and the protein structure is perturbed by cation complexation, two different features can be observed in the difference spectrum: a- negative band or negative feature and b- positive band or positive feature. The negative feature indicates a reduction in the intensity or absorption of certain band upon complexation(Duguid et al., 1994). In this case an indirect interaction of cation with protein can be predicted through cation hydration shell (H-bonding of water with protein C=O and C-N or NH groups). This type of interaction can be associated with protein aggregation.The positive feature is indicative of an increase in the absorption or intensity of a certain band. In this case a direct coordination of metal cation to protein (C=O, C-N, NH or SH groups) is taking place.

The infrared spectra of the LHCII-protein (in the absence of metal ion) (Figure 12) exhibit no major shifting upon metal ion interaction, therefore we have produced the difference spectra ((LHCII + metal ion)-(LHCII)) for the amide I and amide II domain.

From the analysis of the difference spectra of these metal-protein complexes, several interesting and important features were revealed. We will discuss in detail these conformation changes for each metal ion separately. The difference spectra show several positive and negative derivative features in the amide I and amide II regions (1800-1500 cm^{-1}) of the spectra which are explored in order to analyze the metal ion binding mode, protein conformational changes, and the structural variations on metal ion complexation. Positive bands in these spectra arise from the appearance of new conformation compounds, while the negative bands arise from disappearance of the original conformation compounds.

To facilitate the comparison between the effect of metal ions on the conformational changes of LHCII-protein, we found that it is more appropriate to regroup these metal ions in three groups according to the similarities

between some of these metal ions either in their coordination numbers, toxic effect or their existence in the plant as follows:

1) -Cd, Hg, and Pb, **2)** - Cu and Zn, **3)** -Mg, Ca and Mn.

Each group was studied separately and the comparison will be between metal ions in the same group.

4.2 COMPLEXATION OF Cd, Hg, AND Pb WITH LHCII

It has been shown that dangerous environmental pollutants such as Cd^{2+}, Hg^{2+} and Pb^{2+} inhibit the photosynthetic apparatus of plants growing in their presence at the level of pigments and prenylquinone synthesis, decrease the activity of PSII (water splitting system), and cause the degradation of the chloroplast inner structure (Baszynski et al., 1980, Baszynski ,1986; Krupa et al., 1987b). Some specific changes in the amount and structure of Chl-protein complexes have also been observed. The same author showed that Cd^{2+} affectes the structure of light harvesting Chl a/b protein complex II which was reflected by a lower content of its oligomeric form and a higher level of the monomer (Krupa et al., 1987b).

In the present study the results of FTIR experiments designed to elucidate the nature of cadmium, mercury and lead action on the secondary structure of the light-harvesting protein complex are described.

4.2.1 Cd-Protein Binding

The amide A and the C-H stretching vibrations (3300-2800 cm^{-1}) exhibited no major spectral changes upon complexation of LHCII with Cd, whereas the amide I and amide II bands at 1656 and 1549 cm^{-1} showed marked intensity variations in the presence of this ion salt (Figure 13).

At very low cadmium ion concentration (0.01mM) a decrease in the intensity of the amide I band at 1656 cm^{-1} and an increase in the intensity of the amide II band at 1549 cm^{-1} were observed, which are characterized by a strong negative feature at 1625 cm^{-1} and a weak positive feature at 1554 cm^{-1} in the difference spectra (Figure 13). The loss of intensity of the amide I band can be

attributed to the reorientation of the protein in aqueous solution and not to the metal-carbonyl interaction, while the gain in the intensity of the amide II band is due to a direct Cd-nitrogen coordination. As the Cd concentration increases (0.1 to 20 mM), strong positive features appear at about 1650 cm^{-1} and 1550 cm^{-1}, which are due to the increase in the intensities of the amide I and amide II bands, in the presence of Cd ion (Figure 13). The gain in the intensity of these vibrations is related to the direct cadmium-protein interaction through both the C=O and C-N groups. The Cd-proteins bindings to the C=O and C-N groups are reported through structural analysis of metal-protein complexes (Kaegi and Schaeffer, 1988). However, a new positive feature observed at about 1530 cm^{-1} in the difference spectra of the Cd-protein complexes formed at high Cd ion concentrations (10 and 20 mM) can be assumed to the tyrosine band at 1514cm^{-1} (Figure 13). This is likely that the participation of the tyrosine residues in metal-protein interaction increases as Cd ion concentration increases. The presence of a negative features at 1729-1739 cm^{-1} in the difference spectra arising from the loss of intensity of the Chl and lipid carbonyl ester band at 1736 cm^{-1} is indicative of no interaction between the Cd ions and the carbonyl ester of lipid or Chl residues of the LHCII complexes. The difference spectra of Cd-protein complexes obtained at higher metal ion concentrations (more than 20 mM) showed no differences from those of the Cd-protein complexes with Cd ion concentration of 20 mM described in Figure 13. This is indicative of a maximum Cd-protein interaction occurring at 20 mM of metal ion concentration.

The conformation of the protein was perturbed by the presence of Cd ions at high concentration (1, 10 and 20 mM) (Figure 13). The presence of a strong infrared band at 1656 cm^{-1} of the uncomplexed LHC proteins was attributed to the α-helix conformation of the protein as a major conformation species present in solution. The calculated ratio was shown to contain almost 48% α-helical structure (Nabedryk et al., 1984). However, the emergence of positive features at about 1670 cm^{-1} and 1650 cm^{-1} on the higher and lower frequency sides of the amide I band can be attributed to the formation of the β-sheet and turn structures upon Cd ion interaction. An estimation of the relative amounts of each conformation can be deduced by the ratio of the integrated intensities of each band. Such calculation gives about 30% of the α-

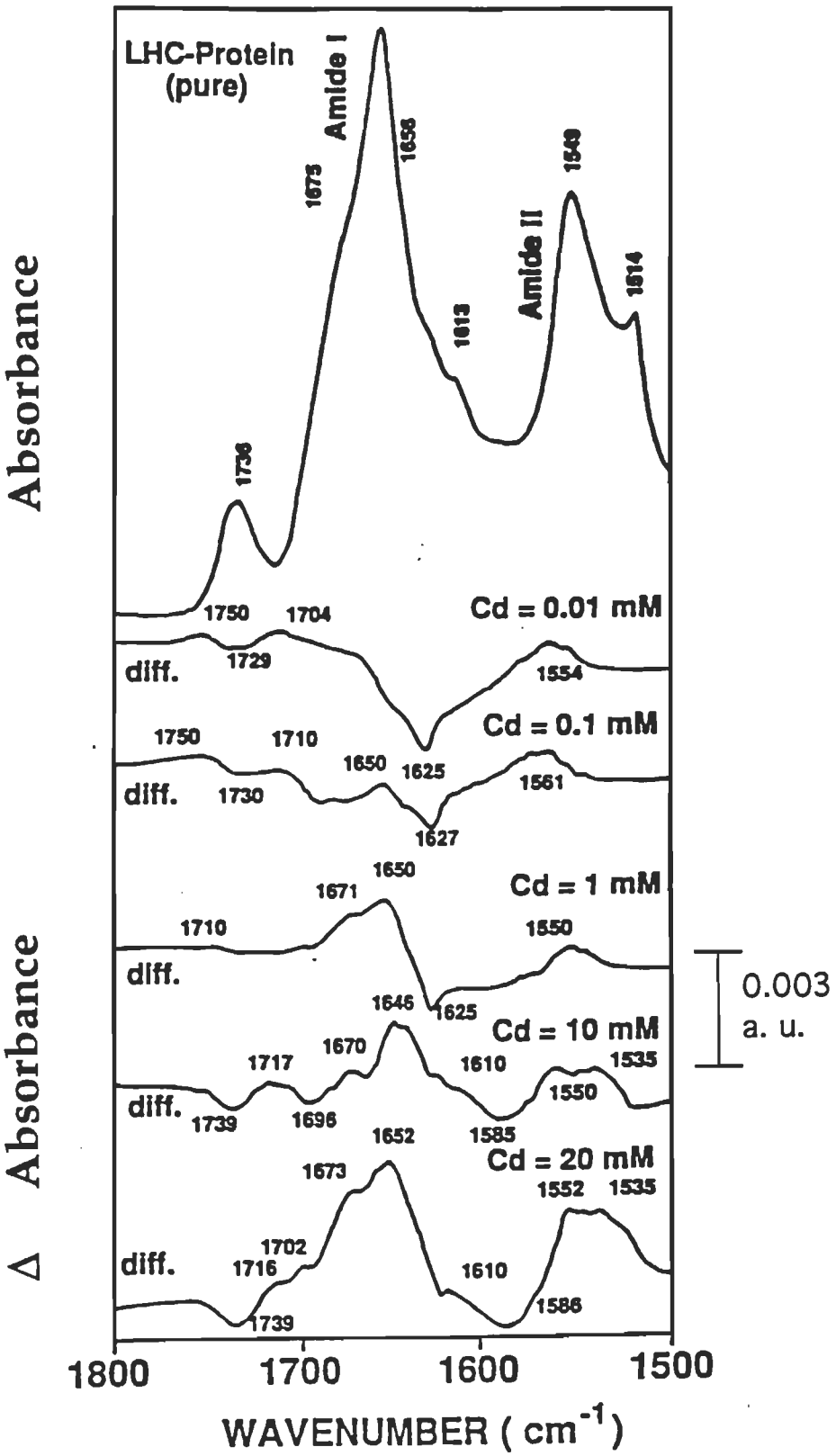

Figure 13 : FTIR spectra and difference spectra [(LHCII + metal ion)-(LHCII)] of LHCII and its cadmium complexes in aqueous solution in the region of 1800-1500 cm^{-1}.

α-helix and the rest is β-sheet and turn structures. This is a major conformational change from about 48% of α-helix in the uncomplexed LHCII protein (Nabedryk et al., 1984) to 30% in the presence of Cd ions at high concentration.

These results are in agreement with the conclusions of Krupa (1988) where at low cadmium concentration the amino acids composition of LHCII and LHCII treated with cadmium are similar with the identical polarity indexes equal 0.34 typical for high hydrophobic, intrinsic membrane proteins.

4.2.2 Hg-Protein Binding

At very low mercury cation concentration (0.01 and 0.1 mM) metal ion binding is mainly through protein carbonyl groups. Evidence for this comes from positive features at about 1660 and 1700 cm^{-1} as results of the increase in the intensity of the amide I band (Figure 14). No such positive feature was observed for the amide II at 1550 cm^{-1}, which is indicative of no major metal ion binding *via* the protein C-N group (Figure 14).

At higher mercury ion concentration (1 mM) more metal-carbonyl binding is observed with the major positive features at 1666 and 1702 cm^{-1} become more pronounced (Figure 14). However, as the cation concentration increased (10 mM), spectral changes were observed, which are characterized by strong positive derivative features at 1642 and 1670 cm^{-1} and a negative feature at about 1550 cm^{-1} (Figure 14). The positive features come from the major increase of the intensity of the band at 1656 cm^{-1}, due to a major Hg-carbonyl binding. The negative feature at about 1550 cm^{-1} arises from the loss of intensity of the amide II band at 1549 cm^{-1} and is characterized by no major metal-nitrogen atom interaction. On the other hand, a positive feature observed at 1530 cm^{-1} in the spectra of Hg-protein complex at high metal ion concentration (10 and 20 mM) is coming from the tyrosine vibration at 1514 cm^{-1} (Figure 14), which is due to the major mercury protein interaction through tyrosine moieties. Similar gain in the intensity of the amide I band was observed as the Hg concentration reached 20 mM, with strong positive peaks at 1646 and 1670 cm^{-1} and a negative feature at 1552 cm^{-1} (Figure 14), which indicates a continued participation of the protein carbonyl groups in

metal-ligand binding. However, the negative feature observed at 1552 cm^{-1} is an evidence for no mercury-nitrogen interaction (Figure 14). A previous study also showed major Hg-carbonyl binding in a series of mercury-polypeptides complexes (Alex et al., 1987). Although the spectroscopic evidence showed the participation of the protein carbonyl groups as major binding sites, mercury binding to the sulfur donor groups of protein is well-documented (Murthy et al., 1989). It is important to note that from the study of the amide I and amide II domains, one cannot draw a certain conclusion on the nature of Hg-sulfur donor binding. Since the Chl/lipid absorption band at 1736 cm^{-1} exhibited no major spectral changes in the presence of Hg ions, the possibility of Hg-Chl/lipid interaction cannot be included (Figure 14).

Drastic conformational changes of the protein were observed in the presence of concentrated Hg ions (10 and 20 mM). The emergence of positive spectral features at 1670 and 1642 cm^{-1} in the difference spectra are due to the protein structural changes on metal complexation (Figure 14). As the concentration increases (20 mM), the positive features at 1670 and 1646 cm^{-1} gain intensity and appear as major components of the difference spectra (Figure 14), which is indicative of drastic conformational changes from α-helix to β-sheet and turn structures, upon Hg ion coordination. The ratio of the integrated intensity of these vibrations showed the decrease of the α-helix from 50% in the uncomplexed protein to 30% for 10 mM and to 20% for 20 mM mercury ion concentrations. The conformational changes observed in the presence of Hg ions are more effective than those observed for the Cd-protein complexes (Figure 13 and 14).

4. 2. 3 Pb-Protein Binding

At low Pb ion concentration (0.01 and 0.1mM), minor interaction of the Pb-protein through the C=O groups was observed. Evidence for this comes from the presence of a weak positive derivative feature at about 1650 cm^{-1} in the difference spectra due to the minor increase in the intensity of the amide I band (Figure 15). As the concentration of metal ion increases (1 to 20 mM), the positive peak at about 1550 cm^{-1} appears as a broad and strong feature of the difference spectra of the Pb-protein complexes (Figure 15). The considerable

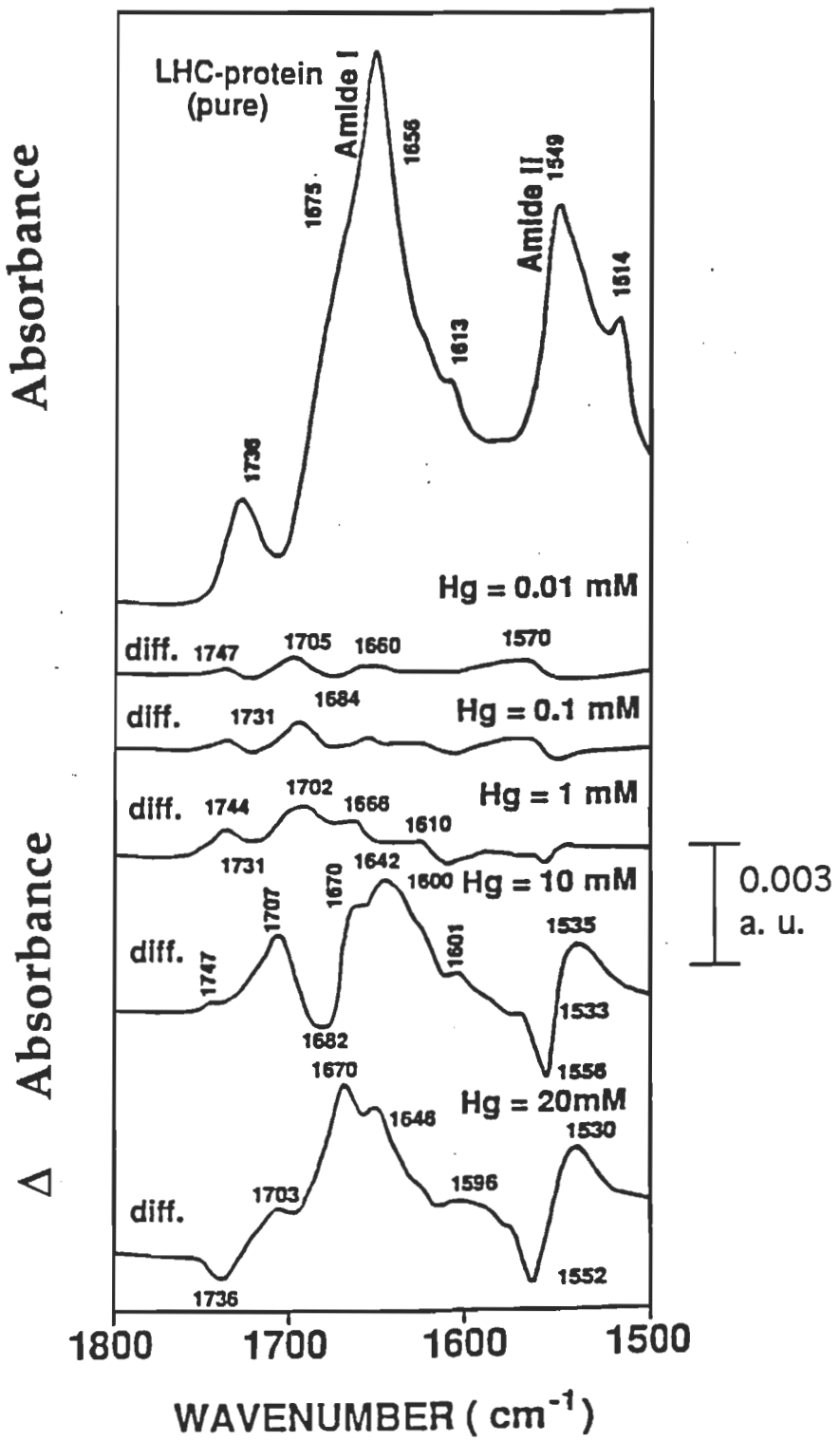

Figure 14 : FTIR spectra and difference spectra [(LHC-II + metal ion)-(LHC-II)] of LHC-II and its mercury complexes in aqueous solution in the region of 1800-1500 cm^{-1}.

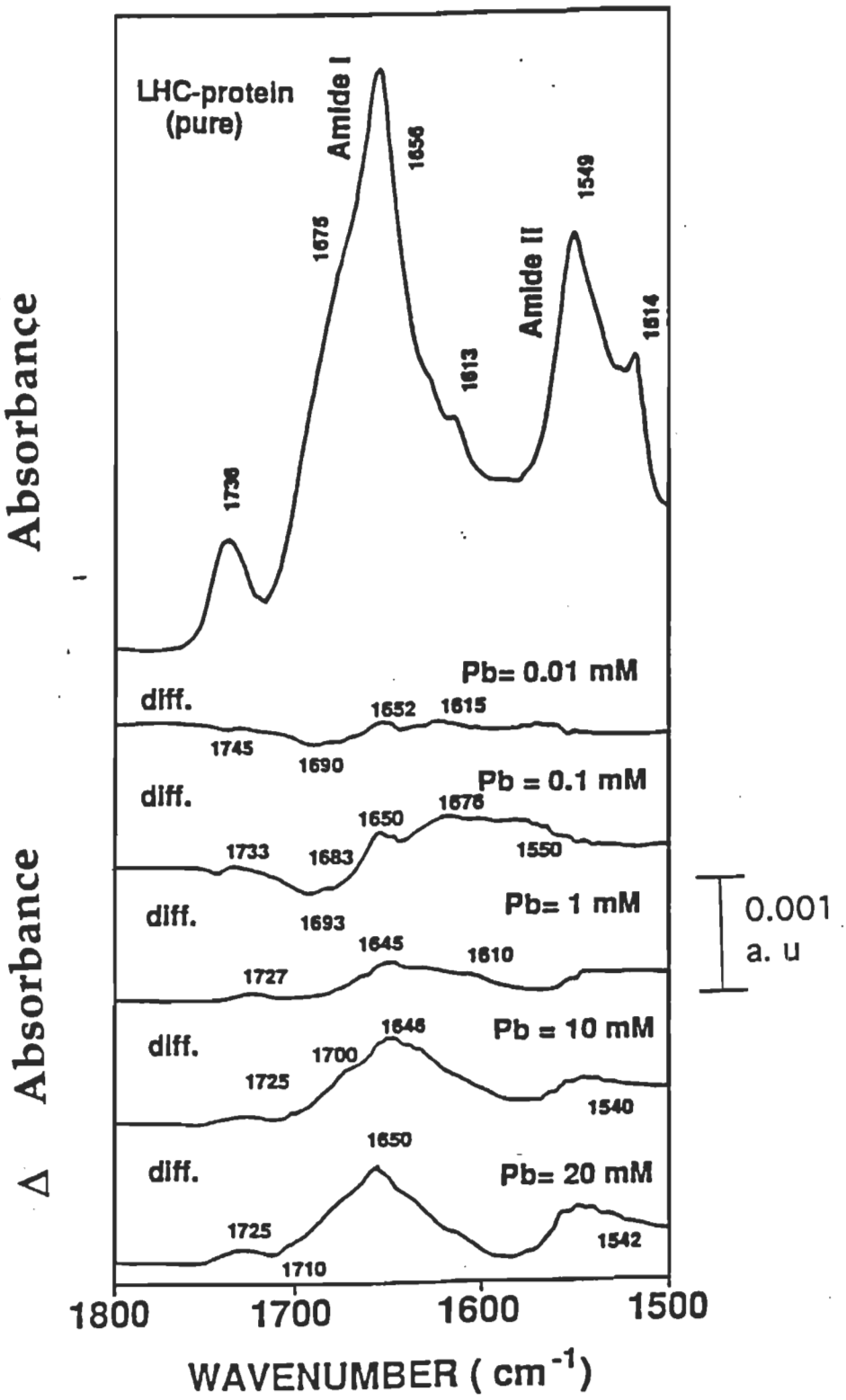

Figure 15 : FTIR spectra and difference spectra [(LHCII + metal ion) - (LHCII)] of LHCII and its lead complexes in aqueous solution in the region of 1800 - 1500 cm^{-1}.

gain in intensity of the amide I band is related to the major metal-carbonyl interaction occurring at high lead ion concentration. Similarly, the presence of a weak positive derivative features at about 1550 cm^{-1} of the amide II domain could be attributed to some degree of lead-protein interaction via the C-N at 1636 cm^{-1}. The possibility of lead-Chl interaction is excluded here. The absence of major conformational marker features at about 1670 and 1640 cm^{-1} in the difference spectra of lead-protein complexes can be related to no major conformation variations of the LHC proteins, upon lead cation interaction. It should be noted that the addition of more concentrated Pb ion solution (more than 20 mM) produced similar spectral changes as observed for the Pb-protein complexes of 20 mM metal cation concentration. This is indicative of maximum perturbations of proteins structure occurring at 20 mM lead ion concentration. Similar behaviors were also observed for the Cd-and Hg-protien complex. However, the interaction of the lead ion brought less perturbation of the protein secondary structures than those of the Hg or Cd ion discussed here (Figures 13, 14, and 15).

4.3. ZINC AND COPPER

The infrared spectral features of the protein amide I and amide II regions of the free LHCII showed no major shifting in the presence of copper and zinc cations (Figure 16) and thus the difference spectra [(LHCII + metal ion)-(LHCII)] were reproduced and are presented in Figures 17 and 18.

4.3,1 Zn-Protein Complexes

At low zinc ion concentrations (0.01-0.1 mM), no major spectral changes were observed in the difference spectra of Zn-protein complexes (Figure 17). This is indicative of no major perturbation of the protein structure by metal cation. As the concentration of metal ion increases (1 mM), several positive features were observed at 1670, 1640, 1610 and 1530 cm^{-1}, which are due to the presence of a strong metal-protein interaction (Figure 17). A strong positive feature at 1640 cm^{-1} is due to the increase of the intensity of the amide I mode as the result of direct Zn-carbonyl interaction. Similarly, the positive feature at 1530 cm^{-1} would come from the spectral variations of tyrosine mode at 1514 cm^{-1} and can be indicative of metal-tyrosine complexation (Figure 16). The

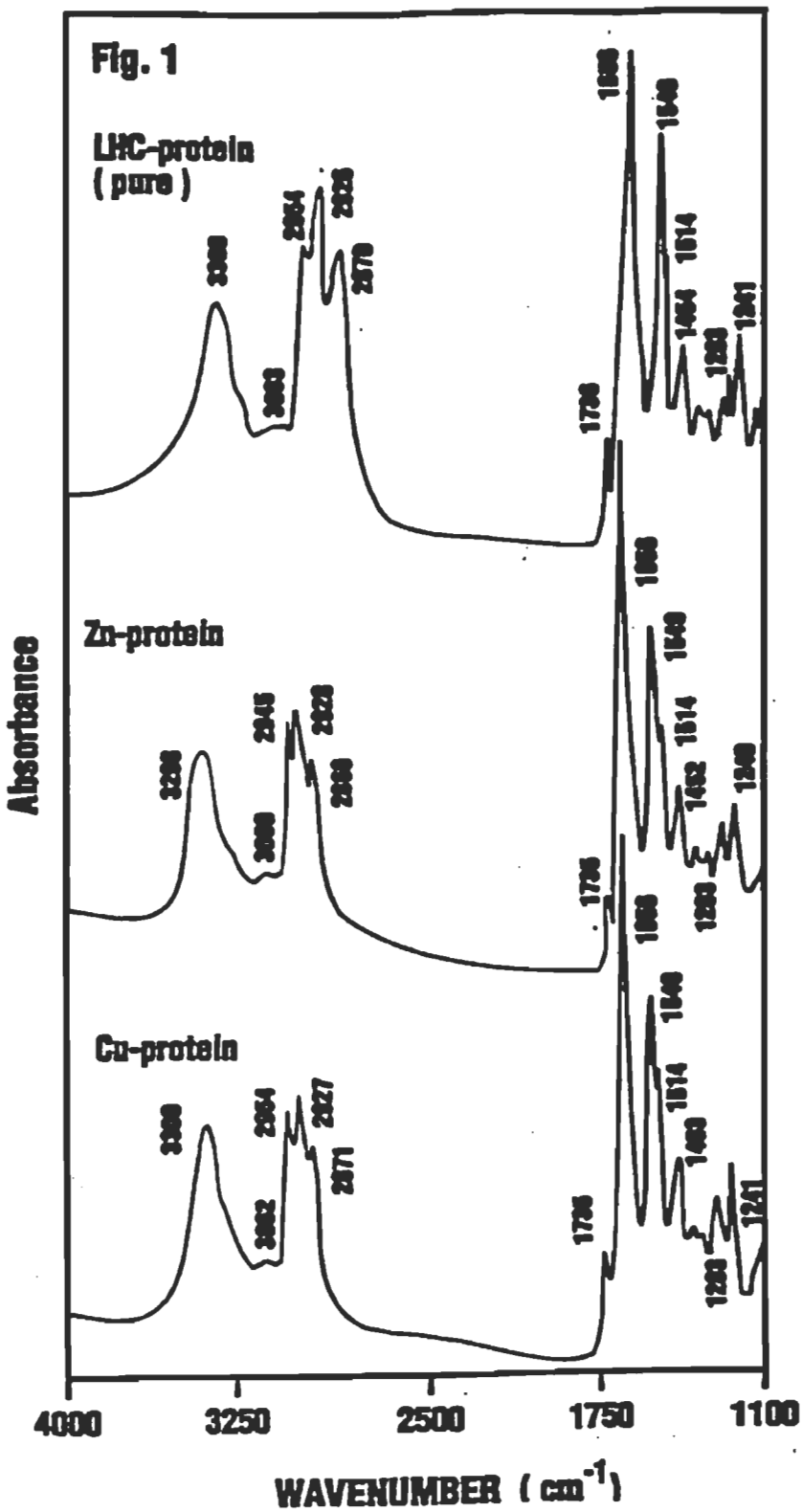

Figure 16 : FTIR spectra of the LHCII protein in the presence of Zn and Cu ions (1 mM) in aqueous solution in the region of 4000-1100 cm^{-1}.

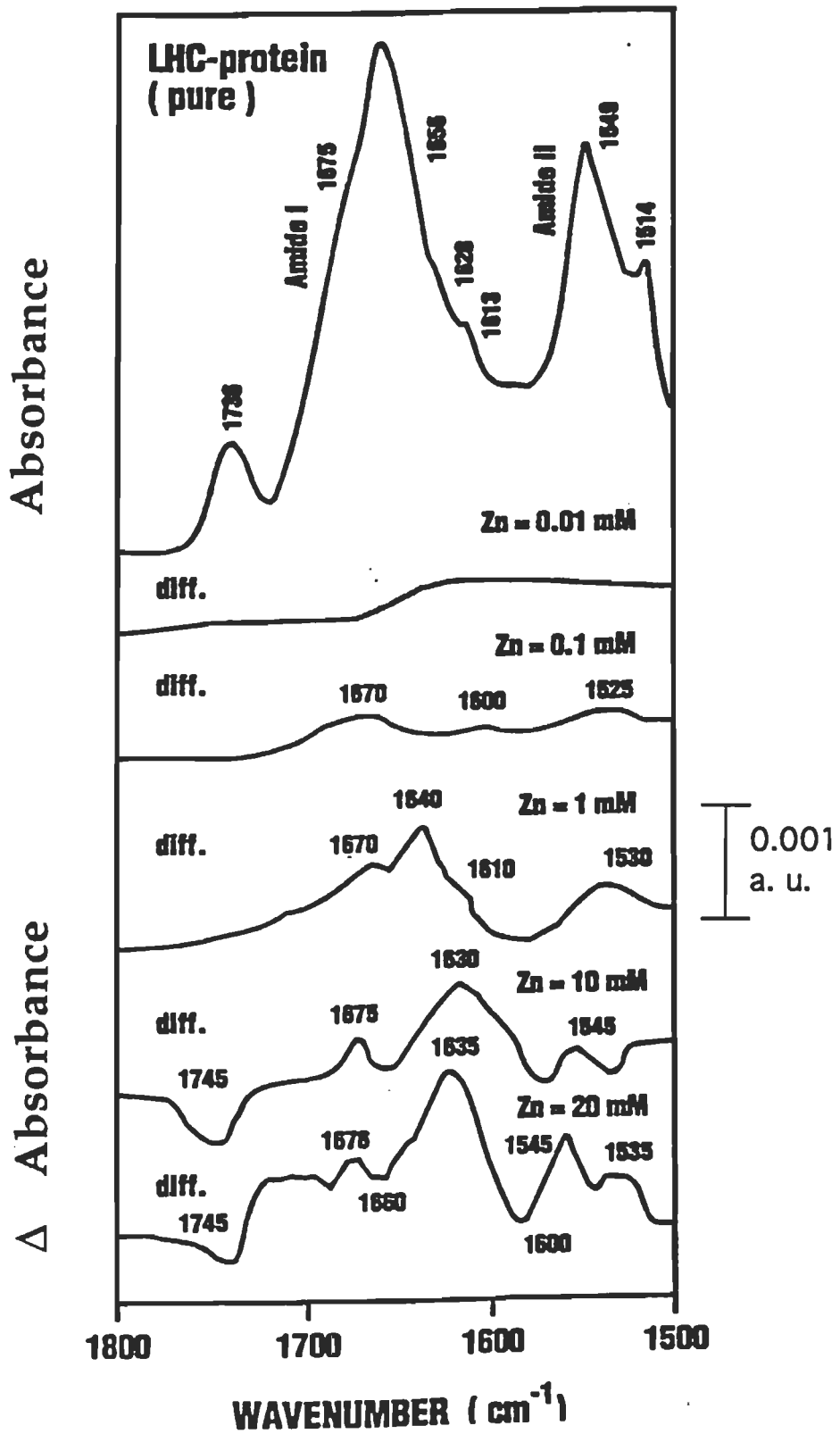

Figure 17. FTIR spectra and difference spectra [(LHCII + metal ion)-(LHCII)] of LHCII and its zinc complexes in aqueous solution in the region of 1800-1500 cm^{-1}.

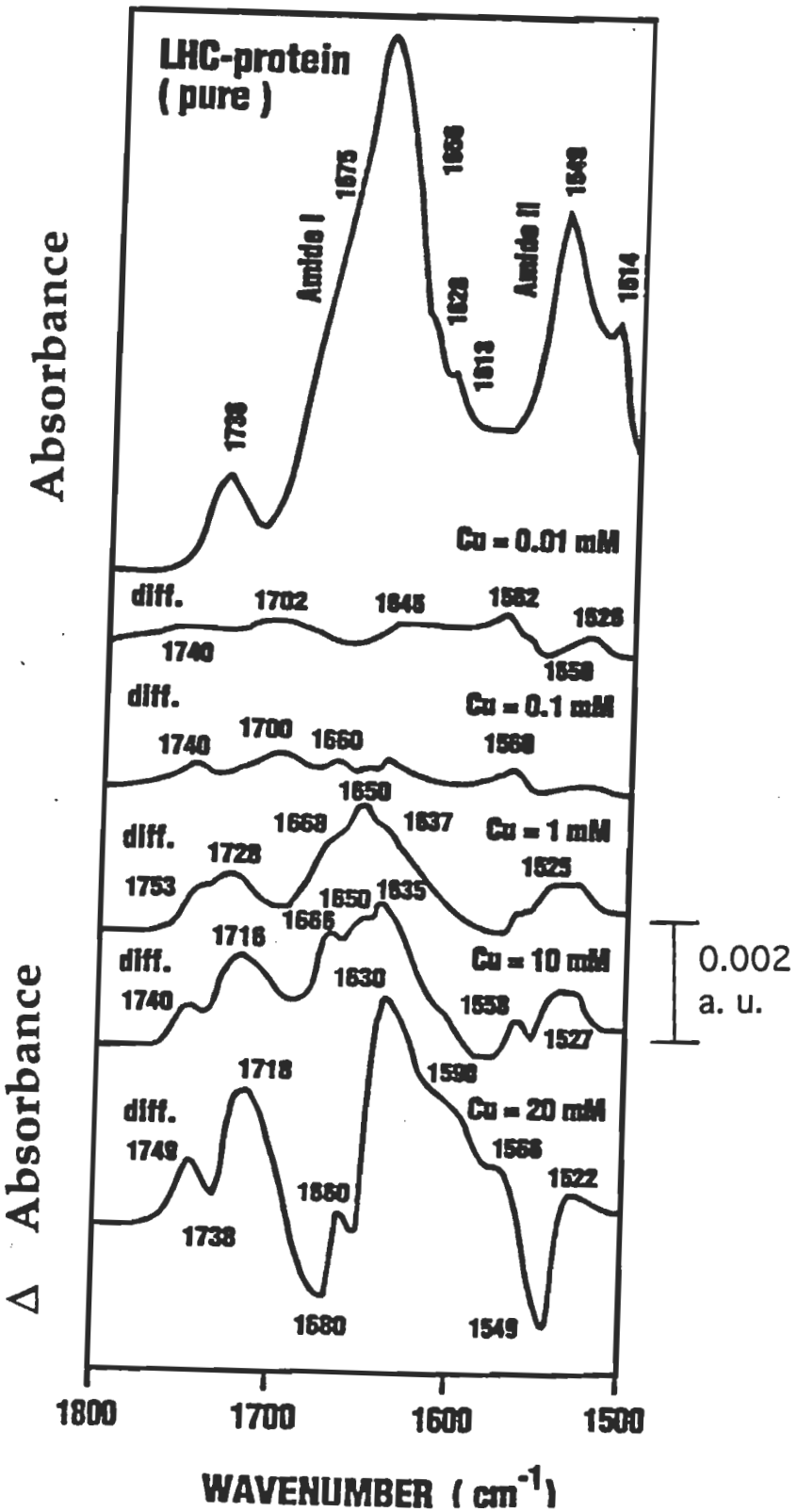

Figure 18 : FTIR spectra and difference spectra [(LHCII + metal ion)-(LHCII)] of LHCII and its copper complexes in aqueous solution in the region of 1800-1500 cm^{-1}.

weak derivative features at 1670 and 1610 cm^{-1} are related to the Chl vibrations (Nabedryk et al., 1984).

At higher metal cation concentration (10-20 mM), major spectral modifications occurred in the presence of zinc ion. A strong derivative feature at about 1630 cm^{-1} was observed in the difference spectra of the metal-protein complexes as a result of an increase in the intensity of the amide I band at 1656 cm^{-1}, that can be attributed to the major Zn-carbonyl interaction (Figure 17).

Similarly, two positive derivative features with medium intensities at 1545 and 1535 cm^{-1} are related to the increase of the intensity of the amide II and the tyrosine modes, that are characteristic of metal-protein interaction *via* C-N and the tyrosine residues. A negative feature observed at about 1745 cm^{-1} is due to the loss of intensity of the carbonyl stretching of the Chl groups, which is indicative of no Zn cation interaction with Chl moieties of the PSII system (Figure 17) (Tajmir-Riahi and Ahmed,1993).

The secondary structure of the protein was perturbed by the presence of Zn ion at high metal concentrations (10 and 20 mM). The presence of a strong infrared band at 1656 cm^{-1} of the uncomplexed LHCII protein was attributed to the α-helical structure of the protein as a major species present in aqueous solution (Nabedryk et al., 1984). However, the presence of positive features at about 1630 and 1675 cm^{-1} in the difference spectra of Zn-protein complexes formed at 10 and 20 mM metal ion concentrations (Figure 16), are due to the major conformational variations from α-helix to β-sheet and turn structures (Dong et al., 1992). An estimation of the relative amounts of each conformation can be calculated from the ratio of the integrated intensity of each band. Such calculation gives about 25% of the α-helix and the rest in β-sheet and turn structures, which is a major conformational variation from the α-helical structure of the uncomplexed protein (48%).

4.3.2 Cu-Protein Complexes

The copper ion perturbed the protein structure more effectively than the zinc cation. At very low concentration of copper ion (0.01, 0.1 mM), the difference spectra of copper complexes exhibited weak positive derivative

features at about 1650, 1560 and 1526 cm^{-1}, that are characteristics of a small increase of the intensities of the amide I and amide II vibrational modes (Figure 18). The observed spectral changes are indicative of some degree of copper ion binding with the protein C=O and C-N groups. However, at higher metal ion concentration (1 to 10 mM), major spectral changes were observed by the appearance of a strong derivative feature at 1650 cm^{-1}, a weak band at 1525 cm^{-1} and the two shoulder features with medium intensities at 1668 and 1637 cm^{-1} (Figure 18). The emergence of the two positive features at 1650 and 1525 cm^{-1} as the result of major intensity increases of the amide I band at 1656 and tyrosine band at 1514 cm^{-1} are due to strong Cu-carbonyl and Cu-tyrosine interactions, while the presence of the two other bands at 1637 and 1668 cm^{-1} are related to the protein conformational changes from the major α-helix in the uncomplexed LHCII to those of the β-sheet and turn structures in Cu-protein complexes (Tajmir-Riahi and Ahmed, 1993). Quantitative analysis of integrated intensity of each band showed protein conformational changes from α-helix of 48% (uncomplexed protein) to 40% and the formation of the β-sheet and turn structures in aqueous solution in the presence of copper ion. When the copper ion concentration increases to 10 mM, the amount of α-helix reduced to almost 30%, while the amounts of β-sheet and turn structures raised to almost 30%, with strong copper ion coordination to both carbonyl and the C-N groups (Figure 18). Evidence for this comes from the emergence of strong derivative features at 1635, 1650 and 1666 cm^{-1}, that are the marker bands for the β-sheet, α-helix, and turn structures, respectively. However, at 20 mM metal ion concentration, the β-sheet structure appeared as a major species in aqueous solution (50%) with a strong positive feature centered at 1630 cm^{-1} while the other conformers (α-helix and turn) were the minor components in solution (Figure 18). The protein carbonyl and the C-N groups were the major binding sites of the copper cation at high concentration with major perturbation of the tyrosine groups.

It should be noted that the concentration of 20 mM of metal ion solution brought the maximum spectral changes for both Zn and Cu ions and no further spectral modifications was observed upon addition of more concentrated metal ion solution (more than 20 mM).

In conclusion, LHCII proteins are very strong metal ion binders, and at low metal ion concentrations, zinc ion was less effective than copper cation (0.01-0.1mM). At higher metal ion concentrations, both Zn and Cu ions are binding to the protein carbonyl and C-N groups with the participation of tyrosine residues, resulting in major protein conformational changes from α-helix to β-sheet and turn structures. However, copper ion induced more perturbation of the protein secondary structure with respect to the zinc cation at high metal ion concentrations.

4.4 Mg, Ca, and Mn

Due to the minor spectral shifting of the amide I and amide II bands upon metal ion interaction (Figure 19), the difference spectra [(LHCII +metal ion salt)-(LHC-II)] were produced and they are shown in (Figures 20, 21 and 22).(Ahmed and Tajmir-Riahi, 1994).

4.4.1 Mg-Protein Interaction

At very low Mg ion concentration (0.01 mM), no major spectral changes were observed, in the difference spectra of the Mg-protein complexes (Figure 20). The negative derivative features observed at 1665 and 1550 cm^{-1} at low metal ion concentrations, are due to the reduction of the intensities of the amide I and amide II bands as the results of protein aggregation in the presence of the Mg(I) ions. The aggregation of the LHCII proteins in the presence of the magnesium ion is well known (Williams et al., 1987). At higher Mg ion concentrations (0.1 and 1 mM), two positive features were observed at about 1670 and 1647 cm^{-1}, because of an intensity increase of the amide I band at 1656 cm^{-1} and they are indicative of direct Mg-protein interaction, through protein carbonyl groups. The negative feature observed at about 1580 cm^{-1} is indicative of no participation of the C-N group, in Mg-protein complexation (Figure 19). At very high metal ion concentrations (10 and 20 mM), major spectral changes occurred, by the presence of strong and broad positive derivative features at about 1639-1635 cm^{-1} and the weaker positive features at about 1558-1566 cm^{-1}, in the difference spectra of Mg(II)-protein complexes (Figure 20). The observed spectral differences are the results of a major intensity increase of the amide I and amide II vibrations, due to the presence of a strong Mg-protein interaction,

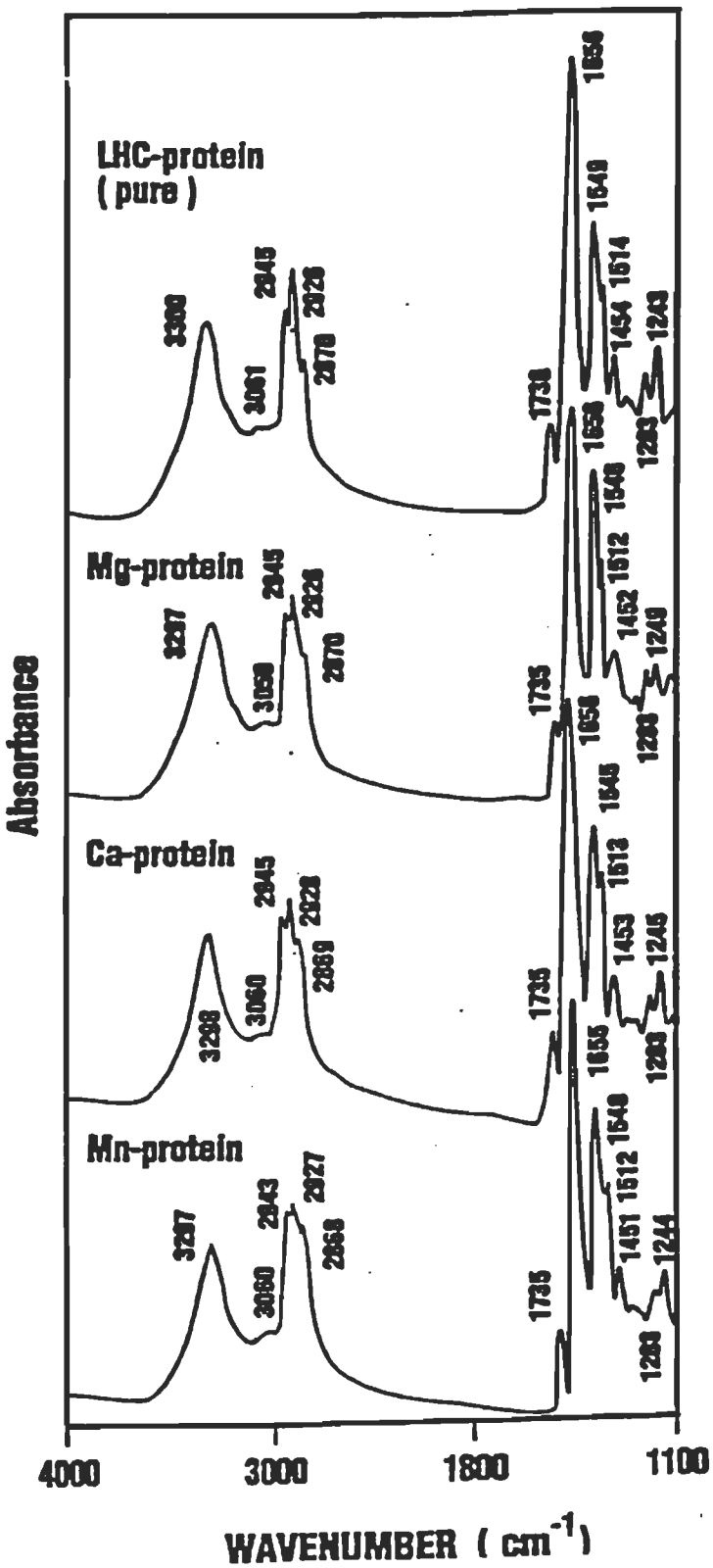

Figure 19 : FTIR spectra of the LHCII proteins in the presence of Mg, Ca and Mn (1 mM) in aqueous solution in the region of 4000-1100 cm^{-1}.

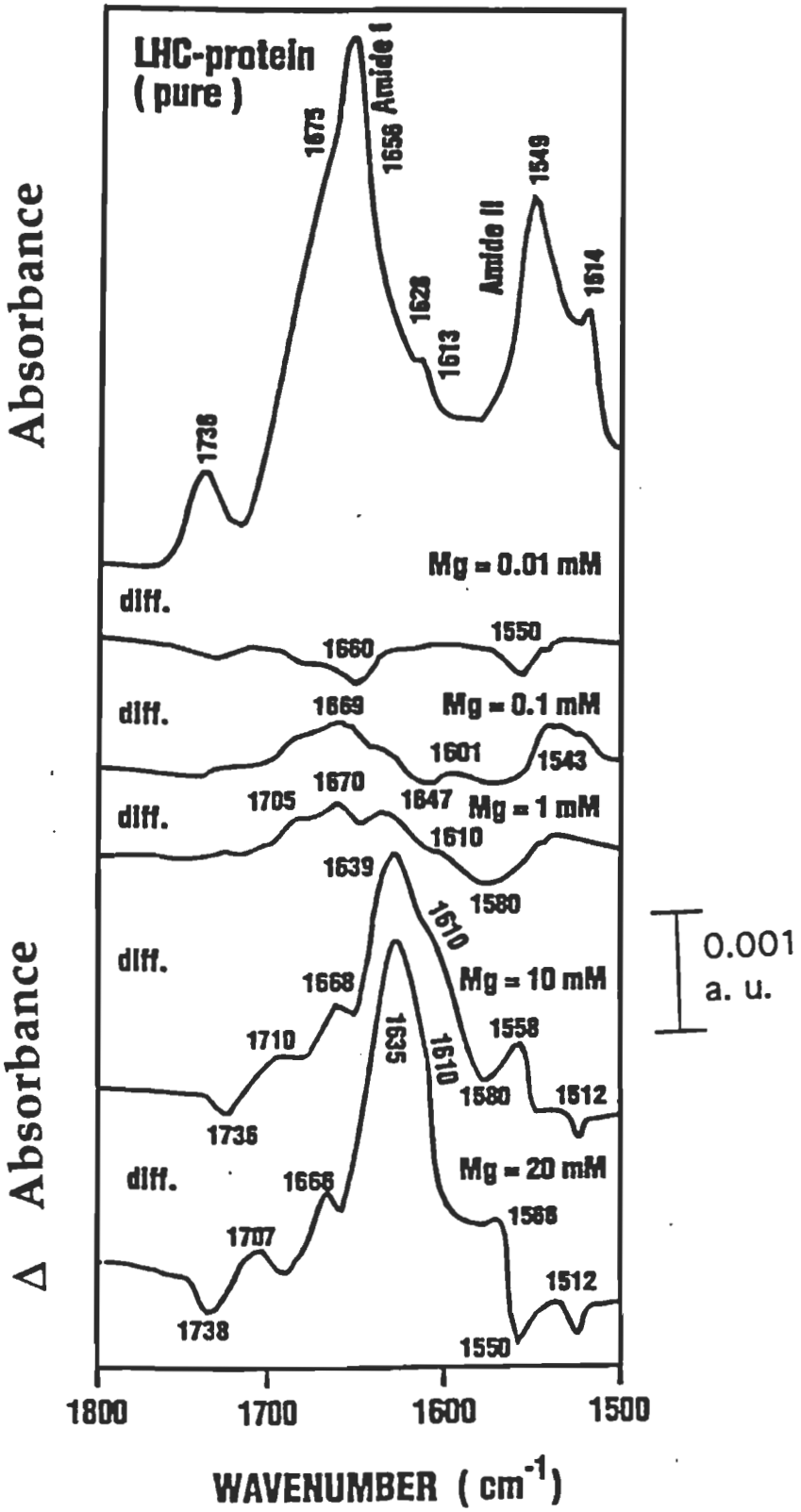

Figure 20 : FTIR spectra and difference spectra [(LHCII + metal ion)-(LHCII)] of LHCII and its Mg complexes in aqueous solution in the region of 1800-1500 cm^{-1}.

through the protein C=O and the C-N groups, and major protein conformational variations, in the presence of high metal ion concentrations. A weak negative derivative feature observed at 1512 cm^{-1}, related to the tyrosine residues is indicative of no direct metal-tyrosine interaction. Similarly, the presence of a negative feature at about 1736-1738 cm^{-1} due to the Chl vibrations (Nabedryk et al., 1984) is indicative of no metal-Chl interaction (Figure 19). The free LHCII proteins show mainly α-helical structure (48%) with minor contributions from β–sheet and turn conformations (Nabedryk et al., 1984). Evidence for this comes from the presence of the amide I band at 1656 cm^{-1}, as a strong feature of the infrared spectra, while the bands at 1628 and 1675 cm^{-1} are less pronounced (Figure 20). Upon Mg ion interaction, a positive derivative feature at 1647 cm^{-1} grows in intensity and appears as a major component of the difference spectra, at high metal ion concentrations (10 and 20 mM) (Figure 20). The decrease in the intensity of the amide I derivative feature at about 1660 cm^{-1} and the increase in the intensity of the components at 1639-1635 cm^{-1} are characteristic features of conformational changes from that of the α-helix to β-sheet and turn structures, in the presence of the Mg ion at high concentrations. A quantitative estimation of the amount of each component can be calculated from the ratio of the integrated intensity of each band. Such calculations predict about 48% of the α-helix in the uncomplexed LHCII, whereas a gradual decrease of the α-helicity to the β-sheet and turn structures was observed with the α-helix 43%, in the presence of the Mg ion at 20 mM concentration. The decrease in the amount of the α-helix was associated with the gradual increase of the β-sheet and turn structures as the metal ion concentration increases (Figure 20).

4. 4. 2 Ca-Protein Interaction

Ca^{2+} is considered to be an essential cofactor of photosynthetic oxygen evolution in higher plants and cyanobacteria (Homann 1990, Yocum 1991). Oxygen-evolving PSII preparations isolated from higher plants and cyanobacteria contain Ca^{2+} which cannot be extracted with various chelating

reagents (Kashino et al., 1986, Cammarata and Cheniae, 1987; Shen et al; 1988a, Ono and Inoue, 1988).

Recent studies by Han and Kato (1993) provided evidences suggesting a functioning of Ca^{2+} in the light-harvesting assembly of PSII. LHCII solubilized from PSII membranes contained one bound Ca^{2+} per PSII. This Ca^{2+} cannot be ascribed to external Ca^{2+} unspecifically bound to the Chl a/b-protein and this Ca^{2+} is not a metal cation that bound to the binding sites of LHCII. This Ca^{2+} binding site is rather related to the minor 22 kDa component of LHCII which is present roughly in a stoichiometric amount to the PSII reaction center, and it may be suggested that the Ca^{2+} is located inside an oligomeric complex of LHCII containing the 22 kDa protein (Peter and Thornber, 1991, Dainese and Bassi, 1991). As such the Ca^{2+} is inaccessible to chelators used for extraction it may play an important structural role to stabilize the association of Chl-proteins or the binding of the antenna complex to the PSII reaction center complex, on the other.

LHCII is known to bind Ca^{2+} strongly and abundantly (Davis and Gros, 1975) and binding of Ca^{2+} to even denaturated LHCII proteins has been reported (Webber and Gray, 1989). There are two types of binding sites : site one binds 1.5 to 4.0 μ moles Ca^{2+} per mg Chl with Kd of 2.5 μM, while 9.5 μ moles Ca^{2+} per mg Chl bind to site II with Kd of 32 μM. Thus site I alone can bind most, if not all the Ca^{2+} present LHCII suspensions.

The interaction of Ca ion with LHCII proteins is rather different from that of the Mg ion. At low metal ion concentration (0.01, 0.1 and 1 mM), there was some degree of Ca-protein interaction *via* protein carbonyl and the C-N groups. Evidence for this comes from two weak positive derivative features, observed at about 1660 and 1540 cm^{-1}, in the difference spectra of Ca-protein complexes (Figure 21). The two weak derivative features observed at about 1660 cm^{-1} and 1540 cm^{-1} are the results of minor intensity increase of the amide I and amide II bands, on Ca ion interaction. It should be noted, that at similar metal ion concentrations, there was no Mg ion binding with the protein C-N group (Figure 20). The presence of a weak negative derivative feature at 1737 or 1738 cm^{-1}, due to the Chl/lipid ester carbonyl vibrations, is indicative of the

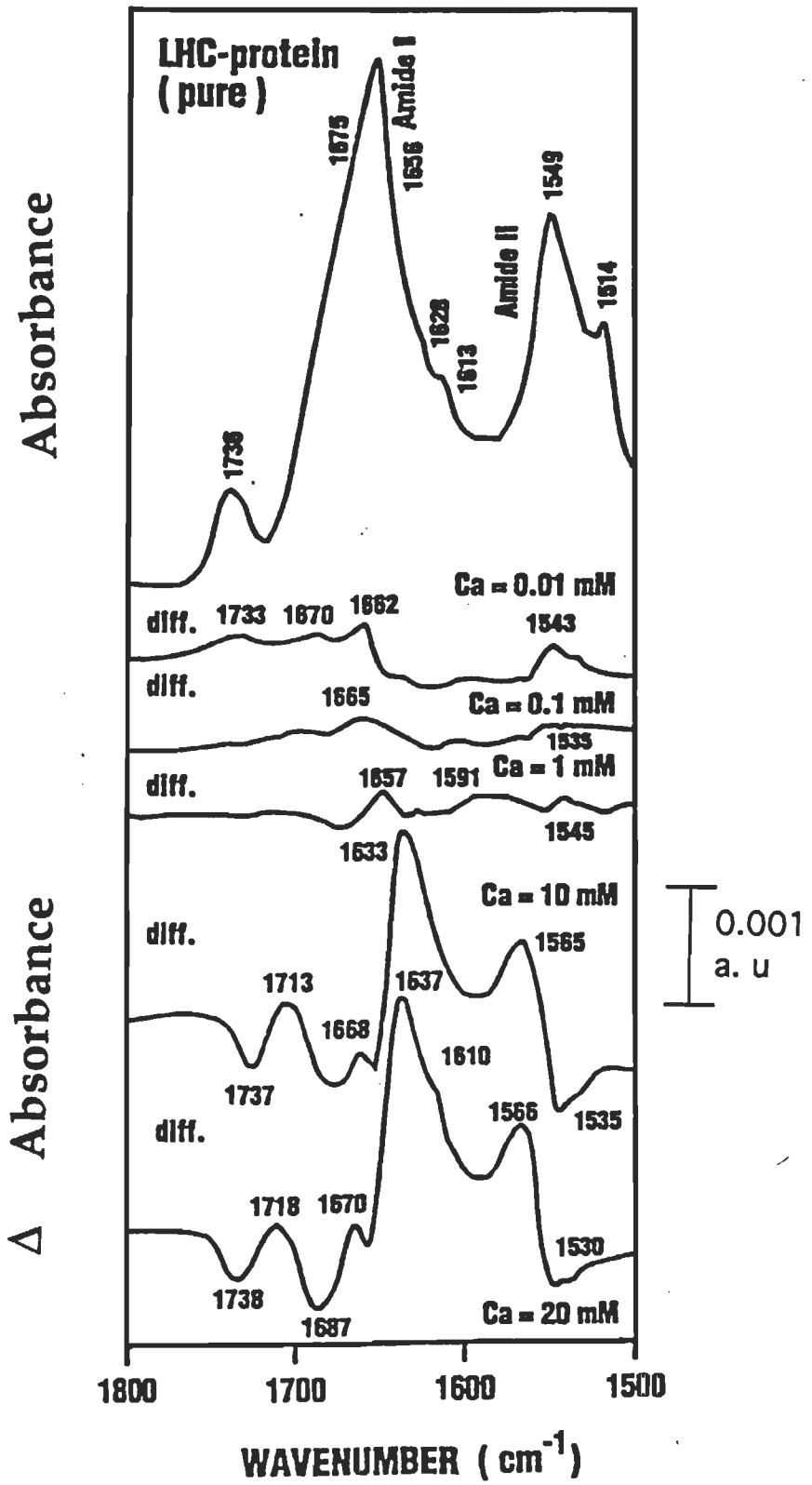

Figure 21 : FTIR spectra and difference spectra [(LHCII + metal ion)-(LHCII)] of LHCII and its Ca complexes in aqueous solution in the region of 1800-1500 cm^{-1}.

absence of any Ca-Chl interaction (Figure 21). However, at high Ca ion concentrations (10 and 20 mM), major metal ion bindings were observed through protein C=O and C-N groups. The presence of two strong positive derivative features at about 1640 and 1565 cm^{-1}, in the difference spectra of the Ca-protein complexes, that formed at high metal ion concentrations (10 and 20 mM) are indicative of a strong metal-protein complexation and of the presence of major protein conformational changes, on calcium ion interaction (Figure 21).

The major conformational changes, occurring in the presence of Ca ion with concentrations of 10 and 20 mM, are characterized with the emergence of strong positive features at 1640 (10 mM) and 1643 cm^{-1} (20 mM), that are the marker infrared bands for the β-sheet conformation (Figure 21). The quantitative analysis of the integrated intensities of the bands at 1640 and 1643 cm^{-1} (β-sheet) and that of the band at about 1670 cm^{-1} (turn structure), showed marked conformational transitions from that of the α-helix in the free LHCII (48%) to 40% (20 mM), in the presence of the Ca ions in aqueous solution

4.4.3 Mn-Protein Interaction

At very low Mn ion concentration (0.01 mM), no major spectral changes were observed for LHCII on metal ion interaction. As metal ion concentration increased to 0.1 and 1 mM, several weak positive derivative features were observed at 1653 and 1551 cm^{-1}, in the difference spectra of the Mn-protein complexes. These are the results of the intensity increase of the amide I and amide II vibrations (Figure 22). The observed spectral changes are due to the participation of the protein C=O and C-N groups, in metal ion complexation. At high Mn ion concentrations (10 and 20 mM), drastic spectral changes were observed, with the appearance of broad and strong positive derivative features at 1635 cm^{-1} (10 mM) and 1630 cm^{-1} (20 mM), as well as other medium derivative features at 1556, 1530 cm^{-1} (10 mM) and 1560, 1532 cm^{-1} (20 mM) (Figure 22). The observed spectral modifications are due to a major Mn-protein interaction, through the C=O and C-N groups. However, the weak positive derivative features observed at about 1530 cm^{-1} (10 and 20 mM), due to the increase in the intensity of the tyrosine mode at 1514 cm^{-1}, are indicative of the

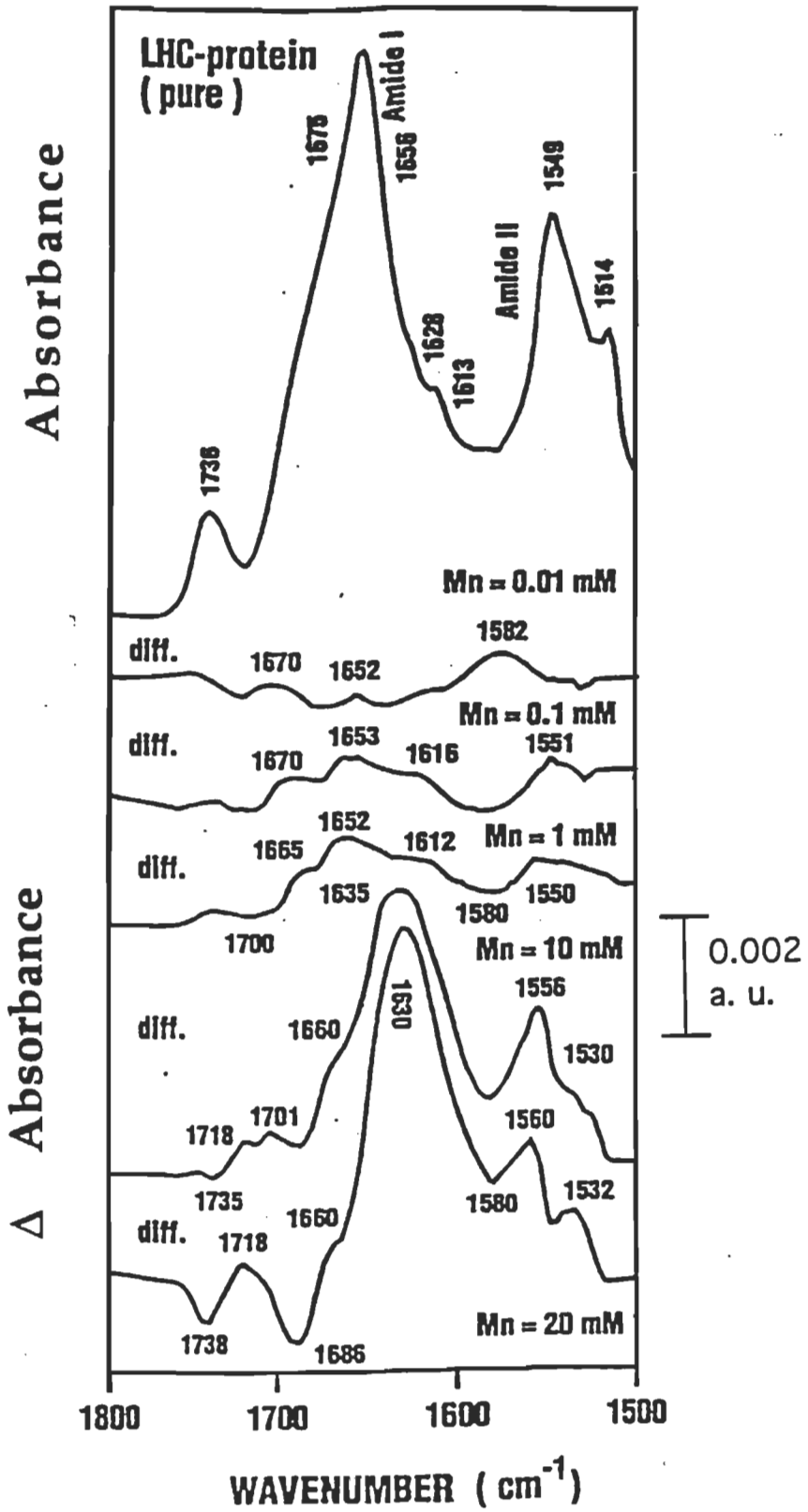

Figure 22 : FTIR spectra and difference spectra [(LHCII + metal ion)-(LHCII)] of LHCII and its Mn complexes in aqueous solution in the region 1800-1500 cm^{-1}.

participation of the tyrosine residue, in the Mn-protein complexation. Such metal ion interaction with tyrosine groups was not observed for the Mg and Ca ions, as we discussed above.

The presence of the strong derivative features at about 1635-1630 cm^{-1} and those of the weak features at about 1670 cm^{-1} are also indicative of major conformational changes from that of α-helical structure, which predominated in the uncomplexed LHCII proteins. The measurements of the integrated intensities of bands, at about 1635 and 1660 cm^{-1} in the difference spectra (10 and 20 mM), have shown major conformational variations from that of the α-helix in the uncomplexed proteins (48 %) to 40% (20 mM) in the presence of the Mn cation (Figure 22). Such major protein conformational variations, observed in the presence of both Ca and Mn ions, could be one of the major factors that contributes to the vital role of these metal cations in water oxidation and oxygen evolution in photosynthetic reaction centers.

4.5 CONCLUSIONS

In our investigations we used three different types of metal cations: I- Mg(II), Ca(II) and Mn(II) cations with strong affinity towards oxygen donor groups (hard acid) such as the oxygen atom of the H_2O or polypeptide C=O groups (Cotton and Wilkinson, 1988). This group of cations are present in the photosystem apparatus and their interactions with photosynthetic reactions are of great importance. Their complexation with certain polypeptides of PSII result in water oxidation and oxygen evolution. II- Zn(II) and Cu(II) cations shown major interaction with nitrogen donor atoms (intermediate acid), such as polypeptides C-N groups. These cations are also present in the photosystems as micronutrients and play an important role in activation of several enzymes. However, when the concentration of these cations increases in the chloroplast, inhibition of electron transport and reduction in rate of oxygen evolution are observed. III- Cd(II), Hg(II) and Pb(II) cations with strong affinity towards polypeptides sulfur donor atoms (soft acids) such as SH groups of cysteine residues. These cations are not present in the photosystem but they are reaching them as major contaminants and by binding to polypeptide sulfur groups thus inhibit the electron transport and oxygen evolution in PSII.

As it is evident from the diversity of acidic nature of these metal ions, different coordination chemistry is associated with each group of cations used in this study. For instance, divalent Mg with coordination number (C.N) of 6 an Ca(II) with C-N=6 to 8, Mn with C-N = 6, Hg with C.N =2, Cd with C.N = 6, Pb with C.N = 4-6, Zn with C.N = 6 and Cu with C.N=4 and 6. These cations show various affinities towards protein donor groups (C=O, C-N and SH groups) and also towards H_2O (Emsley, 1991). Each one binds to different number of water molecules and the replacement of water of hydration from each cation coordination shell will take place with various degree of stabilities (Greenwood and Earnshaw, 1984).

We have used these different cations to monitor their interactions with protein donor groups of LHCII complex and to evaluate the effects of these cations on the protein secondary structures. Indeed each group of metal cations exhibited different affinities towards light-harvesting proteins. Mg(II), Ca(II) preferred mainly polypeptide C=O binding with less interaction towards C-N group. These cations are highly hydrated even when they are protein bound (few numbers of H_2O can be replaced from cation hydration shell by protein coordination). Mn(II) cation prefers peptide C-N and C=O groups. Hg(II), Cd(II) and Pb(II) are sulfur and C=O or C-N bonded, while Zn(II) and Cu(II) cations are coordinated to both C=O and C-N groups. Each cation binds with different intensities to portion donor groups. From careful examination of the difference spectra obtained{(protein + cation) - (protein)} here, the difference in the degree of interactions for each cation have been determined (each set of difference spectra has a different absorbance intensity scale). Particularly, at high cation concentrations, major differences are evident even though the difference spectra seem to be very similar (they have different absorption scales). From these degree of interaction for each metal cation we calculated the amounts of protein secondary structures at different cation concentrations. The differences in the coordination chemistry of these cations prompted us to undertake the present investigation and the results obtained here are in good agreements with the coordination chemistry of these elements and can be extended to other protein complexes of the chloroplast membrane.

One of the major questions that should be addressed, is there any contribution from Cl^- anion associated with each cation to the spectral changes observed for metal-protein complexes under investigation here? If the observed spectral differences are mainly due to the anion (and not due to cation), the difference spectra obtained should be identical for all cation-protein complexes (divalent metal chloride salt used in this study contain similar amounts of Cl^- for all the complexes). Since such similarities were not observed for all the cation complexes, particularly at high salt concentrations, the spectral changes occurred are mainly due to cation interaction and not coming from Cl^- anions.

4. 6 STRUCTURE OF CHLOROPHYLL $P680^+$

It was demonstrated that upon illumination of Mn-depleted PSII-membranes by continuous actinic light in the presence of artificial electron acceptors, i.e. 500 μM potassium ferricyanide and 10 μM silicomolybdate, an absorbance change ΔA with a maximum at 678-680 nm is observed. This maximum absorbance is due to the formation of $P680^+$ resulting from photooxidation of the primary donor P680 (Allakhverdiev and Klimov 1992; Telfer and Barber, 1989; Van Gorkom et al., 1975).

Therefore we feel it is necessary to explain in the first place the result of the experiment which has been conducted in this regard to obtain $P680^+$ by these authors, where our experimental part strongly depends on their conclusion.

Figure 23 shows the kinetics of these absorbance changes at 678 nm. When PSII membranes are used before removal of the manganese cluster, even under oxidizing conditions (presence of 500 μM potassium ferricyanide and 10 μM silicomolybdate) only a weak absorbance change is seen upon illumination (Allakhverdiev and Klimov, 1992) (Figure 23, trace 1). Under these conditions, the active oxygen evolving complex (OEC) keeps the reaction center and the secondary donor Tyrosine Z mostly in the reduced state. However, removal of the manganese cluster from PSII membrane (PSII-Mn-depleted), inactivates the water splitting enzyme which donates electrons to Z, inhibits reduction of $P680^+$. Upon the illumination of PSII-Mn depleted, a

strong absorbance change occurred, this absorbance change is reversible in the dark (Figure 23, trace 2). Addition of 10 μM $MnCl_2$ leads to a decrease of the ΔA to the value characteristic of native PSII-membrane (Figure 23, trace 3), that can be explained by an increase of the rate of $P680^+$ reduction under reconstitution of the oxygen evolving complex, which acts as secondary electron donor to $P680^+$.

Thus, the light-minus-dark difference spectrum of the reversible absorbance change seen in Figure 24 under the conditions used for (Figure 23, trace 2) is typical of $P680^+$ accumulation (Klimov et al., 1982; Van Gorkom et al., 1975). Such a spectrum is created presumably because silicomolybdate is able to accept electrons from reduced pheophytin (directly or possibly through the non-heme iron) thus allowing the photoacumulation of $P680^+$.

Therefore, in our investigation we used conditions similar to the one described above to accumulate $P680^+$ for a time long enough to detect it by FTIR spectroscopy. It was previously demonstrated that these conditions also result in the formation of radical ($Z^\bullet$) (Ghanotakis and Babcock, 1983).

Figure 25 shows that the infrared spectra of the depleted PSII membranes exhibit no major shifting upon illumination, therefore we have produced the light-minus-dark difference ($P680^+$-P680) spectrum, by subtraction of the spectrum of PSII-Mn depleted before illumination from the spectrum of PSII-Mn depleted during illumination in the range between 1500 cm^{-1} and 1800 cm^{-1}. From the analysis of the difference spectra of light-minus-dark measurements, several interesting and important features were revealed. In Figure 25, the IR spectra of the preparation before (a) and during illumination (b) are presented together with the light-minus-dark difference spectrum (c). In the difference, the bands that arise from P680 and Z appear as negative absorption changes while the bands that originate from the formation of $P680^+$ and $Z^\bullet$ (tyrosine radical) are seen as positive absorption changes.

In the region below 1650 cm^{-1} the analysis of Chl vibrations associated with the formation of $P680^+$ is complicated by the possible superposition of

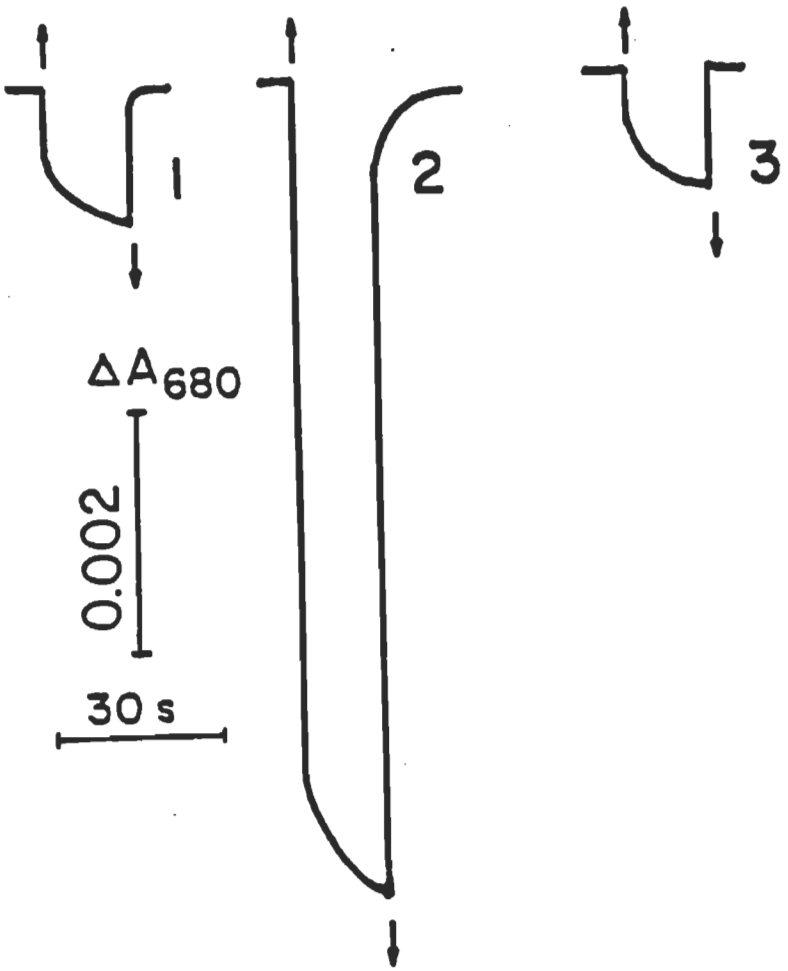

Figure 23 : Kinetics of photoinduced absorbance changes (ΔA) at 678 nm related to P680 photooxidation in the presence of 500 μM potassium ferricyanide and 10 μM Silicomolybdate in the PSII preparations before (1) and after (2,3) a complete removal of Mn without (2) and with addition of 10 μM $MnCl_2$(3). Up and down arrows indicate light on and off, respectively (Allakhverdiev and Klimov, 1992).

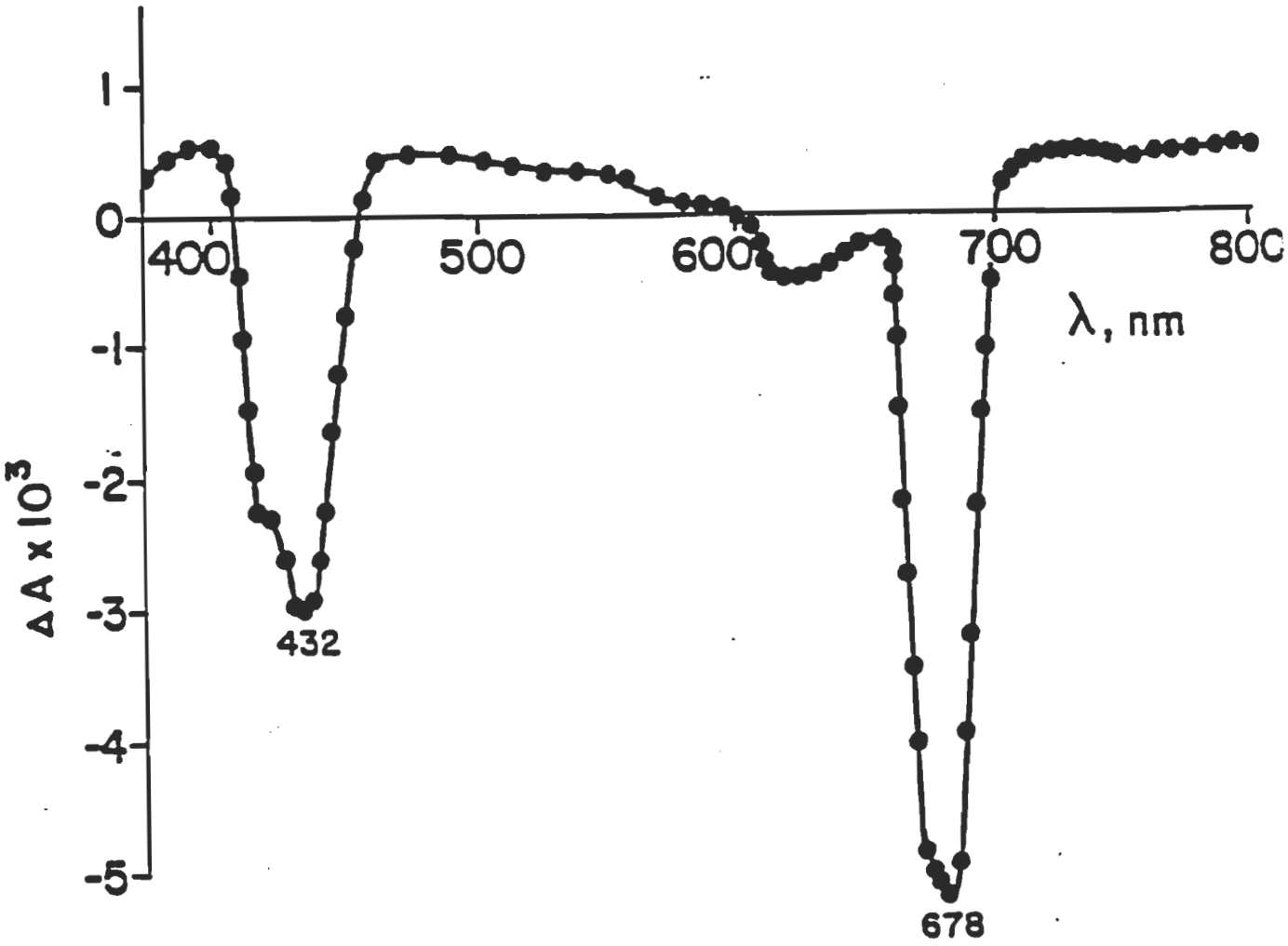

Figure 24 : Light-minus-dark difference spectrum of the reversible absorption changes seen in Mn-depleted photosystem II preparations in the presence of 500 μM potassium ferricyanide and 10 μM silicomolybdate.(Allakhverdiev and Klimov, 1992).

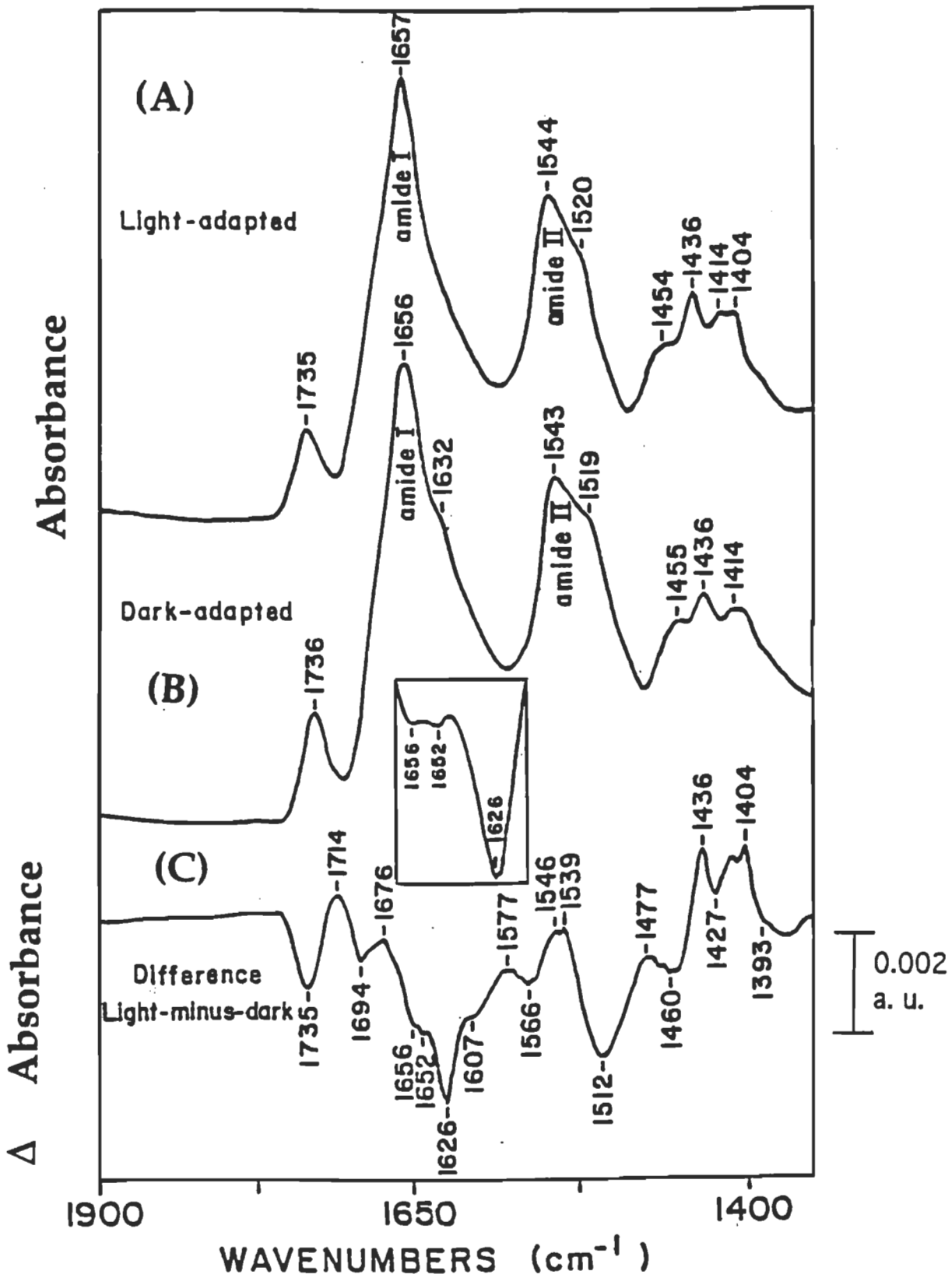

Figure 25 : FTIR spectra of Mn-depleted PSII preparations in the presence of 500 μM potassium ferricyanide and 10 μM silicomolybdate obtained in the dark or during illumination and the resulting light-minus-dark difference spectrum. Inset: expanded portion (1620-1650 cm^{-1} region) of the light-minus-dark difference spectrum.

changes in the redox state of Cyt b559, plastoquinone, tyrosine, or from other amino groups that might be subjected to some modification of their interacting milieu following photooxidation of Z and P680. The IR spectra of the light-and dark-adapted Mn-depleted particles exhibited no major difference (frequency shifts) in the amide I (1657 cm^{-1}) and amide II (1544 cm^{-1}) domains, thus excluding any large conformational changes occurring upon charge separation which confirms the previous observations of Tavitian et al., (1986). Minor difference in the intensities of the amide I and amide II bands are reflected by shoulder peaks at 1656 and 1546 cm^{-1} in the difference spectrum.

Comparison of the light-minus-dark spectrum of Figure 25 with the known FTIR spectra does not give any clear evidence for the participation of Cyt b559 or plastoquinone in this spectrum. In fact, in the spectral region studied, Cyt b559 in its reduced form was characterized by vibration modes at 1685, 1673, 1641, 1620, 1545, and 1406 cm^{-1}, and the oxidized form absorbed at 1656, 1628, and 1608 cm^{-1} (Berthomieu et al., 1992). This pattern of bands is absent in the difference spectrum. At most, only a few minor bands or shoulders could correspond to the above-mentioned maxima and be assigned to the Cyt. In the case of plastoquinone, none of the bands associated with its vibration modes (Borthomieu et al., 1990) are found. In contrast with the study of (McDonnell and Barry, 1992), a positive band at 1514 cm^{-1} which they assign to oxidized tyrosine, is not found. Instead, a negative band at 1512 cm^{-1}, corresponding to loss of intensity of the tyrosine band at 1519 cm^{-1} in the IR spectrum obtained from the illuminated particles, is observed in the difference spectrum together with negative shoulder at 1607 cm^{-1}. These vibrations are characteristic of the ring modes of phenol groups that are absent in the tyrosine radicals (Tripathi and Schuler, 1984). The positive band at 1477 cm^{-1} may be tentatively associated with the C-C stretch mode of the tyrosine radical (Tripathi and Schuler, 1984). On the other hand, the positive features centered at 1400-1477 cm^{-1} are related to C-O stretching and C-H bending modes and can originate from either Chl or tyrosine.

The main and most interesting Chl bands are found in the region between 1735 and 1650 cm^{-1} in the difference spectrum of Figure 25 where their ester and ketone vibration modes are evidenced. Chl a usually shows two

bands in that region. An absorption band originates from its two ester groups at 1735 cm^{-1}, and a peak at 1694 cm^{-1} is due to the vibration modes of free (not hydrogen bonded) 9-keto C=O in ring V of the porphyrin (Ballschmiter and Katz, 1969). These two bands are found in the difference spectrum as negative features together with a third band at 1652 cm^{-1}, further evidenced in the inset of Figure 25, that could also be assigned to 9-keto C=O group. The presence of an absorption band at 1652 cm^{-1} was used as a diagnostic of aggregation interaction between Chl a molecules since it originates from coordinated C=O in Chl solutions (Ballschmiter and Katz, 1969). The occurrence of the peak at this frequency in the difference spectrum (Figure 25 and inset) could indicate that P680 is formed by coordinated Chl dimer. The above would imply the coordination of 9-keto function from one Chl to the central Mg ion of the other Chl which keeps its 9-keto group free (Ballschmiter and Katz, 1969). Alternatively, the strong negative band appearing at 1626 cm^{-1} can also be attributed to strongly associated 9-keto function (Chapados, 1988; Chapados et al., 1991) as similarly assigned in the difference spectrum obtained for triplet P680 (Noguchi et al., 1993).

Upon photooxidation of P680, the band at 1694 cm^{-1} that originates from the free 9-keto groups is shifted to higher frequencies and appears as positive absorption at 1714 cm^{-1} in the difference spectrum as in the case of photooxidation of monomeric Chl a or of the P700 Chl in the PSI reaction center complex (Nabedryk et al., 1990), indicating that this group is now in an environment with even less interaction or with lower dielectric constant (Chapados, 1988). On the other hand, the band at 1652 or the one at 1626 cm^{-1} assigned to strongly associated 9-keto group is shifted to 1676 cm^{-1}, a frequency still in the position of an associated ketone (possibly hydrogen-bonded) (Chapados, 1988; Chapados et al., 1991), but not indicative of coordination bond. We must note that in the difference spectrum, the absorption peaks cannot be quantitatively evaluated because of the presence of both positive and negative bands. Thus, it is not clear if the band at 1676 cm^{-1} originates from a shift of the band at 1652 or from that at 1626 cm^{-1}.

The occurrence of two pairs of bands attributed to 9-Keto groups (1714/1694 cm^{-1}, and 1676/1652-1626 cm^{-1}) demonstrate the dimeric nature of

P680 (Allakhverdiev et al., 1994) in agreement with recent FTIR studies of the triplet state of this reaction center (Noguchi et al., 1993). The above data are also in agreement with the known structure of the bacterial reaction center (Michel and Deisenhofer, 1988). The occurrence of a dimeric P680 with the radical of the charge separated state delocalised on one of the Chl could explain the conflicting interpretation of most of the data reported on the structure (monomeric or dimeric) of this reaction center (Van der Vos et al., 1992).

4. 7. EFFECT OF BETAINE AND SUCROSE ON PSII MEMBRANES

To investigate the effect of glycinebetaine and sucrose on the integrity of PSII-membrane protein, we have undertaken the analysis of the FTIR spectra of PSII-membranes incubated with betaine and sucrose separately at different temperatures, 20, 40, 60 and 70 °C, using resolution-enhancement and curve fitting techniques based on the amide I mode.

From the recorded absorption spectra of treated PSII-membranes or untreated PSII-membranes one cannot visualize any shift in the amide I bands. This special region (1700-1600 cm^{-1}) consists of a number of broad overlapping bands that cannot be resolved into individual components by an increase of the instrumental resolution. The amide I band consists of a number of individual bands at the frequencies characteristic for specific types of secondary structure (Susi and Byler, 1986, Surewicz and Mantsh, 1988), the secondary derivative analysis permits the direct separation of the amide I band into its sub-components (Dong et al., 1990). The various amide I bands identified in the resolution-enhanced spectra reflect different components of the protein secondary structure. Based on systematic studies of the frequency distribution of amide I bands of a number of proteins with known secondary structure (Byler and Susi, 1986), the assignment of the individual segments to specific components of this structure is feasible. Identification of the component bands in the second-derivative of amide I band contours not only enriches the qualitative interpretation of infrared spectra but also provides a basis for the quantitative analysis of the protein secondary structure.

SECOND-DERIVATIVES

To resolve the bands under the amide I of untreated and treated PSII we performed the derivative techniques using Spectra Calc. Algorithm. The second derivative mode and 9 points which gave a best fit were used. All the recorded absorption spectra were manipulated under similar conditions.

The intrinsic shape of the amide I band is approximated by a Lorentzian function (Surewicz and Mantsh, 1988). In the second-derivative spectrum, the peak frequency of an absorbance is identical with the original peak frequency, but the half-bandwidth of the original is reduced by a factor of 2.7 (Susi and Byler, 1983, 1986). The height of a second-derivative peak is proportional to the square of the original peak height with an opposite sign, and the half-bandwidth is inversely proportional to the square of the original half-bandwidth (Susi and Byler, 1983, 1986). The close correlation between the relative areas of assigned amide I bands in second-derivative spectra and known three dimensional structures (Dong et al., 1990) supports the use of the second-derivative infrared spectrum for the quantitative as well as qualitative evaluation of protein secondary structure.

The original spectra of all the measured untreated or treated PSII samples show a relatively narrow amide I band maxima at around 1656 ± 2 cm^{-1}. The frequency of amide I bands indicates that these complexes are enriched in α-helical character (Byler and Susi 1986; Krimm and Bandekar, 1986) secondary structure even when high temperature 70 °C were used. Compared with the infrared spectrum of the reaction center complex isolated from purple photosynthetic bacterium, *R.sphareoides.*(Nabedryk et al., 1982, 1988) the amide I band of the PSII membranes appeared to be narrower in bandwidth and more symmetric. This is indicative of a higher content of α-helices in the PSII membranes than in the bacterial counterpart.

The second derivative spectra of untreated and treated PSII-membranes (in the presence of 1M of betaine or sucrose) under elevated temperature are shown in Figures 26, 27 and 28. Upon application of second-derivative to the absorption spectra of untreated and treated PSII at the amide I region, seven

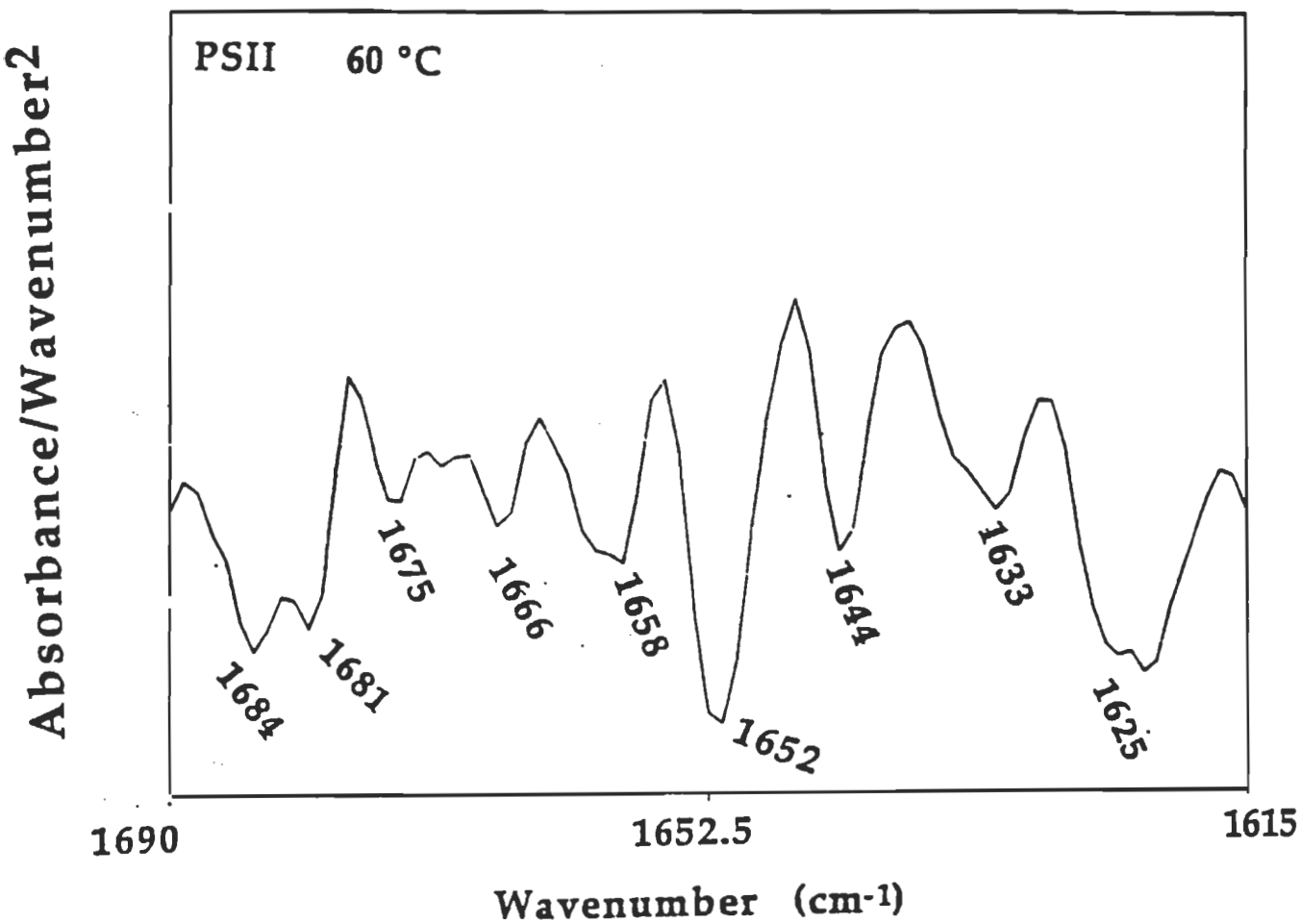

Figure 26 : FTIR spectrum in the amide I region of PSII membranes at 60 °C after resolution enhancement by Fourier second-derivative.

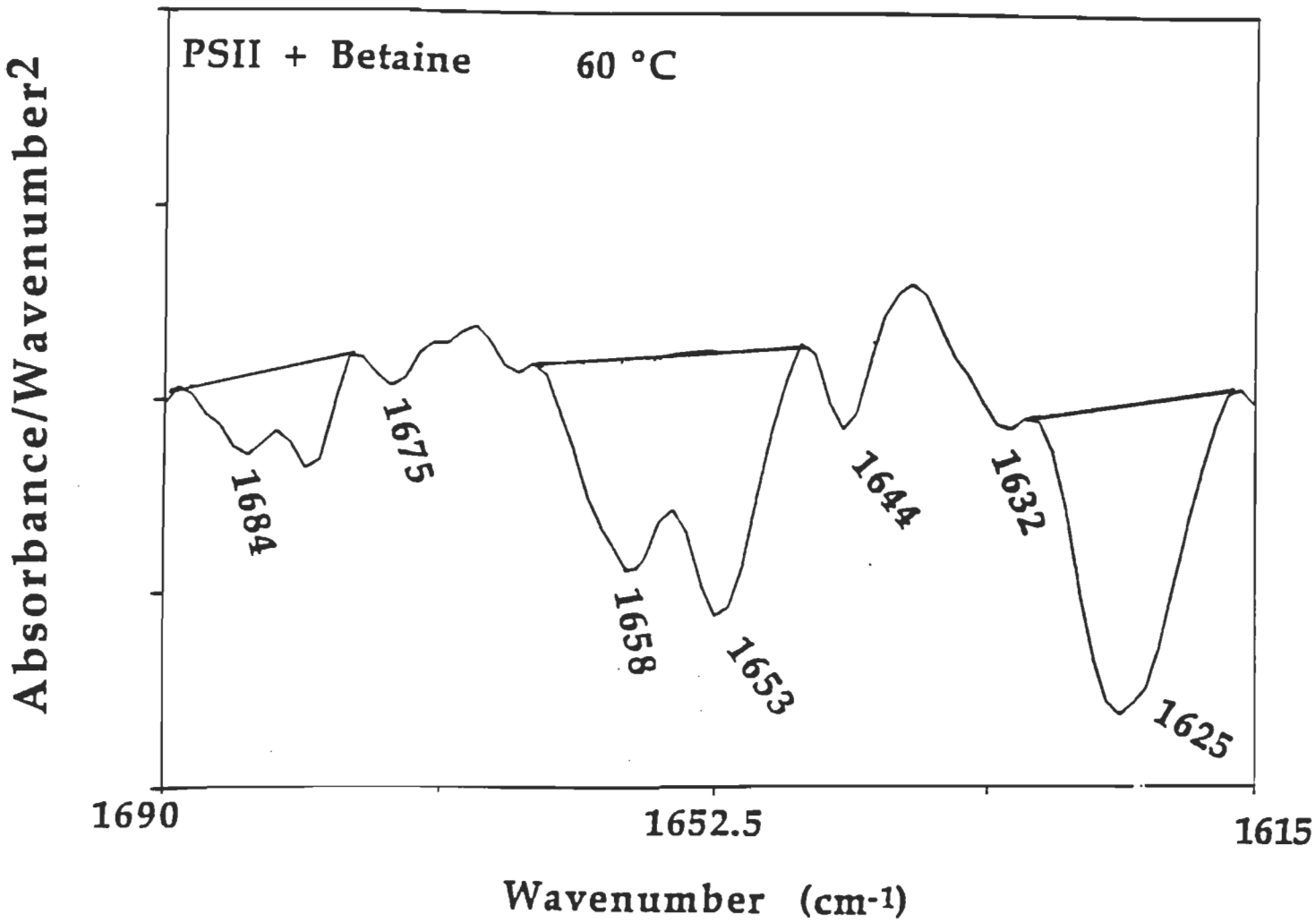

Figure 27 : FTIR spectrum in the amide I region of PSII membranes in the presence of betaine at 60 °C after resolution enhancement by Fourier second-derivative.

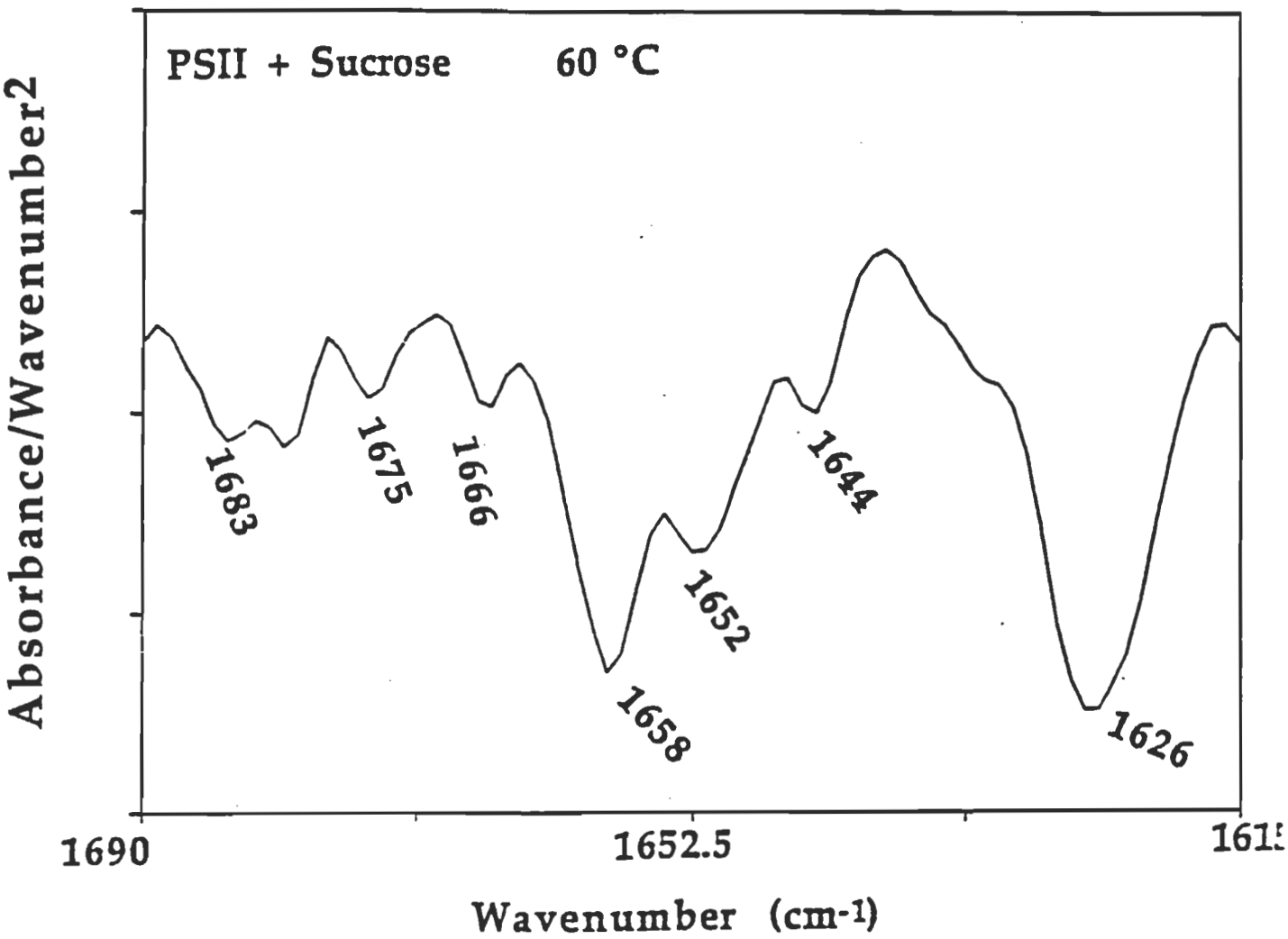

Figure 28 : FTIR spectrum in the amide I region of PSII membranes in the presence of sucrose at 60 °C after resolution enhancement by Fourier second-derivative.

major bands at the following frequencies, 1626, 1635, 1643, 1652, 1658, 1675, and 1684 cm^{-1} were revealed.

To quantify the amount of each type of secondary structures (α-helix, β-sheet, random, antiparallel) we calculated the area under each band in the second derivative spectra. Knowing the frequency of each component we determined the relative amount of each type.

The accuracy of measured band areas in amide I second-derivative spectra is dependent upon the correct positioning of the base line. In this regard Figure 27 will be used to explain how the bands under amide I can be measured, we utilized the procedure of (Dong et al., 1992) for this task. The dashed horizontal lines on second derivative spectrum of Figure 27 represent the base lines used to compute the relative amounts of each kind of secondary structure. Choice of base-line location can be reliably made if it is recognized that excursion above the true base line occurs. It was reported that the presence of a strong α-helix band results in unusually strong positive lobes on each side of the α-helix band (Martin, 1959; Kauppinen et al., 1981b). For this reason we could not draw an appropriate single base line because the spectrum of PSII-membranes has an extremely high α-helix content (Figure 27). Fortunately, small deviations in base-line position above or below the true base line only subtly affect the calculated relative percentages of major secondary structures. However, a three-base lines approach as shown in the spectrum for PSII-membranes in Figure 27 permits an approximate distribution among secondary structures to be determined. All bands peak area under the amide I band (region 1615-1690 cm^{-1}) for each frequency appearing in the second derivatives were calculated. Then the percentage of each band area was calculated by dividing the band area by the amide I band area. This procedure was carried on for three times on three different samples for each condition and the average of these measurements along with their coefficient of variation were calculated. The relative amounts of α-helix, β-sheet, turns and antiparallel secondary structures of treated and untreated PSII-membrane were calculated.

The second-derivative spectra at 20 and 40 °C for betaine-PSII and sucrose-PSII revealed that no major conformation changes were detected at these temperatures. However, at elevated temperature (60 °C and 70 °C) there were significant changes regarding β-structures, where some of the other structures were converted to β-sheet. The bands at 1633 and 1626 cm^{-1} were replaced by a single strong band at 1626 cm^{-1}. The amount of α-helix structure was not much affected in the presence of osmolite (glycinebetane or sucrose).

In the absence of the osmolite (glycinebetaine or sucrose) the intensity ratio of the peak at 1654 cm^{-1} to that at 1625 cm^{-1} decreases as temperature increases. This suggests that the content of β-sheet increases at the expense of α-helices and some other structures. However the temperature-induced spectral changes are not rapid and progress gradually over a wide temperature range.

The present data indicate that the thermally induced alteration in the secondary structure of untreated PSII-membrane is not a sharp event but it rather takes place over a wide temperature range. One of the consequences of the increased temperature is the reduction of the content of α-helical conformation. However when PSII-membranes were treated with betaine or sucrose at the different temperatures, this conformation change in α-helix content was very low.

CURVE-FITTING

Curve-fitting technique could be used individually or as a complementary method for second-derivatives to quantify the amount of the amide I band substructures. Once the number and approximate frequencies of the individual bands are determined from second derivative spectra, they can be used as input parameters for curve fitting analysis of the original spectrum, without this knowledge curve fitting would be meaningless, or risky at best. Initial band positions were taken directly from the second-derivative spectra (Figures 26, 27 and 28) and no additional band was added. During the curve-fitting process, the heights, widths, and positions of all bands were varied simultaneously. The relative integrated intensity of each band was then

calculated from final fitted band heights and widths. We repeated these experiments three times and the calculation was performed three times for each sample, then the average of these calculations along with their coefficients of variation were calculated

Figures 29, 30 and 31 illustrate the results of such curve-fitting applied to the original absorption spectra of PSII membranes, and treated PSII-membranes under different temperatures. It can be seen that the amide I band contour of the untreated and treated PSII-membranes consist of a strong center band at around 1655 cm^{-1} and few shoulder bands, two on each side of the 1655 cm^{-1} band. The exact positions of these shoulder bands are given in Table 3 along with their total areas as integrated intensities which in turn are related to the population of the corresponding substructures. If the amide I bands are of comparable absorptivities (a reasonable approximation), their integrated intensities are a measure of their relative concentrations. It should be emphasized here that the component bands identified by the curve-fitting analysis of the Figures, 29, 30 and 31 are essentially the same as those found with second-derivative enhancement, and no extra bands were assigned.

The component bands derived from the curve-fitting analysis of the amide I mode are best interpreted as reflecting at least four types of substructure in the untreated and treated PSII membrane. The amide I band at 1650-1660 cm^{-1} can be assigned unambiguously to α-helices, while the components band at 1620-1640 cm^{-1} are due to β-sheet ; in fact, the concomitant appearance of a band in the range 1680-1690 cm^{-1} has been associated with β-antiparallel structures (Susi et al., 1967). This leaves the bands in the range 1666-1675 most likely assigned to turns (Susi and Byler, 1983).

From the integrated intensity of these bands, the fractional percentage of all components structures under amide I band were determined.

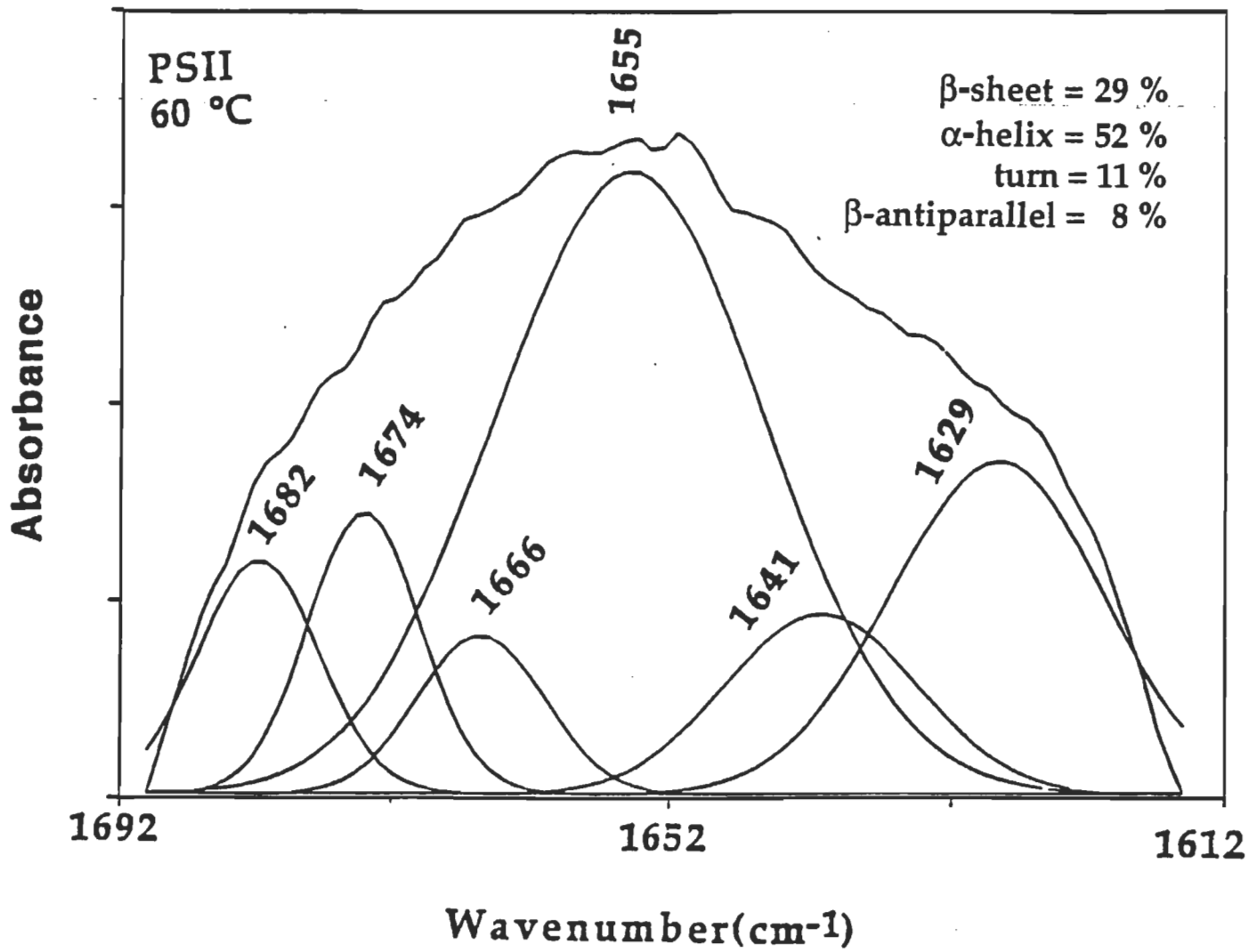

Figure 29 : The amide I band contour (1615-1690 cm^{-1}) with the best fitted individual component bands for Photosystem II-membrane protein at 60 °C.

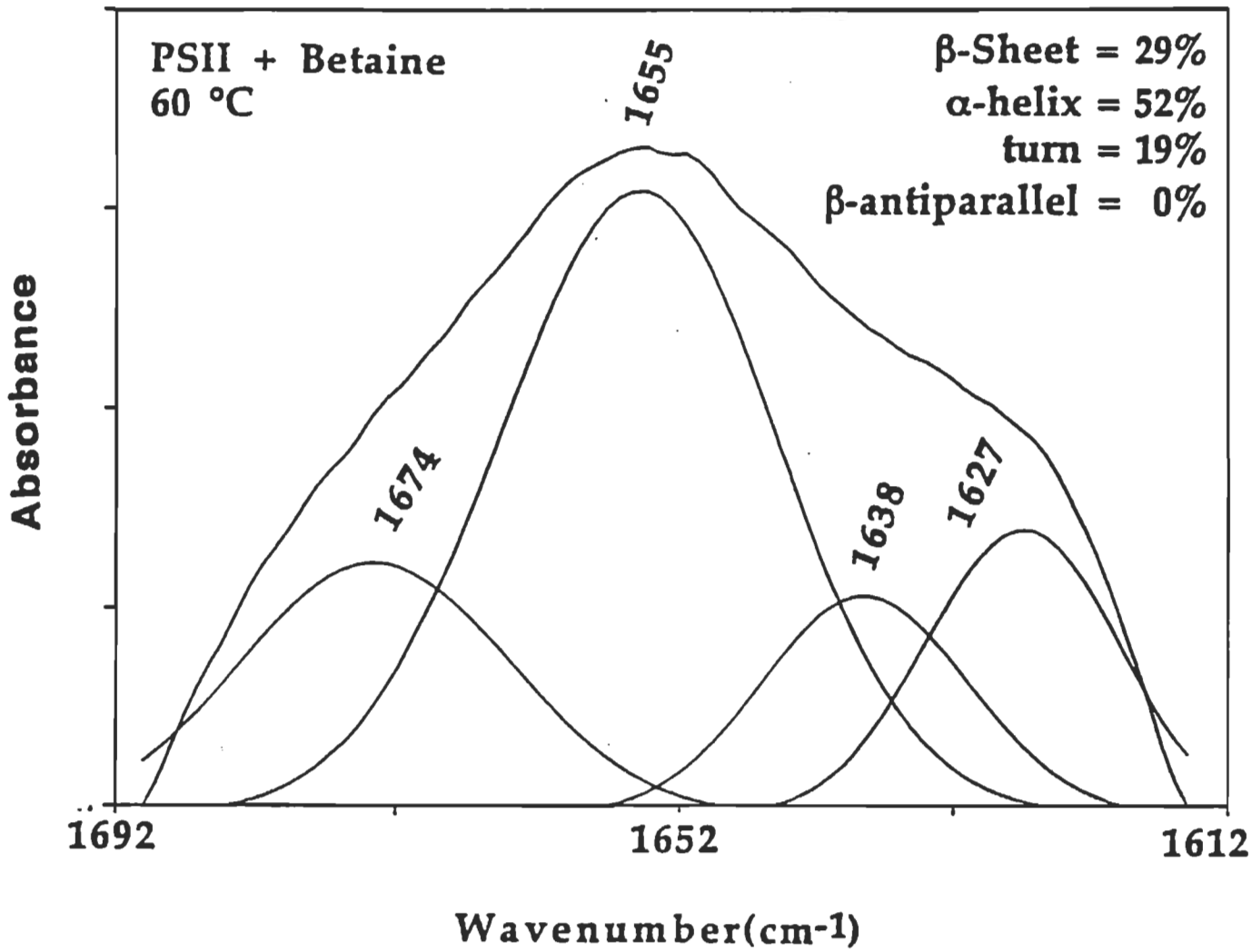

Figure 30 : The amide I band contour (1615-1690 cm^{-1}) with the best fitted individual component bands for Photosystem II membrane protein in the presence of betaine at 60 °C.

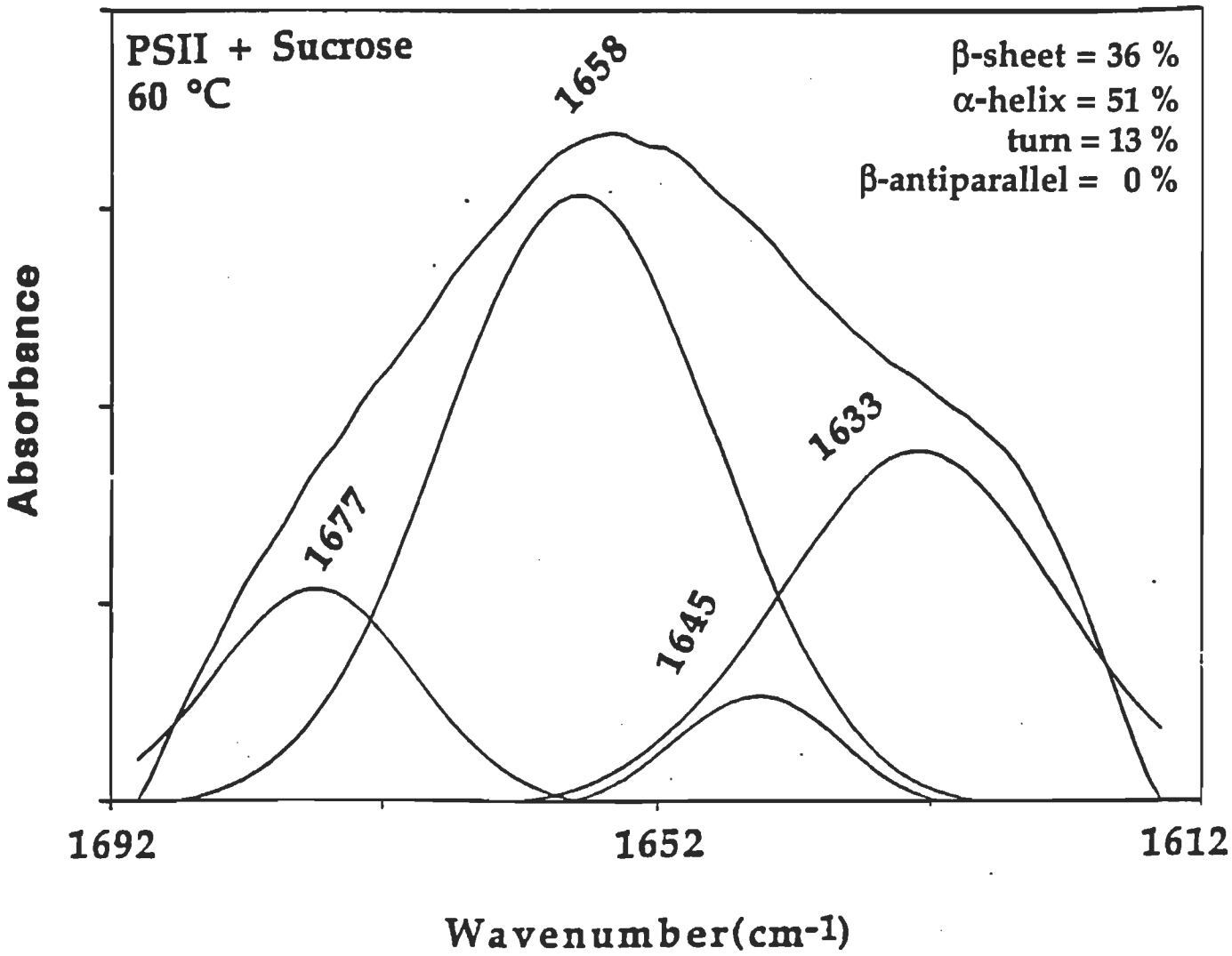

Figure 31 : The amide I band contour (1615-1690 cm^{-1}) with the best fitted individual component bands for Photosystem II membrane protein in the presence of sucrose at 60 °C.

The results of second-derivative and curve-fitting calculations are presented in Table 3. Each value on the Table represents the average of the two sets of measurements, for a second derivative and curve-fitting values.

The close agreement among these two methods (second-derivative and curve-fitting) adds confidence to the analysis and suggests that these infrared bands reflect real structural details, curve-fitting then provides the added advantage that it allows the relative contributions of the component bands to be estimated.

Data in Table 3 can explain the effect betaine and sucrose have on PSII-membranes at different temperatures. These results showed that the α-helix structure of PSII membrane was protected against increasing temperature. At 20 °C the α-helix content was about 58%, while β-sheet was 25%, turn structure 12 % and β-antiparrarllel 7.5 %. As the temperature increased to 40, 60 and 70 °C, the amount of α-helix decreased when osmolite was not present, but when osmolite was added the content of α-helix remained almost constant (50%). No major differences were observed for the betaine and sucrose in protecting the integrity of the PSII-protein structures under elevated temperature. However, the amount of β-sheet was increased as the temperature increasesd (10%), while the other structures decreased by temperature increases. The changes observed indicate that the thermal stability of the protein structure of PSII membrane increased in the presence of osmolite (glycinebetaine and sucrose).

In this context its worth mentioning the extensive studies by (Lee and Timasheff, 1981; Arakawa and Timasheff, 1982a, 1984a, 1985) on protein-solute-solvent interactions. According to these authors'concept, the determining factor for the protein response to specific solute was whether the thermodynamics of the protein-solute-solvent system dictated a preferential binding of the solute to the protein, or its preferential exclusion.

First, preferential solute binding typically favors changes of the native structure of the protein and, hence, causes protein denaturation. This can be rationalized intuitively with the favorable effect of an increased available protein surface (Gekko, 1983; Low, 1985; Arakawa et al., 1990). For the same

Table 3: The relative amounts of α-helix, β-sheet, turns and antiparrarel secondary structures of treated an untreated PSII along with the standard deviation. (number of measurements = 3).

Amide I Components (Cm^{-1})	Conformation PSII free				Conformation PSII + Betaine				Conformation PSII + Sucrose			
	20°C	40°C	60°C	70°C	20°C	40°C	60°C	70°C	20°C	40°C	60°C	70°C
1620-1640 β-sheet	23 ± 2	26 ± 5	29 ± 5	37±6	27± 2	26 ± 3	29 ± 4	23 ± 2	26 ± 3	22 ± 3	36 ± 4	30 ± 4
1650-1660 α-helix	58 ± 7	53 ± 5	52 ± 6	48 ± 4	53 ± 4	58 ± 5	52 ± 3	52 ± 4	53 ± 4	50 ± 4	51 ± 5	50 ± 5
1666-1680 Turn structure	12 ± 4	16 ±3	11 ±3	15 ± 3	16 ± 3	16 ± 3	19±3	15 ± 3	16 ± 2	20 ± 3	13 ± 2	20 ± 2
1680-1690 β-antiparallel	7±1	5 ± 1	8 ± 1	0	4 ±1	0	0	10 ± 2	5 ± 1	8 ± 1	0	0

reason, a binding of solutes tends to induce dissociation of polypeptides aggregates into their components.

Secondly, selective exclusion of a solute from the protein surface forces individual polypeptides as well as polypeptides assemblies to minimize their surfaces. This is accomplished by retaining native conformation and associations. Because proteins have a smaller surface in the native or folded state in comparison with their denaturated state, the tighter packaging of the proteins result in their stabilization (Ollis and White, 1990).

The entropic and enthalpic factors that determine preferential solute binding or preferential hydration, i.e., solute exclusion, vary with the nature of the solute but, to some degree, also with the protein (Gekko, 1983; Arakawa and Timasheff, 1985a). Consequently, the effectiveness of protectants may vary with the target proteins.

Our FTIR spectroscopy results, in Table 3 is in line with the framework of the second concept of Timasheff's group since selective exclusion of solute from protein surface forces individual polypeptides as well as polypeptides assemblies to minimize their surfaces. The results we obtained showed that the integrity of the PSII-protein was protected in the presence of betaine or sucrose. There were no indications for protein denaturation under the effect of these two solutes, where the amount of α-helical and β-sheet structures suffered no major conformation changes even when high temperature (60 and 70 °C) were applied. Accordingly the result obtained by our method are in favors of the second concept of Timasheff and his group, and exclude the preferential binding of the solute to the protein, which can result in the changes of the native structure of the protein, and hence denaturation, which is not the case for our data.

A similar interpretation was also postulated by Stewart and Bendal (1981) who proposed that the presence of highly hydrophobic solutes such as glycinebetaine reduces the concentration of free water at the protein interface and therefore intensifies hydrophobic interactions. This interpretation also explains the stabilization of multisubunit protein complexes as confirmed by the stabilization of the binding of the extrinsic polypeptides in the oxygen

evolving complex of PSII (Stamatakis and Papageorgiou, 1993; Williams and Gounaris, 1992).

Regardless of the mechanism involved, it is apparent that the structure stabilizing or modifying effects of betaine or sucrose in the suspension media of PSII membranes preparations cannot be ignored. Sometimes they are taken for granted, e.g., when sucrose is routinely included in the storage and assay media or even required for activity (Satoh and Katoh, 1985), or when the preparations are stored as highly concentrated suspensions in which the membrane protein assemblies themselves may act as mutually stabilizing preferentially hydrated constituents (Collins and Washabaugh, 1985).

4. 8. SECONDARY STRUCTURE OF 33 kDa PROTEIN

The manganese-stabilizing protein (33 kDa), which was isolated by a two-step salt washing procedure, showed a high degree of purity when analyzed by SDS-PAGE (Figure 32, lane 3). No contamination with either the 24, or 17-kDa extrinsic proteins was evident with Coomassie Blue staining even on heavily overloaded gels (20 μg of 33 kDa-protein). It should be noted that this result was only obtained when freshly isolated membranes were used for the protein isolation; PSII-membranes which had been stored overnight on ice or which had been frozen yielded manganese-stabilizing protein preparations which exhibited significant contamination by the 24, and 17-kDa proteins.

Figure 33 shows the densitograms of the purified manganese-stabilizing protein which was deposited in lane 3 in the electrophoreses. It is obvious that only one component was obtained in this purification procedure, at 33-kDa range, there is no traces of neither 17 nor 24-KDa extrinsic protein. From the integrated area the percentage of 33-kDa was more than 99%. These are clear indications that the 33-kDa which we used for the FTIR measurement was pure protein, and only one type of extrinsic protein.

Vibrational spectra of 33 kDa protein consists of several characteristic bands in the mid-infrared region. Figure 34 shows the absorption spectra of 33 kDa protein, the spectrum exhibits absorbance maxima for amide I and amide II near 1650 and 1545 cm^{-1}, respectively. The vibrational mode most useful for

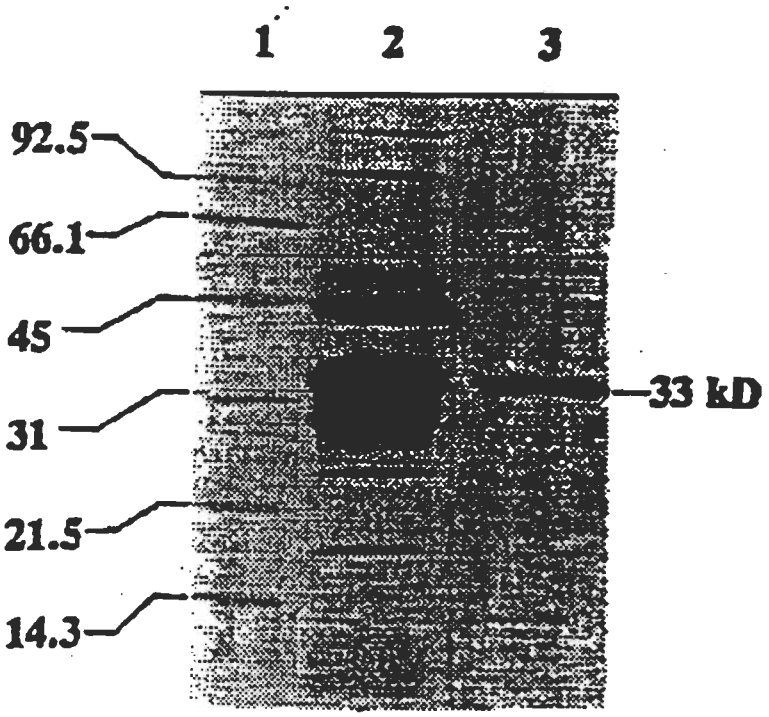

Figure 32 : Polyacrylamide gel electrophoresis of pure 33 kDa extrinsic polypeptide. Lane 1, molecular weight standards (for phosphorylase B, bovine serum albumin, ovalbumin, carbonic anhydrase, soybeal tripsin inhibitor, and lysozyme); lane 2, polypeptide profile of the PSII submembrane fraction; lane 3 isolated 33 kDa extrinsic polypeptide (15 μg).

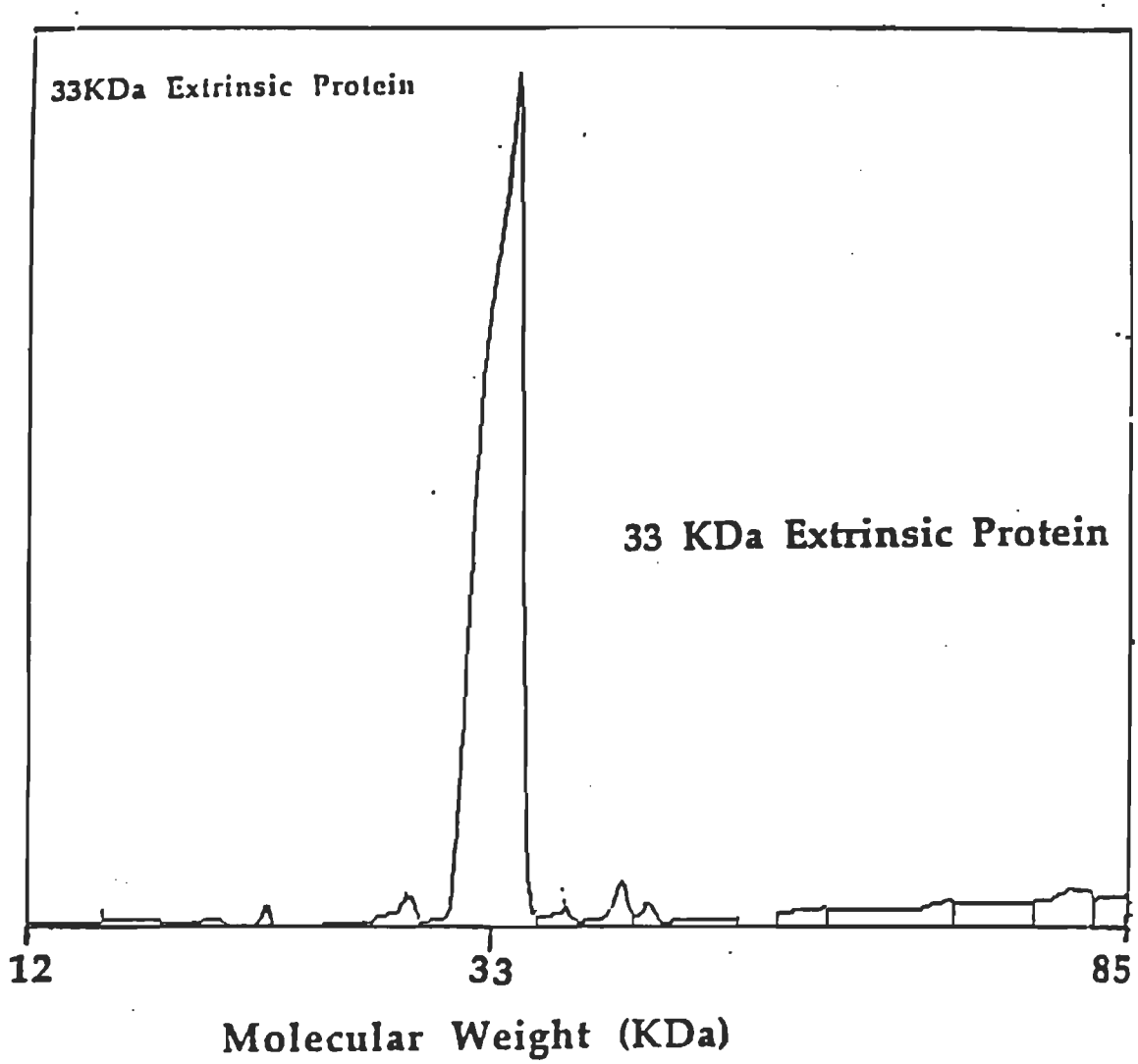

Figure 33 : Densitogram of manganese-stabilizing protein (33 kDa).

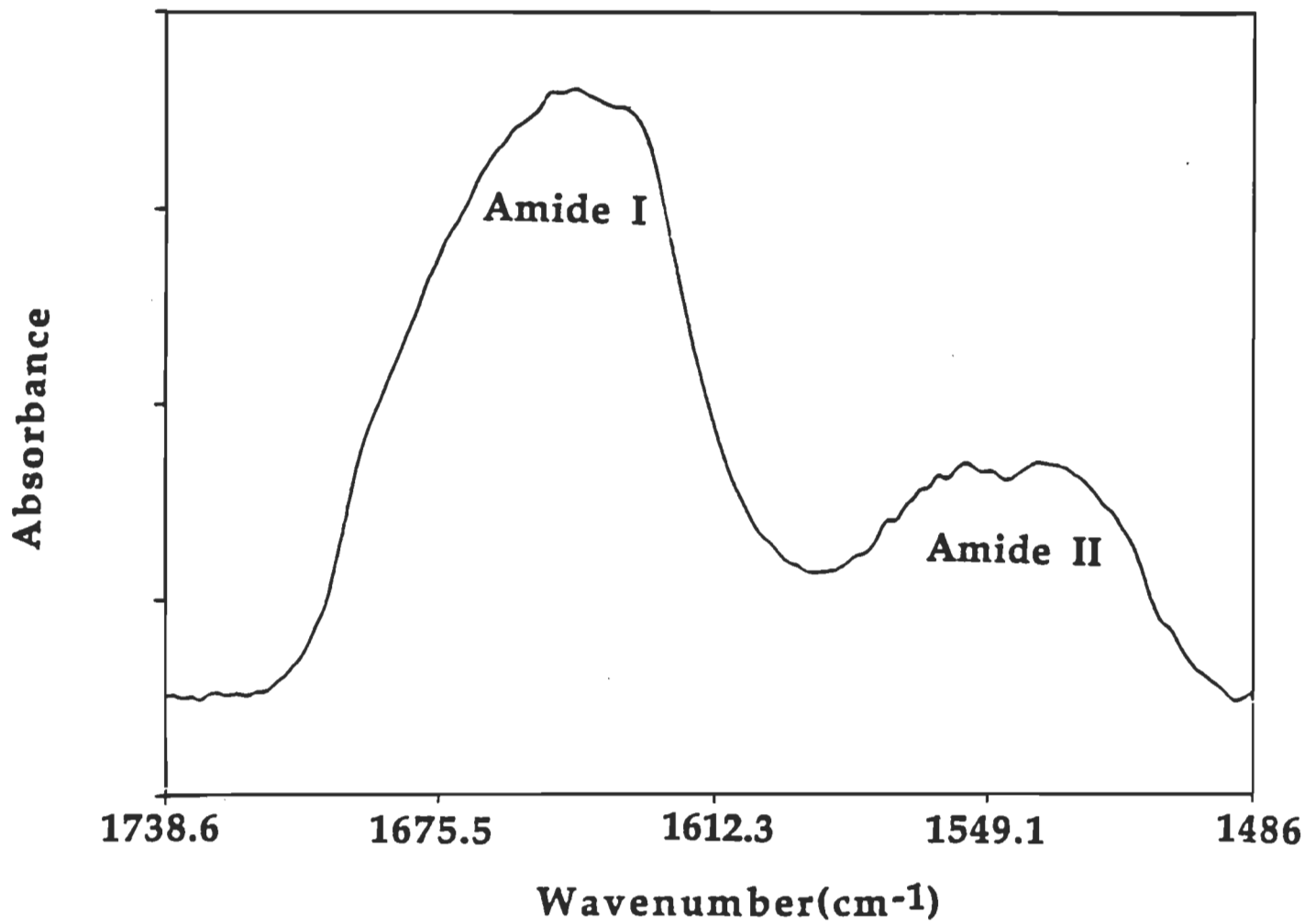

Figure 34 : FTIR absorption spectrum of manganese-stabilizing protein (33 kDa) in the region of the amide I and amide II.

the analysis of protein secondary structure is the amide I band between approximately 1600 and 1700 cm^{-1}. The amide I region of the infrared spectrum of 33 kDa shows a maximum at about 1648 cm^{-1} and a very intense shoulder between 1620 and 1635 cm^{-1} (Figure 34). While these two spectral features already indicate the presence of both α-helical and β-type conformations (Susi et al., 1967; Parker, 1983) further details are likely to be hidden by the partial overlapping of bands that are characteristic of various components of protein secondary structure (Susi and Byler, 1983, 1986; Byler and Susi, 1986; Yang et al., 1987). Indeed, the Fourier-deconvolved spectrum and secondary derivative shown in Figures 35 and 36 respectively reveal the presence of about five components in the amide I region of the 33 kDa protein. The frequencies of component bands identified in the resolution-enhancement spectra can be used subsequently as input parameters for curve-fitting of the original broad amide I band contour (without knowing the number and approximate positions of the components any curve-fitting analysis would be meaningless). The results of such curve-fitting analysis of the spectral region of the amide I band of 33 kDa protein is shown in Figure 37. The frequencies of the best fitted component bands correspond closely to those identified in the resolution enhanced spectrum (Ahmed et al., 1995).

The most prominent feature in the amide I region of the infrared spectrum of the 33 kDa protein is a band at 1629 cm^{-1} (Figures 36 and 37). This component, which accounts for 36% of the total area of the amide I band, can be assigned unambiguously to protein segments in the β-sheet conformations (Susi and Byler, 1986; Susi et al., 1969; Byler and Susi, 1969). In fact, the presence of more than "β-component" in the spectrum region between 1620 and 1646 cm^{-1} has been observed for a number other proteins (Byler and Susi, 1969). These components most likely represent β-type segments with a slightly different pattern of hydrogen bonding. Although tempting, the assignment of the different "β-bands" to specific classes of β-strand (i. e parallel and antiparallel) is not straightforward and, at least at present, would be purely speculative.

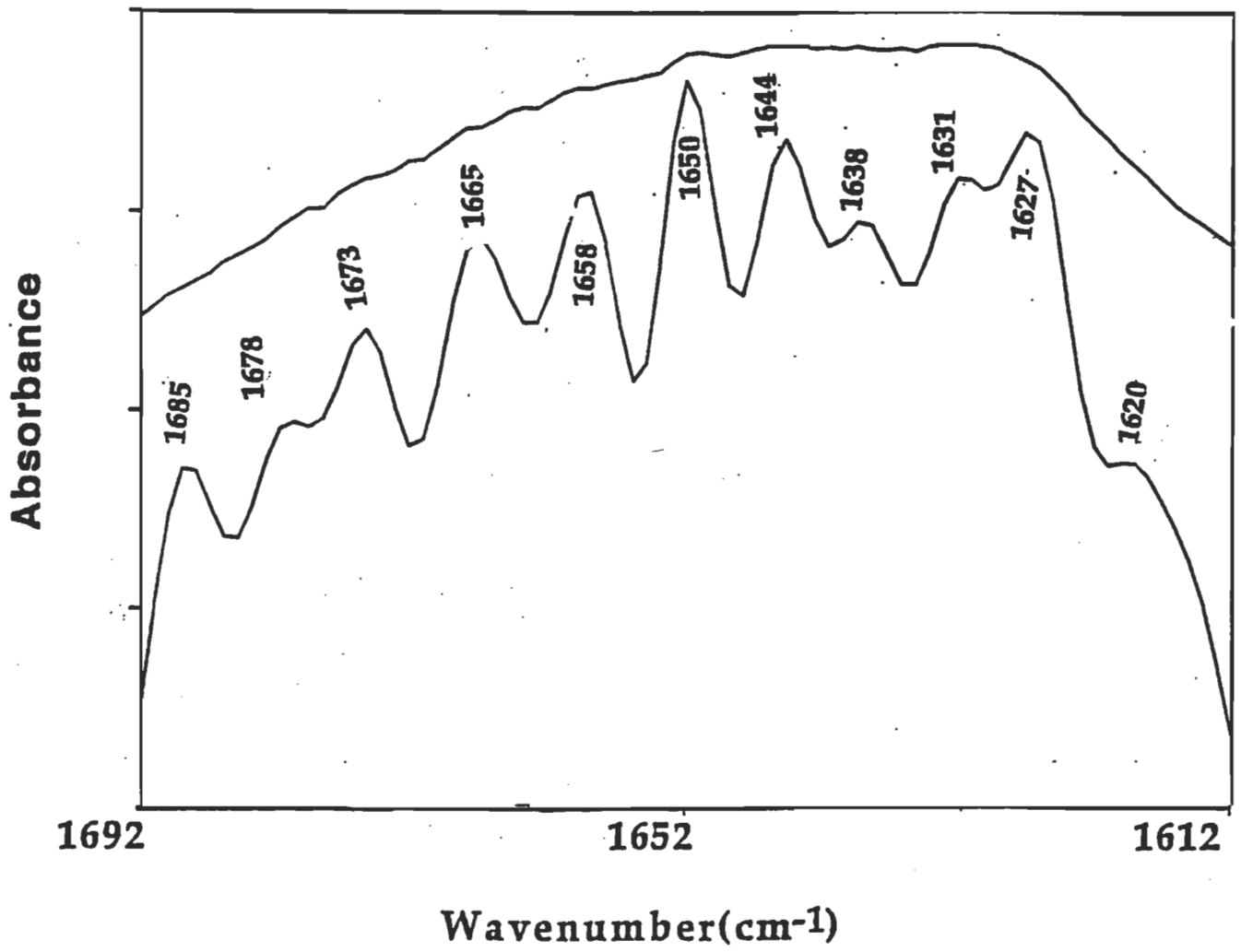

Figure 35 : FTIR spectrum in the amide I region of manganese-stabilizing protein (33 kDa) after band narrowing by Fourier deconvolution.

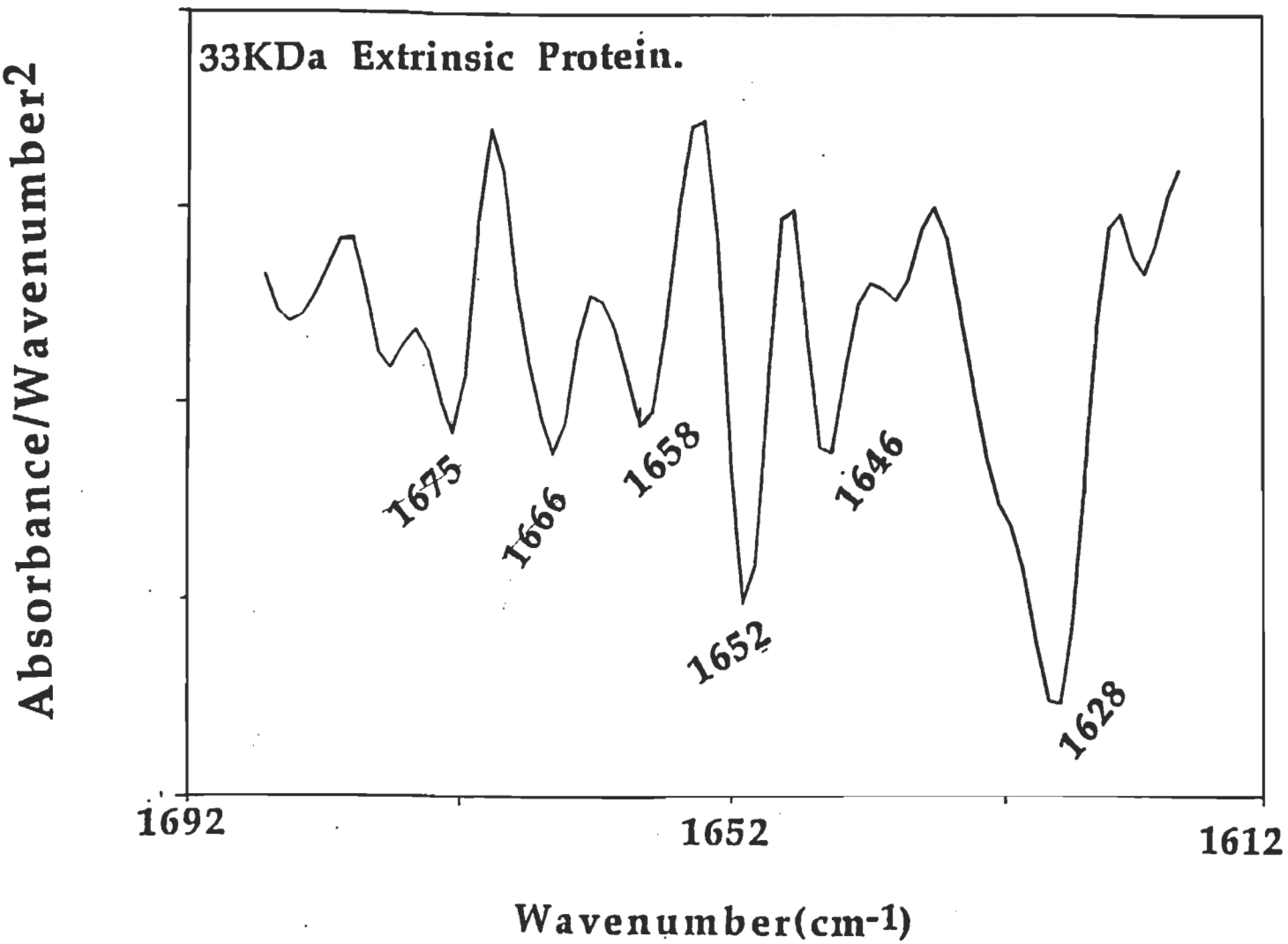

Figure 36 : Second-derivative amide I infrared spectrum of manganese-stabilizing protein (33 kDa).

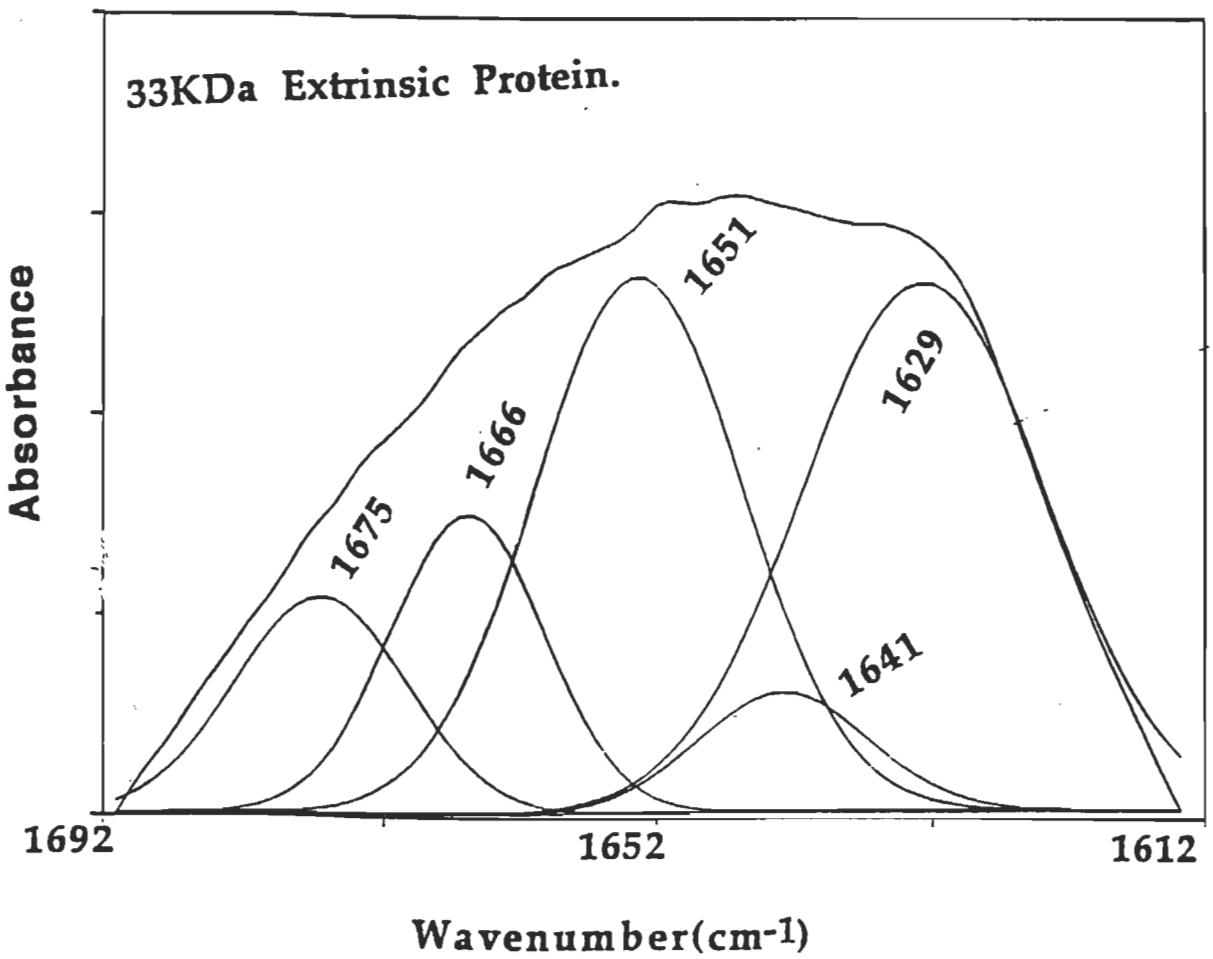

Figure 37 : The amide I band contour (1612-1692 cm^{-1}) with the best fitted individual component bands for manganese-stabilizing protein (33 kDa).

Fourier resolution enhancement reveals that the other bands seen in the original spectrum of Figure 34 consists of five bands with major bands at 1652, 1658 and three smaller bands at 1666, 1675 and 1685 cm^{-1}. The frequency of 1652 and 1658 cm^{-1} bands are highly characteristic of α-structures (Byler and Susi, 1986; Yang et al., 1987).

The assignment of the three minor components at 1666, 1673 and, 1685 cm^{-1} (Figures 36 and 37) is less certain as both bands due to turn structure (1666, and 1675 cm^{-1}) are coupled with high frequency vibrations of β-segments (1685 cm^{-1}) which might contribute to the spectruml region between 1666 and 1690 cm^{-1} (Susi and Byler, 1986; Haris et al., 1986). The frequencies of bands due to these different structures may in certain cases be very close or even coincide. In previous analyses of infrared spectrum of water soluble proteins, turns have been assigned to bands around 1666 cm^{-1} as well as to frequencies above 1680 cm^{-1} (Byler and Susi, 1986; Yang et al., 1987). A usually weak band occurring at around 1675 cm^{-1}, on the other hand, has been attributed to in-phase vibrations of β-segments in antiparallel conformation (Byler and Susi, 1986).

Table 4 shows the secondary structure fractions which were determined from the FTIR spectroscopy using resolution enhancement and curve-fitting procedures. It is obvious from the data presented in Table 4 that the 33 kDa extrinsic protein contains a relatively large proportions of β-sheet structure (36%) and a sizable amount of α-helical structure (27%).

The secondary structure analysis obtained by FTIR were also compared with those of other results predicted from either unconstrained Chou-Fasman analyses (Chou and Fasman, 1978) or from the methods of Biou et al.,(1988) as implemented by Beauregard for the 33 kDa extrinsic protein (Beauregard, 1992).

Neither computational approach provides a satisfactory description of the secondary structure contents. Chou-Fasman estimates α-helix to represent 28 % of the protein domains, which is similar to our method, however it seriously underestimates the amounts of β-sheet and turn conformations. The analysis of Beauregard, (1992) seriously underestimated β-sheet (9%) and

Table 4 : Secondary Structure Analysis of the 33 kDa Extrinsic Polypeptide.

Secondary structure type	Circular[a] Dichroism	Chou-Fasman[b]	Beauregard[c]	FTIR[d]
α-Helix	9%	28%	13%	27 ± 3%
β-sheet	38%	25%	9%	36 ± 4 %
Turn	17%	12%	------	24 ± 3%
Other	35%	35%	------	13 ± 2%

[a] from (Xu and Bricker, 1994).

[b] from (Chou-Fasman, 1978).

[c] from (Beauregard, 1992).

[d] this study, number of measurements =3, (Ahmed et al., 1995).

α-helix (13%) contents of this protein and besides, it could not predict the amount of turn or antiparallel structure in the polypeptide.

The secondary structure fractions recently obtained from the circular dichroism method (Xu and Bricker, 1994) yields fairly reliable appraisal of the amount of β-structure (38%) but the amount of α-helix (9%) and turn (17%) were seriously underestimated (Table 4). The present infrared spectroscopic study shows that the main components of the secondary structures of the 33 kDa polypeptides is β-sheet. Qualitatively, this is in agreement with the results obtained from (Xu and Bricker, 1994). However, quantitative measurement of the protein secondary structure obtained from the analysis of the infrared and circular dichroism data are considerably different (Table 4).

The reasons for the discrepancies between the estimates of 33 kDa obtained from the analysis of circular dichroism and infrared data are not fully clear. The source of potential error in these two approaches are different. The CD spectrum of protein is affected by interfering absorption and, particularly in a membrane environment, by light scattering (Mao and Wallace, 1984). Quantitative analysis of circular dichroism spectra relies on the set of reference data (Chang et al., 1978). These data, obtained from the spectra of aqueous solutions of globular protein of known three-dimensional structure, may be not fully applicable to membrane proteins in a hydrophobic environment or for membrane bound protein even after their isolation. Estimates of the secondary structure based on circular dichroism spectra are also influenced by uncertainties in protein concentration.

The approach used in this study seems to be free of most of the problems listed above. Particularly, the analysis based on infrared spectra does not depend on any transferred secondary structure data. On the other hand, a potential source of uncertainty in quantitative interpretation of infrared data arises from the ambiguity in the assignment of the component bands between 1670 and 1680 cm^{-1}. This problem concerns particularly those cases where the characteristic "turn" band around 1665 cm^{-1} is not observed in the infrared spectra. Under certain circumstances the above ambiguity may effect the accuracy of the estimate of the α-helix content. Another problem with analysis of infrared spectra arises from the unknown intrinsic absorptivities of the amide I vibrations of C=O groups in differential conformational states. The present approach is based on the assumption that the various amide I bands have comparable absorptivities and, accordingly, that the total fractional areas of band assigned to various components of the secondary structure represent the real content of these structures. The good correlation that was found for more than 20 proteins between the secondary structure estimates obtained from X-ray data and infrared analysis (Goormaghtigh et al., 1990) strongly suggests that this assumption provides a realistic approximation that will not lead to systematic errors.

Thus, although certain approximations are involved in the quantitative interpretation of infrared spectra, we believe that the present estimate of a

secondary structure, and particularly the relatively high content of β-type conformations, represents a real structural property of 33 kDa. In fact, the main spectral features characteristic of β-structure are seen even without deconvolution or second derivatives, and the overall shape of the amide I band contour is similar to that of other protein containing both β-structure and sizable amount of α-helix conformation.

The quantitative interpretation of the infrared spectra obtained from the isolated 33 kDa polypeptide must be taken with caution because the extrinsic protein may undergo some minor conformational changes during its removal from the PSII membranes. We believe that the present analysis of the secondary structure, and particularly the relatively high content of β–type conformation, represent a real structural property of the polypeptide in solution but some rearrangements may occur upon binding to the PSII core.

CHAPTER IV

CONCLUSIONS

The objective of this work was to use FTIR spectroscopy with its enhancement-resolution techniques to investigate the following:

I-The effect of metal ions on the isolated Light Harvesting Complex (LHCII)
2-The structure of Chl $P680^+$
3-Effect of heat treatment on PSII in the presence of osmolite
4-Secondary structure of 33 kDa extrinsic protein.

In the course of this study we can draw the following conclusions:

1- Fourier-transform infrared spectroscopy is a valuable method for the study of protein conformation in solution primarily because of the sensitivity to conformation of the amide I band (1700-1620 cm^{-1}) which arises from the backbone C=O stretching vibration. Combined with resolution-enhancement techniques such as derivative spectroscopy and self-deconvolution, plus the application of iterative curve-fitting techniques, this method provides a wealth of information concerning protein secondary structure. Further extraction of conformational information from the amide I band is dependent upon discerning the correlations between specific conformational types and component bands in the amide region.

2-There were several reports in the literature which dealt with the factors affecting the composition and structure of LHCII among these factors, the effects of radiant energy, herbicides, low temperature, mineral deficiency, heavy metal pollution and specific mutations were investigated. The results of these authors unequivocally indicate a positive correlation between the level of trans-16 : 1 acid and the oligomerization of LHCII. These studies concluded

in vivo and in vitro these factors disturb the association of the proteins subunits into the oligomeric form of this complex. The most visible symptom of the metal ion toxicity is the loss of chloroplast membrane constituents such as carotenoids and lipoquinones. A decrease in Chl content was observed and the changes observed in the photochemical activities may have resulted from ultrastructural changes in chloroplast under the metal ion trearement.
In this work we investigated the effect of several heavy metal ions on the secondary structure of the light-harvesting protein complex using Fourier transform infrared with its resolution enhancement techniques.

The interaction of divalent heavy metal ions with the light-harvesting (LHC-II) proteins of chloroplast thylakoids membranes was investigated in aqueous solution at different metal ion concentrations (0.01 to 20 mM), using Fourier transform infrared (FTIR) difference spectroscopy. The infrared difference spectroscopic results for the amide I and amide II regions (1800-1500 cm^{-1}) have shown a strong metal-protein interaction at high metal ion concentrations, whereas at a very low concentration the metal cation binding is negligible. The metal ion binding is mainly *via* the protein carbonyl group at low cation concentration, whereas metal ion coordination to the protein C=O and C-N groups were observed at higher cation concentrations. The metal-tyrosine binding was also observed for some ions at high metal ion concentrations. Major conformational changes from α-helix to those of the β-sheet and turn-structures were observed, in the presence of these metal cations at high concentrations. There have been several reports in the literature concerning the functional effect of metal ion on the LHCII.

3-The structure of the primary electron donor of photosystem II $P680^+$ was studied to examine if it is composed of Chl monomer or dimer. In this study, FTIR spectroscopy was used to analyze the changes in the vibration modes occurring upon photooxidation of $P680^+$ in a Mn-depleted PSII. It is demonstrated that illumination of the above in the presence of artificial electron acceptors (500 μM potassium ferricyanide and 10 μM silcomolybdate) results in a light-minus-dark absorbance change typical of the formation of $P680^+$. The light-minus dark FTIR spectrum obtained under similar conditions is characterized by two negative peaks located at 1694 and 1652 or 1626 cm^{-1} that

can be assigned to the 9-keto groups of the P680 Chl, the latter band being indicative of a strongly associated group. These vibrations are shifted to 1714 and 1626 cm^{-1}, respectively in the positive features of the difference spectrum attributed to $P680^{+}$. The occurrence of two pairs of bands attributed to 9-keto groups is discussed in terms of P680 being formed of a Chl dimer.

4-The integrity of Photosystem II membranes isolated from chloroplast thylakoids is profoundly affected by the solute environment. Recently it was shown that glycinebetaine was effective in protecting the evolution of oxygen against heat, prevented the dissociation of the 18, and 23 kDa extrisic proteins from the photosystem II complex in the presence of 1 M NaCl. It also prevented the dissociation of 33-kDa extrinsic protein.

Using FTIR spectroscopy we studied the heat treatment effect on the secondary structure of PSII-protein in the presence of glycinebetaine and sucrose. It is concluded that glycinebetaine and sucrose act as protecting agent for the PSII-membrane protein under elevated temperature. Some of the β-structures were converted to β-sheet, where the integrity of α-helical structure was almost protected (table 5) and no major conformation changes were observed. The presence of a high percentage of α-helical structural at even elevated temperature (70 ^{o}C) was a great indication of the protection of PSII-protein at high temperature in the presence of glycinebetaine or sucrose. These results can be accommodated readily in a concept developed by Timasheff and his coworkers according to which the responses of proteins to their solute environment are consequences of interaction preferences among the constituents of the solvent -protein-solute systems.

5-The 33 kDa extrinsic protein of PSII is an important component of the oxygen-evolving apparatus which functions to stabilize the manganese cluster at physiological chloride concentrations and to lower the calcium requirement for oxygen evolution. Chou-Fasman analysis of the amino acid sequence of this protein suggests that this component contains a high proportion of α-helical structure. A computational study using more sophisticated techniques concluded that the protein contained little periodically ordered secondary structure. In this study, we have measured the relative proportions of

secondary structure present in 33 kDa protein using FTIR spectroscopy. Our results indicate that, the manganese-stabilizing-protein (33 kDa) contains a large proportion of β-structure (36%), relatively small amount of α-helical structure (27%), 24% turn and 13% other structures.

6-Finally these studies demonstrate that the real power of FTIR spectroscopy lies in the ability to corroborate secondary structure or to follow relative changes in protein structure as a function of selected variables. This ability of resolution-enhanced FTIR to provide a rapid, reliable structural characterization is of importance when structural information from X-ray crystallography is unavailable.

REFERENCES

Abadia, A., Ambard-Bretteville, F., Remy, R., Tremolieres, A. (1988). "Iron deficiency in pea leaves: effect on liquid composition and synthesis". Physiol Plant. 72, 713-717.

Ahmed, A., Tajmir, H. A. (1993). "Interaction of toxic metal ions Cd^2, Hg^{2+},and Pb^{2+} with light harvesting complex proteins of chloroplast thylakoids membranes an FTIR spectroscopic study". **J. Inorg. Biochem.**, 50 , 235-243.

Ahmed, A., Tajmir, H. A. (1994). "Interaction of Mg(II), Ca(II), and Mn(II) with light harvesting complex of chloroplast thylakoids membranes". **J. Molec. Struct.,** 319, 145-151.

Ahmed, A., Tajmir-Riahi, H. A., Carpentier, R. (1995). "A quantitative secondary structure analysis of 33kDa extrinsic polypeptide of photosystem II by FTIR spectroscopy". **FEBS. Lett.,** 363. 65-68

Alberdi, M., Corcuera, L.J. (1991). "Cold acclimation in plants". **Phytochemistry,** 30, 3177-3184.

Alex, S., Tajmir-Riahi, H. A, Savoie, R. (1987). "The methyl mercury (II) binding on the conformation of poly (L-glutamic acid) and poly (L-lysine): A Raman spectroscopic study". **Biopolymers,** 26, 1421.

Allakhverdiev, S.I., Shafiev, M. A, Klimov, V. V. (1986). "Effect of reversible extraction of manganese on photooxidation of chlorophyll P680 in photosystem II preparation". **Photobiochem. Photobiophys.**, 12, 61-65.

Allakhverdiev, S.I., Klimov, V. V. (1992). "Topography of photosystem II reaction center components in thylakoid membranes". **Z. Naturforsch,** 47c, 57-62.

Allakhverdiev, S. I., Klimov, V. V., Carpentier, R., (1994). ´´Variable thermal emission and Chlfluorescence in photosystem II particles". **Proc. Natl. Acad. Sci., USA**, 91, 287-285

Allakhverdiev, S. I., Ahmed, A., Tajmir-Riahi, H. A., Klimov, V. V., Carpentier, R. (1994). "Light-Induced Fourier Transform Infrared spectrum of the Cation Radical $P680^+$". **FEBS Lett.**, 339, 151-154.

Allen, J. P., Feher, G., Yeates, T. O., Komiya, H., Rees, D. C. (1987). "Structure of the reaction center from Rhodobacter sphaeroides R-26: The protein subunits". **Proc. Natl. Acad. Sci. USA**, 84, 5730-5734.

Andersson, B., Akerlund, H-E. (1987). "Protein of the oxygen evolving complexe in the light reactions. in : Topics in Photosynthesis., (Barber, J., eds.), Vol 8, pp. 379-420, Elsevier, Amsterdam.

Andersson, B., Critchely, C., Ryrie, J., Jansson, C., Larsson, C., Anderson J. B. (1984). "Modification of chloride requirement for photosynthetic O_2 evolution, the role of 23 kDa polypeptide." **FEBS Lett.**, 168, 112-115.

Andersson, B., Styring, S. (1991). in : Current Topics in Bioenergetics (Lee, C.P. eds.) Vol 16, pp 1-81, Academic Press , San Diego.

Andreaesson, L. E., Vangard, T. (1988). "Electron Transport in Photosystem I and II." **Ann. Rev. Plant Physiol. Plant Molec. Biol.**, 39, 379-411.

Arakawa, T., Carpenter, J. F., Kita, Y. A., Crowe, J. H. (1990). "The basis for toxicity of certain cryoprotectants: A hypothesis." **Cryobiology,** 27, 401-415.

Arakawa, T., Timasheff, S. N. (1982a). "Preferential interactions of proteins with salts in concentrated solutions". **Biochemistry**, 24, 6544-6552.

Arakawa, T., Timasheff S. N. (1984a). "Protein stabilization and destabilization by guanidinium salts". **Biochemistry**, 23, 5912-5923.

Arakawa, T., Timasheff, S. N. (1985a). "The stabilization of proteins by osmolytes". **Biophys. J.**, 47, 411-414.

Arakawa, T., Timasheff, S. N. (1985b). "Mechanism of poly (Ethyleneglycol) interaction with proteins". **Biochemistry**, 24, 6756-6762.

Arnon, D. T. (1949). "Copper enzymes in isolated chloroplats Polyphenoloxidase in Beta vulgaris". **Plant Physiol.**, 24, 1-15.

Arnon, D.T. (1991). "Photosynthetic electron transport emergence of a concept, 1449-1459". **Photosynth. Res.**, 29, 117-131.

Bagley, K., Dolinger, G., Eisenstien, L., Singh, A. K., Zimanyi, L. (1982). "Fourier transform infrared difference spectroscopy of bacteriorhodobsin and its photoproducts". **Proc. Natl. Acad. Sci. USA,** 79, 4972-4976.

Barber, J. (1987). "Photosynthetic reaction centers: a Common link". **Trends Biochem. Sci.**, 12: 321-326.

Baron, A., Areuano, J.B., Schroder, W., Lachica, M., Chueca, A. (1993). "Copper binding sites associated with photosystem 2 preparation". **Photosynthetica**, 28, 195-204.

Baszynski, T. (1986). "Interference of Cd^{2+} in functioning of the photosynthetic. apparatus of higher plats". **Acta Soc. Bot. Pol.**, 55, 291-304.

Baszynski, T., Wajda, L., Krol., M., Wolinska, D., Krupa, Z., Tukendorf, A. (1988). "Photosynthgetic activities of cadmium-treated tomato plants". **Physiol, Plant,** 48, 365-370.

Beauregard, M., (1992). Modelling of the photosystem II 33 kDa protei: structure, function and possible sulfate-sensitive sites derived from sequence-encoded information". **Envir. exp. Bot.**, 32, 411-423

Bennet, J., Williams, R., Jones, E., (1984). "Chlorophyll protein complexes of higher plants : phosphorylation and preparation of monoclonal antibodies". in Advances in photosynthesis research, (C. Sybesma, eds.) Vol, 3, pp 99-106, Martinus Nijhoff publishers. The Hague.

Berthold, D.A., Babcock, G. T., Yocum, C. A. (1981). "A highly resolved oxygen-evolving photosystem II preparation from spinach thylakoid membranes". **FEBS Lett.**, 134, 231-234.

Berthomieu, C., Boussac, A. Mantele, W., Breton, J., Nabedryk, E. (1992). "Molecular changes following oxidoreduction of Cyt b559 characterized by Fourier tranbsform infrared difference spectoscopy and electron paramagnetic resonance: photooxidation in Photosystem II and electrochemistry of isolated Cyt b559 and iron protoprophyrin IX-Bisimidazole model compounds."**Biochemistry,** 31, 11460-11471.

Berthomieu, C., Nabedryk, E., Boussac, A., Mantele, W., Breton, J. (1990b). "Charecterization by FTIR spectroscopy of the photoreduction of the primary quinone acceptor QA in Photosystem II". **FEBS Lett.**, 269, 363-367.

Berthomieu, C., Nabedryk, E., Boussac, A., Mantele, W., Breton, J. (1990a). "Charecterization of cytochrome b559 and of the primary acceptor Q_A of photosystem II by FTIR difference spectroscopy". **Biophys., J.** 57, 566.

Borthakur, D., Haselkorn, R. (1989). "Nucleotide sequence of the gene encoding the 33 kDa water oxidizing polypeptide in Anabaeana sp. strain PCC 7120 and its expression in Escherichia coli Pl". **Molec. Biol.,** 13, 427-439.

Bou, V., Gibrat,J., Levin, J. M., Garnier, J. (1988). "Secondary structure prediction: combination of three different methods". **Protein Engin.**, 2, 185-191.

Boussac, A., Rutherford, A. W. (1988 a). "The involvement of Ca^{2+} in the Ca^{2+} effect on photosystem II oxygen evolution". **Photosynth. Res.**, 33, 208 209.

Bradford, M. (1976). "A rapid and sensitive method for the quantitation of microgram quantities of protein utilizing the principle of protein-dye binding". **Anal. Biochem,** 72,248-254.

Braiman, M. S., Rothschild, K. J. (1988). "Fourier transform Infrared Techniques For Probing Membrane Protein Structure". **Annu. Rev. Biophys. Biophys. Chem.**, 17, 541-570.

Bricker, T. M. (1992) "Oxygen Evolution in the Absence of the 33-Kilo dalton Manganese-Stabilizing protein". **Biochemistry**, 31, 4623-4628.

Brog, D.C., Fajer, J., Felton, R.H., Dolphin, D. (1970). "The π-cation radical of chlorophyll a". **Proc. Natl. Acad. Sci. USA**, 67, 813-820.

Brudvig, G. W., Beck, W. F., De Pula, J. C. (1989). "Mechanism of photosynthetic water oxidation". **Annu. Rev. Biophys. Biophys. Chem.**, 18, 25-46.

Brudvig, G.W. (1987). "The Tetranuclear Manganese Complex of Photosystem II". **J. Bioenergy Biomembr.**, 19, 91-104.

Brudvig, G.W., Casy, J. L., Sauer, K. (1983). "The effect of temperature on the formation and decay of the multiline EPR signal species associated with photosynthetic oxygen evolution". **Biochim. Biophys. Acta**, 723, 366-371.

Bryce, J. H., Hill, S. A. (1993). "Photosynthesis" In Plant Biochemistry and Molecular Biology". (Lea, P. J. and Leegood, R. C., ed.), Vol 1, pp. 1-26. John Wiley publishers, Chichester, England.

Burke, J. J., Ditto, C. J. Arntzen, C. J. (1978). "Involvement of the light-harvesting complex in cation regulation of excitation energy distribution in chloroplasts". **Arch. Biochem. Biophys.**, 187, 252-263.

Burnap, R. L., Sherman, L. A. (1991). "Deletion mutagenesis in Synechocystis sp. PCC6803 indicates that the Mn-stabilizing protein of Photosystem II is not essential for O_2 evolution". **Biochemistry**, 30, 440-446.

Byler, D. M., Susi, H. (1986). "Examination of the seconderay structure of proteins by deconvolved FTIR spectra". **Biopolymers**, 25, 469-487.

Calver, J. G., Pitts, J. N. (1967). "Light and the low of Photochemistry". in: Photochemistry. pp 1-123, John Wiley publishers, Chicheste, England.

Camm, E. L., Green, B. R., Allred, D. R., Staehelin, L.A. (1987). "Association of the 33 kDa extrinsic polypeptide (water splitting) with PSII particles: Immunochemical quantification of residual polypeptides after membrane extraction". **Photosynth. Res. 13**, 69-80.

Cammarata, K.V., Chenaie, G. M. (1987). "studies on 17, 24 kDa depleted photosystem II membranes. I. Evidence for high and low affinity calcium sites in 17, 24 kDa depleted PSII membranes from wheat versus spinach". **Plant Physiol.** 84: 587-595.

Chang, C. T., Wu, C. S. C., Yang, J. T. (1978). "Circular dichric analysys of protein conformation inclusion of the β-turns". **Anal. Biochem.** 91, 13-31.

Chang, C., H., Tiede, D., Tang, J., Smith, U., Norris, J., Schiffer, M., (1986). "Structure of Rhodopseudomonas sphaeroides R-26 reaction center". **FEBS Lett.**, 205, 82-86

Chapados, C. (1988). "Aggegation of chlorophyll a species absorbing near 700 nm^{-1}, the infrared carbonyl bands". **Photochem. Photobiol.**, 47, 115-131.

Chapados, C., Lemieux, S., Carpentier, R. (1991). "Protein and chlorophyll in Photosystem II probed by infrared spectroscopy". **Biophys. Chem.**, 39, 225.

Chirgadze, Y. N., Shestopalov, B.V., Venyaminov, S.Y. (1973). "Intinsities and other spectral parameters of infrared amide bands of polypeptides in the β- and random forms". **Biopolymers,** 12, 1337-1351.

Chou, P. Y., Fasman, G. D. (1978). "Prediction of the secondary structure of protein from their amino acids sequence". **J. Adv. Enzym.** 47, 45-148.

Clayton, R.K. (1980). "photosynthesis: Physical Mechanism and chemical Patterns". I. U. P. A. B. Biophysic series, Cambridge University Press, London.

Collins, K. D., Washabaugh, M. W. (1985). "The hofmeister effect and the behavior of water at interfaces". **Q Rev. Biophys.**, 18. 323-422.

Colman, W. J., Govinddjee (1977). "A model for the mechanism of chloride activation of oxygen evolution in photosystem II". **Photosynth. Res.**, 13, 199-223.

Cotton, F. A., Wilkinson, G. (1988). "Advanced inorganic chemistry (5th edn), John Wiley and Sons, New York.

Cramer, W. A., Theg, S. M., Widger W. R. (1986). "On the structure and function of Cytochrome b559". **Photosynth. Res.** 10, 393-403.

Critchely, C. (1985). "The role of chloride in photosystem II". **Biochim Biophys. Acta.**, 811, 33-46.

Crawford, I. P, Niermann, T., Kirschner, K. (1987). "Prediction of secondary of evolutionary comparison: application to the alpha subunit of tryptophan synthase". **Proteins,** 2, 118-129.

Csonka, L. N. (1989). "Physiological and genitic responses of bacteria to osmotic stress". **Microbiol. Rev.,** 53, 121-147.

Dainese, P., Bassi, R. (1991). "Subunit stoichiometry of the chloroplast photosystem II antenna system and aggregation state of the component chlorophyll a/b binding proteins". **J. Biol. Chem.**, 266, 8136-8142.

Davis, M. S., Forman, A., Fajer, J. (1979). "Ligated chlorophyll cation radicals: their function in photosystem II of plant Photosynthesis". **Proc. Natl. Acad. Sci. USA**, 76, 4170-4174.

Davis, D. J., Gross, E. L.(1975). "Protein-protein interactions of light-harvesting pigments protein from spinach chloroplasts. I. Ca^{2+} binding and its relation to protein assosciation". **Biochim. Biophys. Acta,** 387, 557-567.

Deisenhofer, J., Epp, O., Miki, K., Huber, R., Michel, H. (1985). "Structure of the protein subunits in the photosynthetic reaction center of Rhodopseudomonas viridis at 3A resolution". **Nature,** 318, 618-624.

Dekker, J. P., Van Gorkom, H. J. (1987). "Electron Transfer in the water-oxidizing complex. of photosystem II". **J. Bioenerg. Biomembr.**, 19, 125-152.

Dismukes, G. C. (1988). "The spectroscopically derived structure of the manganese site for photosynthetic water oxidation and a proposal for the protein binding sites for calcium and manganese". **Chemica Scripta,** 28A, 99-104.

Dismuks, G.C. (1981). "Intermediates of a polynuclear Manganese Center Involved in Photosynthetic Oxidation of water". **Proc. Natl. Acad. Sci. USA**, 78, 274-278.

Dong, A., Caughey, B., Caughey, W. S. (1990). "Determination of Protein secondary Structure Using factor Analyasis of Infrared Spectra". **Biochemistry**, 29, 3303-3308.

Dong, A., Caughey, B., Caughey, W. S., Bhat, K.S, Coe, J. E. (1992). "Secondary structure of pentraxin female protein in water determined by infrared spectroscopy: Effects of calcium and phosphorylcholine". **Biochemistry** 31, 9364-9370.

Dousseau, F., Therrien, M., Pezolet, M. (1989). "On the spectral subtraction of water from the FTIR spectra of aqueous solutions of proteins". **Appl. Spectrosc.**, 43, 538-542.

Droppa, M. N., Masojidek, Z., Rozsa, A, Wolak, L. I., Horvath, T., Fakas, G. (1987). "Characteristics of Cu deficiency-induced inhibition of photosysynthetic electron transport in spinach chloroplasts". **Biochim. Biophys. Acta**, 891,75-84.]

Duguid, J. Bloomfield, V. A., Benevides, J., Thomas, G. (1994). "Raman spectroscopy of DNA-metal complexes. 1-Interactions and conformational effects of the divalent cations : Mg, Ca, Sr, Ba, Mn, Co, Ni, Cu, Pd, and Cd ". **Biophys. J.**, 65, 1916-1928.

Duguid, J. Bloomfield, V. A., Benevides, J., Thomas, G. (1995). "Raman spectroscopy of DNA-metal complexes. 2-The thermal denaturation of DNA in the presence of Mg^{2+}, Ca^{2+}, Sr^{2+}, Ba^{2+}, Mn^{2+}, Co^{2+}, Ni^{2+}, Cu^{2+}, Pd^{2+}, and Cd^{2+} ". **Biophys. J.**, 69, 2623-2641.

Durrant, JR., Hastings, G., Joseph, D.M., Barber, J., Porter, J., Klug, D.R. (1992). "Subpicosecond equilibration of excitation energy in isolated photosystem II reaction centerss; Oxygen quenching as a mechanism for photodamage". **Biochem. Biophys. Acta**, 1017, 167-175.

Earnest, T. N., Roepe, P. D., Das Gupta, S. K., Herzfeld, J., Rothschild, K. J. (1987). In "Biophysical studies of retinal proteins". (Ebrey, T. and Nakanishi, K., eds.) pp, 133-143. Urbana, III: Univ. III press.

El-Kabbani, O., Chang, C. H., Tiede, D., Norris, J., Schiffer, M. (1991) "Comparisoon of reaction center from Rhodobacter sphareoides and Rodopseudomonas viridis; overall architecture and protein-pigment interactions". **Biochemistry,** 30, 5361-5369.

Emsley, J. (1991). "The elements". (second eddition) Oxford University press, New York.

Enami, I., Miyaoka, T., Mochizuki, Y., Shen J. R., Satoh, K., Katoh, S. (1989). "Nearst neighbor relationships among constetuent proteins of oxygen-evolving p-hotosystem II membrane binding and function of the extrinsic 33 kDa protein". **Biochem. Biophys. Acta,** 973, 35-40.

Engelhard, M., Gerwert, K., Hess, B., Kreutz, W., siebert, F. (1985). "Light driven protonation of internal aspartic acids of bacterihodopsin: an investigation by static and time-resolves infrared spectroscopy using ^{13}C aspartic acid labeled membrane". **Biochemistry,** 24, 400-407.

Evans, M.C.W, Nugent, J. H. A. (1991). "Absorbing developments". **Nature,** 350, 109-110.

Fasman, G. D. (1991). "The prediction of the secondary structure of proteins". in: Methods in protein sequence analysis. J., LH. G. pp 321-332 Birkhauser, Basel.

Fringeli, U. P., Gunthard, Hs. H. (1980). "Membrane, Spectroscopy" In: Molecular Biology, Biochemistry and Biophysics". (Grell, E. eds.). Vol. 31, pp 270-332. Berlin: Springer.

Gabbay-Azaria, R., Tel-Or., E., Schonfeld, M. (1988). "Glycinebetaine as an osmoregulant and compatible solute in the marine cyanobacterium subsalsa". **Arch. Biochem. Biophys.,** 264, 333-339.

Gekko, K. (1983). "Mechanism of protein stabilizition by polyols: thermodynamics of transfer of amino acids and protein from water to aqueous polyol solutions". In: Studies in Physiol and Theoritical Chemistry. (Tanaka, N. Ohtaki, H and Tamamushi, R., eds.) Vol 27, pp 339-358. Elsevier Science Publisher, BV, Amesterdam.

Gerlsma, S.Y. (1970). "The effects of polyhydric and monohydric alcohols on the heat induced reversible denaturation of chymotrypsinogen A". **Eur. J. Biochem.,** 14, 150-153.

Gerlsma, S.Y., Stuur, E. R. (1972). "The effect of polyhydric and monohydric alcohols on the heat-induced reversible denaturation of lysozyme and ribonuclease". **Int. J. Peptide protein Res.,** 4, 377-383.

Gerlsma, S.Y., Stuur, E. R. (1974). "The effect of combining two different alcohols on the heat-induced reversible denaturation of ribonucleaseInt". **J. Peptide Protein Res.,** 6, 65-74.

Ghanotakis, D. F., Babcock, G. T., Yocum, C. F. (1984a). "Calcium reconstitutes high levels of oxygen evolution in polypeptides depleted photosystem II preparations". **FEBS Lett.,** 167, 127-130.

Ghanotakis, D. F., Babcock, G. T. (1983). "Hydroxylamine as an inhibitor between Z and P680 in Photosystem II". **FEBS Lett.,** 153, 231-234.

Ghanotakis, D. F., Demetriou, D. M., Yocum, C.F. (1987). "Isolation and characterization of an oxygen-evolving Photosystem II reaction center core preparation and a 28 kDa Chl-a-binding protein". **Biochem. Biophysic. Acta.**, 891, 15-21.

Ghanotakis, F., Yocum, C.F. (1990). "Photosystem II and the oxygen-evolving complex". **Ann. Rev. Plant Physiol. Plant Molec. Biol.**, 41, 255-276.

Gibrat, J. F., Granier, J., Robson, B. (1987). "Further developments of protein secondary prediction using information theory. New parameters and consideration of residue pairs". **J. Mol. Biol.**, 198, 425-443.

Glazer, A. N., Melis, A. (1987). "Photochemical Reaction Centers: Structure, Organization and function". **Ann. Rev. Plant Physiol.**, 38, 11-45.

Giese, A. (1964). "Action of light on Plants". in: Photophysiology 1, General Principles, Academic Press, New york.

Golbeck, J. H., Bryant, D. A. (1991). "Photosystem I". In: Current Topic in Bioenergetics. (Lee, C. P eds.) Vol 16, pp 265-318. Academic press, Inc. San Diego.

Goormaghtigh, E., Cabiaux, V., Ruysschaert, J. M. (1990) "Secondary structure and dosage soluble and membranes proteins by attenuated total reflection Fourier transform infrared spectroscopy on hydrated film". **Eur. J. Biochem.**, 193, 409-420.

Gorga, J. C., Dong, A., Manning, M. C., Woody, R. W., Caughey, W. S., Stominger, J. L. (1989). "Comparison of the secondary structures of lumen class I and class II major histocompatibilty complex antigens by Fourier transform infrared and circular dichroism spectroscopy". **Proc. Natl. Acad. Sci. USA**, 86, 2321-2325.

Gounaris, K., Brain, A.P.R., Quinn, P. J., Williams, W.P. (1983a). "Structural and functional changes associated with heat-induced phase-separations of non-bilayer lipids in chloroplast thylakoid membranes". **FEBS Lett.**, 153, 47-52.

Gray, J.C., Hird, S. M., Wales, R., Webber, A. N., Willey, D. L. (1989). "in Techniques and New Developments in photosynthesis". (Baltscheffsky, M., eds.) Vol 3, 461-468. Kluwer Academic Publishers, Dordrecht, The Netherlands.

Green, B. R. (1988). "The chlorophyll-protein complexes of higher plant photosynthetic membranes or just what green babd is that?". **Photosynth. Res.**, 15, 3-32.

Greenwood, N. N., Earnshaw, A.(1984). "Chemistry of the elements". Programon press, Oxford.

Guy, C. L. (1990). "Cold acclimation and freezing stress tolerance: role of protein metabolism". **Ann. Rev. Plan. Physiol. Plant Mol. Biol.,** 41, 187-223.

Haag, E., Irrgang, K.D., Boekema, E. J., Renger, G. (1990). "Functional and structural analysis of photosystem II core complex from spinach with high oxygen evolution capacity". **Eur. J. Biochem.**, 189, 47-53.

Hanson, A. D., May, A. M., Grumet, R., Bode, J., Jamieson, G. C., Rhodes, D. (1985). "Betaine synthesis in chenopods: locolization in chloroplasts". **Proc. Natl. Acad. Sci. USA,** 82, 3678-3682.

Hansson, O., Wydrzynski, T. (1990). "Current perceptions of photosystem II". **Photosynth. Res.** 23, 131-162.

Haris, P. I., Lee, D. C., Chapman, D. (1986). "A Fourier transform infrared investigation of the structural differences between ribonuclease A and ribonuclease S". **Biochem. Biophys. Acta,** 874, 255-265.

Hearst, J. E. (1987). "Primary structure and function of the reaction center polypeptides of Rohodopseudomonas capsulate-the structural and functional analogies with the photosystem II. Polypeptides of plants". in : Encyclopedia of plant physiology New seriesIn Staehelin L. A. and Arntzen C.J. eds.) , Vol 19, photosynthesis III, 382-389 Springer-verag, Berlin.

He, W. Z, Newell, W. R, Harris, P.I, Chapman, D., Barber, J. (1991). "Protein secondary structure of the isolated photosystem II reaction center and conformational changes studied by Fourier Transform infrared spectroscopy". **Biochemistry,** 30, 4552-4557.

Henderson, R., Baldwin, J. M.,, Ceska, T. M., Zemlin, F., Beckmann, E., Downing, K.H. (1990). "Model for the structure of bacteriorhodopsin based on high resolution cryo-electron microscopy". **J. Mol. Biol.**, 213, 899-929.

Homann, P. H. (1992). "Stabilization of the water oxidizing polypeptide assembly on photosystem II membranes by osmolytes and other solutes". **Photosynth. Res.**, 33, 29-36.

Homannn, P. H. (1987). "The relation between the chloride, calcium and polypeptide requirements of photosynthetic water oxidation". J. **Bioenerg. Biomem.** 19, 105-123.

Homman, P. H. (1990). "The role of calcium in biological systems". (Anghileri, L. J., eds.) Vol 4, pp 79-96, CRC Press, Boca Ration, Florida.

Hoff, A.J. (1987). "Electron paramagnetic resonance in photosynthesis". In: New Comprehensive Biochemistry (Photosynthesis), (Amesz J. eds.) Vol 15, pp 97-123, Elsevier, Amsterdam.

Huner, N. P. A., Krol, M. Williams, J. P., Maissan, E., Low, P., Roberts, D., Thompson, J. E. (1987). "low temperature development induces a specific decrease in trans-Δ^3-hexadecenoic acid content which influences LHCII organization. **Plant Physiol.**, 84, 12-18.20

Imaoka, A., Akabori, K., Yanagi, M., Izumi, K., Toyashima, Y., Kawamori, A., Nakayana, H., Sato, J. (1986). "Roles of three lumen-surface proteins in the formation of S_2 state and O_2 evolution in photosystem particles from spinach thylakoid membranes". **Biochem. Biophys. Acta,** 848, 201-206.

Incharoensakdi, A., Takabe, T., Akazawa, T. (1986). "Effect of betaine on enzyme activity and subunit interaction of Ribuose-1,5 Biphosphate carboxylase oxygenase from Aphanothece halophytica". **Plant Physiol.**, 81, 1044-1049.

Isoagai, Y., Yamamoto, Y., Nishimura, M. (1985). "Association of the 33-KDa polypeptide with the 43-KDa component in photosystem II particles'. **FEBS Lett.**, 187, 240-244.

Jackson, M., Haris, P. I., Chapman, D. (1989). "Fourier transform infrared spectroscopic studies of lipids, polypeptides and proteins". J. **Mol. Struct.**, 214, 329-355.

Jursinic, P., Govindjee (1977). "Temperature dependence of delayed light emission in the 6 to 340 microsecond range after a single flash in chloroplasts". **Photochem. Photobiol.**, 26, 617-628.

Kagi, J. H. R., Schaeffer, A. (1988). "Biochemistry of metallothionein". **Biochemistry,** 23, 8509-8515.

Kahino, Y., Satoh, K., Katoh, S. (1986). "A simple procedure to determine Ca^{2+} in oxygen-evolving preparations from synechococcus sp. **FEBS Lett.**, 205, 150-154.

Katz, J. J. Shipman, L. L., Norris, J.R. (1979). "Structure and function of photoreaction center chlorophyll, in : Chlorophyll Organization and Energy Transfer in Photosynthesis". (Katz, J. eds) pp 1-40, Ciba foundation Symposium 61. Excerpta Media, Amsterdam.

Kauppinen, J. K., Moffat, D. J., Mantsch, H. H., Cameron, D. G. (1981). "Fourier self-deconvolution: a method for resolving intrinsically overlapped bands". **Appl. Spectrosc.**, 35, 271-276.

Kauppinen, J. K., Moffat, D. J., Cameron, D. G., Mantsch, H. H., (1987). "Fourier self-deconvolution: a method for resolving intrinsically overlapped bands". **Appl. Spectrosc.**, 20, 1866-1879.

Kishikawa, K. (1983). "Assessment of secondary structure prediction of proteins, Comparison of computerized Chou-Fasman method with others". **Biochim. Biophys. Acta,** 748, 285-299.

Kleffel, B., Garavito, R. M., Baumeister, W., Rosenbusch, J. P. (1985). "Secondary structure of a channel-forming protein: porin from E. coli outer membranes". **EMBO J.**, 4, 1589-1592.

Klimov, V. V., Allakhverdiev, SI., Demeter, S., Krasnovskii, A. A. (1979). "phyeophytin reduction in Photosystem II of chloroplasts in relation to oxidation-reduction potential of medium". **Dokl. Akad. Nauk. USSR,** 249, 227-2330.

Klimov, V. V., Klevanik, A. V., Shuvalov, V. A., Krasnovsky, A. A. (1977). "Reduction of phephytin in the primary light reaction of photosystem II". **FEBS Lett.,** 82, 183-186.

Klimov, V. V., Krasnovsky, A. A. (1981). "Pheophytin as a primary electron acceptor in photosystem II reaction center". **Photosynthetica,** 15, 592-609.

Kok, B., Forbush, B., McGloin, M. (1970). "Cooperation of charges in photosynthetic oxygen evolution: A linear four steps mechanism". **Photochem. Photobiol.**, 2, 457-475.

Krimm, S., Bandekar, J. (1986). "Vibrational spectroscopy and conformation of peptides, polypeptides, and proteins". **Adv. Protein Chem.**, 38, 181-364.

Krishnan, M., Nguyen, H. T., Burke, J. J. (1989). "Heat shock protein synthesis and thermal tolerance in wheat". **Plant Physiol.**, 90, 140-145.

Krol, M., Huner, N. P. A., Williams, J. P., Maissan, E. (1988). "Chloroplast biogenesis at cold-hadening temperature. Kinetics of trans-Δ^3 hexadecenoic acid accumulation and the assembly of LHCII". **Photosynth. Res.**, 15, 115-132, 1988.

Krupa, Z., Hunter, P. N.A., Williams, J. P., Maisson, E., James, D.R. (1987a). "development at cold-hardening temperatures, the structure and

composition of purified rye light-harvesting complex II". **Plant Physiol.,** 84 19-24.

Krupa, Z., Skorzynska, E., Mksymiec, W., Baszynski, T. (1987b) "Effect of cadmium treatment on the photosynthetic apparatus and its photochemical activities ingreening radish seedings". **Photosynthetica,** 21, 156-164.

Krupa, Z. (1988). "Cadmium-induced changes in the composition and structure of the Light-harvesting chlorophyll a/b protein complex II in Radish cotyledons". **Physiol. Plant.,** 73, 518-524.

Kuhlbrandt, W., Wang, D. N. (1991). "Three-dimensional structure of plant light-harvesting complex determined by electron crystallography". **Nature,** 350, 130-134.

Kuhlbrandt, W., Wang, D. N., Fujiyoshi, Y. (1994). "Atomic model of plant light-harvesting complex by electron crystallography". **Nature,** 67, 614-621.

Kuwabara, T., Reddy, K. T., Sherman, L.A. (1987). "Nucleotide sequence of the gene from the cyanobacterium Anacystis nidulans R2 encoding the Mn-stabilizing protein involved in PSII water oxidation". **Proc. Natl. Acad. Sci. USA,** 84, 8230-8234.

Kyte, J., Doolittle, R. F. (1982). "A simple method for displaying the hydropathic character of a protein". **J. Molec. Biol.,** 157, 105-132.

Laemmli, U. K. (1970). "Cleavage of structural proteins during the assembly of the head of bacteriophage T4". **Nature,** 227, 680-685.

Lawolr, D.W. (1987). "photosynthesis, metabolism, control and physiology". John Wiley and Sons, New York

Lee, D.C, Harris P.I., Chapman, D., Mitchell, R. C. (1990). "Determination of protein secondary structure using factor analysis of infrared spectra". **Biochemistry,** 29, 9185-9193.

Lee, D. C., Hyward, J.A., Restall, C. J., Chapman, D. (1985). "Second-derivative infrared spectroscopy studies of the secondary structures of bacteriohodopsin and Ca^{2+}-ATPase". **Biochemistry,** 24, 4364-4373.

Lee, D.C, Harris, P.I., Chapman, D. (1986). "Infrared spectroscopic studies of biomembranes and model membranes". **Biosci. Rep.**, 6, 235-255.

Lee, J. C., Timasheff, S. N. (1981). "The stabilization of proteins by sucrose". **J. Biol. Chem.**, 256, 7193-7201.

Leech, R. M., Walton, C. A. (1983). "Modification of fatty acid composition during chloroplast ontogeny and the effects on thylakoid appression and primary photochemistry". In: Biosynthesis and function of plant lipids. (Thomson, W. W, Mudd, J. B., Gibbs, M., eds.). pp 56-80. Waverley Press, Baltimore.

Lemoine, Y., Dubacq, J. P., Zabulon, G. (1982). "Changes in the light-harvesting capacities and Δ^3-trans-hexadecenoic acid content in dark-and light grown Picea abies". **Physiol. Veg.**, 20, 487-503.

Levin, J., Garnier, J. (1988). "Improvements in a secondary structure prediction method based on a search for local sequence homologies and iots use as a model building tool". **Biochem. Biophys. Acta,** 955, 283-295.

Lim, V. I. (1974). "Algorithms for prediction of α-helical and b-structural regions in globular proteins" **J. Mol. Biol.**, 88, 873-894

Losche, H., Feher, G., Okamura M.Y. (1988). "The stark effect in photosynthetic reaction centers from Rhodobacter sphaeroides R-26, Rhodopseudomonas viridid and the D1D2 complex of photosystem II from spinach". In: The photosynthetic bacterial reaction center. Structure and Dynamics. (Breton, J., and Vermeglio, A., eds). pp 151-164. New York.

Low, P.S. (1985). "Molecular basis of the biological compatibility of nature's osmolytes". In: Transport Process, Iono-and Osmoregulation.(Gilles R., and Gilles-B., M., eds.) , pp 469-477. Springer-Verlag, Berlin.

McDonald, G. M, Barry, B. A, (1992). "Difference FTIR study of a novel biochemical preparation of photosystem II". **Biochemistry,** 31, 9848-9856.

Mamedov, M., Hayashi, H., Murata, N. (1993). "Effect of glycinebetaine and unsaturation of membrane lipids on heat stability of photosynthetic electron-transport and phosphorylation reaction in Synechocystis PCC6803". **Biochim. Biophys. Acta,** 1142, 1-5.

Mantele, W. G (1992). " The photosynthetic reaction center". (Deisenhofer, J., and Norris, J., eds.) Acadimic Press New York.

Mantele, W. (1993). "Reaction-induced infrared difference spectroscopy for the study of protein function and reaction mechanisms". **Trends in Biochem. Sci.,**18, 197-202.

Mantsch, H. H. (1984). "Fourier transform Infrared spectroscopy". (Theophanides, T., eds.) pp. 125-135. Dordrecht, The Netherlands: Reidel. 192 pp.

Mao, D., Wallace, B. A. (1984). "Analysis of light scattering absorption flattening effects in the circular dichroism spectra of small unilamellar vesicles". **Biophys. J.**, 45, 382a.

Maroc, J., Termolieres, A., Garnier, J. Guyon, D. (1987). "Oligomeric form of the light-harvesting chlorophyll a+b-protein complex CPII, Phosphatidylglycerol, Δ^3-trans-hexadecenoic acid and energy transfer in chlamydomonoas rheinhardtii, wild type and mutants". **Biochim. Biophys. Acta,** 893, 91-99.

Masojidek, J., Droppa, M., Horvath, G. (1987). "Analysis of the polypeptide composition of grana and stroma thylakoids by two-dimer sionol gel electrophoresis". **Eur. J, Biochem.**, 169, 283-288.

Mendelsohn, R., Mantsch, H. H. (1986). " Progress in Protein-Lipid Interactions". (Watts, A. and Depont H.H.M, eds.), pp 103-146. Amsterdam: Elsevier.

Michel, H., Epp. O., Deisenhofer, J. (1986). "Pigment-protein interactions in the photosynthetic reaction center from Rhodopseudonas viridis". **EMBO J.**, 5. 2445-2451.

Michel, H., Deisenhofer, J. (1986). " Encyclopedia of plant physiology". (Staehelin, L. A., and Arntzen, C.J., eds.). Vol 111, pp 371-381, springer Verlog, Berlin.

Michel, H., Deisenhofer, J. (1987). "The structural organization of photosynthetic reaction centers". in Progress in Photosynthesis Research. (J. Biggins. eds.). Vol I, pp 353-362, Martinus Nijhoff Publishers. Dordrecht.

Michel, H., Deisenhofer, J. (1988). "Relevance of the photosynthetic reaction center from purple bacteria to the structure of photosystem II". **Biochemistry**, 27, 1-7.

Millner, P.A., Gogel, G., Barber. J. (1987). "Investigations of the spatial relationships between photosystem 2 polypeptides by reversible crosslinking and diagonal electrophoresis". **Photosynth. Res.**, 13, 185-198.

Miyao, M., Murata, N. (1984a). "Role of 33 kDa polypeptide in preserving Mn in photosynthetic oxygen-evolution system and its replacement by chloride ions". **FEBS Lett.**, 168, 281-286.

Miyao, M., Murata, N. (1989). "The mode of binding of three extrinsic proteins of 33 kDa, 23, kDa and 18 kDa in the photosystem II complex of spinach". **Biochim. Biophys. Acta,** 977, 315-321.

Miyao, M., Murata, N., Maison, P. B., Boussac, A., Etienne, A. L., Lavorel, J. (1987). "Effect of 33 kDa protein on the S-state transition in the oxygen-evolving complex" in: Progress in photosynthesis research (Biggins, J., eds.). Vol 15, pp 613-616, Martinus Nijhoff, Dordrecht.

Moya, J. L., Ros. R., Picazo, I. (1993). "Influence of cadmium and nickel on growth, net photosynthesis and carbohydrate distribution in rice plants". **Photosynth. Res.**, 36, 75-80.

Mullet, J. E., Burke, J. J., Arntzen, C. (1980). "A developmental study of Photosystem I peripheral chlorophyll proteins". **Plant Physiol.**, 65, 814-822.

Murata, N., Miyao, M. (1985). "Extrinsic membrane proteins in the photosynthetic oxygen-evolving complex". **Trends Biochem. Sci.,** 10, 122-124.

Murthy, S.D. S., Sabat, S.C., Mohanty, P. (1989). "Mercury-induced inhibition of photosystem II activity and changes in the emission of fluorescence from phycobillisomes in Intact cells of the cyanobacterium, Spirulina platensis". **Plant Cell Physiol.**, 30, 1153 -1157.

Nabedryk, E., Tiede, D. M., Dutton, P. L., Breton, J. (1982). "Conformation and orientation of the protein in the bacterial photosynthetic reaction center". **Biochem. Biophys. Acta,** 682, 273-80.

Nabedryk, E., Andrianambininitsoa, S., Breton, J. (1984). "Transmembrane orientation of a-helices in the thylakoid membrane and in the light-harvesting complex. a polarized infrared spectroscopy study". **Biochim. Biophys. Acta,** 765, 380-388.

Nabedryk, E., Leohard, M. Mantele, W., Breton, J. (1990). "Fourier transform infrared difference spectroscopy shows no evidence for an enolization of chlorophyll a upon cation formation either in vitro or during P700 photooxidation". **Biochemistry,** 29, 3242-3247.

Nabederyk, E., Andrianambinntsoa, S., Berger, G., Leonard, M., Mantele,W., Breton, J. (1990). "Characterization of bonding interactions of the intermediary electron acceptor in the reaction center of photosystem II by FTIR spectroscopy". **Biochim. Biophys. Acta,** 1016, 49-54.

Nakatani, H.Y., Ke, B., Dolan, E., Arntzen, C.T. (1984). "Identity of the photosystem II reaction center polypeptide". **Biochem. Biophys. Acta,** 765, 347-352

Nanba, O., Satoh, K. (1987). "Isolation of photosystem II reaction center consisting of D-1 and D-2 polypeptides and cytochrome b-559". **Proc. Natl. Acad. Sci. USA,** 84, 109-112.

Nicholls, D.G (1982). "Bioenergitics an introduction to the chmiosmotic theory". Academic Press, London.

Noguchi, T., Ono, T. A., Inoue Y. (1992). "Detection of structural changes upon S1-to-S2 transition in the oxygen-evolving manganese cluster in photosystem II by light-induced Fourier transform infrared difference spectroscopy". **Biochemistry,** 31, 5953-5956.

Noguchi, T., Inoue, Y., Satoh, K. (1993). "FTIR studies on the triplet state of P680 in the photosystem II reaction center: triplet equilibrium within a chlorophyll dimer". **Biochemistry,** 32, 7186-7195.

Oettmeier, W. (1992). "The photosystems: Structure, Function, Molecular biology". (Barber, J., eds.) pp 349-408, Elsevier, Amsterdam.

Olinger, J., M., Hill, D. M., Jakobson, R. J., Brody, R. S. (1986). "Fourier transform infrared studies of ribonucleaswe in H2O and ^{2}H2O solutions". **Biochem. Biophys. Acta,** 869, 89-98.

Ollis, D., White, S. (1990). "Protein crystallization". In: Methods of Enzymolgy (Deutscher, M. P., eds.) Vol 182, pp, 646-659. Academic Press, San Diego.

Ono, T. Inoue, Y. (1984). "Ca^{2+}-dependent restoration of O_2-evolving activity in $CaCl_2$-washed PSII particles depleted of 33, 24 and 16 kDa polypeptides". **FEBS Lett.**, 168, 281-286.

Ono, T. Inoue, Y. (1988). "Discrete extraction of the Ca atom functional for O_2 evolution in higher oplant photosystem Ii by a simple low pH treatment. **FEBS Lett.**, 227, 147-152.

Ort, D.R., Good, N, E. (1988). "Textbooks Ignore photosystem II-dependent ATP formation: Is the Z scheme to blame?". **Trends Biochem. Sci.,** 13, 467-469.

Otte, S. C. M., Van der Vos, R., VanGorkum, H. J. (1992). "Steady state spectroscopy at 6 K of the isolated photosystem II reaction center: analysis of the red absorption band". **J. Photochem. Photobiol.,** (B), 5-14.

Papageorgiou, G.C., Fujimura, Y., Murata, N. (1991). "Protection of the oxygen -evolving photosystem II complex by glycinebetaine". **Biochim. Biophys. Acta,** 1057. 361-366.

Parker, F.S (1983). "Applications of infrared, Raman and Resonance Raman Spectroscopy in Biochemistry". Plenum Press, New York.

Pecoraro, V. L. (1988). "Structural proposal for the maganese centers of the oxygen evolving complex an inorganic chemist's perspective". **Photochem. Photobiol.,** 48, 249-264.

Peter, G. F., Thornber, J. P. (1991) " Biochemical composition and organization of higher plant photosystem II light-harvesting pigments-proteins. **J.Biol. Chem.,** 266, 16745-16754.

Philbrick, J.B., Zilinskas, B. A. (1988). "Cloning, nucleotide sequence and mutational analysis of the gene encoding the photosystem II manganese-stabilizing polypeptide of synechocystis 6803". **Mol. Genet.,** 212, 418-425.

Plamley, F. G., Schmidt, G.W (1987). "Reconstitution of chlorophyll a/b light-harvesting complex; xanthophyll dependent assembly and energy transfer". **Proc. Natl. Acad. Sci. USA,** 84, 146-150.

Potter, W. T., Houtchens, R. A., Caughey, W. S. (1985). "Crystallization-induced changes in protein structure observed by infrared spectroscopy of carbon monoxide liganded to human hemoglobins A and Zurich" **J. Am. Chem. Soc.,** 107, 3350-3352.

Prestrelski, S. J., Byler, D. M., Thompson M.P. (1991). "Effect of metal ion binding on the secondary structure of Bovine α-lactoalbumin as examined by infrared spectroscopy". **Biochemistry,** 30, 8797-8804.

Pschorn, R., Ruhle, W., Wild, A. (1988). "Structure and function of Ferredoxin-$NADP^+$ oxidoreductase". **Photosynth. Res.**, 17, 217-219.

Ptitsyn, O. B. and Finkelstein, A. V. (1983). "Theory of protein secondary structure and algorithm of its prediction". **Biopolymers,** 22 15-25

Rashid, A., Carpentier, R. (1991). "Interaction of Zn^{2+} with the donor side of Photosystem II". **Photosynth. Res.,** 30, 123-130.

Rashid, A., Carpentier, R. (1989). "$CaCl_2$ inhibition of H_2O_2 electron donation to photosystem II in submembrane preparations depleted in extrinsic polypeptides". **FEBS Lett.,** 258, 331-334.

Renger, G. (1992). "In the PSs: Structure, Function and Molecular Biology" (Barber, J., eds.) pp 45-99, Elsevier Science Publishers, Amsterdam.

Renger, G., Eckert, H.J., Hagemann, R., Hanssum, B., Koike, H.,Wacker, U. (1989). "Photosynthesis: Molecular Biology and Bioenergetics". (Singhal, G. S., Barber, J., Dilly, R.A., Govindjee, Haselkom, R. and Mohanty, P., eds.) pp 357-371, Narosa Publishing House, New Delhi.

Rochaix, J. D., Dron, M., Rahire, M., Malone, P. (1984). "Sequence homology between the 32 kDa and the D2 chloroplast membrane polypeptide of Chlamydomonas reinhardtii". **Plant Mol. Biol.** 3, 363-370

Rothschild, K. J., Zagaeski, M., Cantore, W. A. (1981). "Conformational changes of bacteriorhodopsin detected by Fourier transform infrared difference spectroscopy". **Biochem. Biophys. Res. Commum.**, 103, 483-489.

Rutherford, A. W. (1989). "Photosystem II, the water splitting enzyme". **Trends Biochem. Sci.,** 14, 427-432.

Rutherford, A. W. (1986). "How close is the analogy between the reaction center of photosystem II and that of purple bacteria?". **Biochem. Soc. Trans.** 14 15-17.

Rutherford, A. W. (1987). "How close is the analogy between the reaction center of PSII and that of purple bacteria? 2. The electrons acceptor side". In: Progress in Photosynthesis Research (Biggins. J., eds.). Vol 1. pp 277-283, Martinus Nijhoff. Dordrecht. ISBN 90-247-3450-9.

Satoh, K., Ohno, T., Katoh, S. I. (1985). "an oxygen evolving complex with a simple subunit structure-a water-Plastoquinone oxidoreductase-from the thermophilic cyanobacterium synechococcus Sp". **FEBS Lett.,** 180, 326-330.

Schelvis, J. P.M., Van Noort, P. I., Arsma, T. J., Van Gorkom H.J. (1993). "Energy transfer, charge separation and pigment arrangement in the reaction center of Photosystem II". **Biochim. Biophys. Acta.,** 1142, 36-42

Seidler, A., Michel, H. (1990). "Expression in Escherichiacoli of the psbO gene encoding the 33 kDa protein of the oxygen-evolving complex from spinach". **EMBO J.,** 9, 1743-1748.

Shen, J. R., Satoh, K., Katoh, S. (1988a). "Calcium content of oxygen-evolving photosystem Ii preparations from higher plants. Effects of NaCl treatment". **Biochim. Biophys. Acta,** 993, 358-364.

Siebert,F., Mantele, W. (1983). Investigation of the primary photochemistry of bacteriorhodobsin by low-temperature Fourier transform infrared spectroscopy". **Eur. J. Biochem.,** 130, 565-573

Siebert, F., Mantele, W., Gerwert, K. (1983). Fourier transform infrared spectroscopy applied to rhodopsin, The problem of the protonation state of the retinyidene schiff base re-investigated". **Eur. J. Biochem.,** 136, 119-127.

Siefermann, H. D. (1985). "Carotenoids in photosynthesis; I, Location in photosynthetic membranes and light harvesting function". **Biochem. Biophys. Acta,** 811, 325-55.

Staehelin, L.,A.(1986). "Chloroplast structure and supramolecular organization of photosyntetic membranes". in : Ecyclopedia of Plant Physiology , New series (Staehelin, L.A., Arntzen, C., j., eds.), Vol 19, pp 1-84, Springler Verlag. Berlin.

Stamatakis, C., Papageorgiou, G.C. (1993). "Stabilization of photosystem II paricles isolated from the thermophilic cyanobacterium Phormidum laminosum with glycinebetaine and glycerol". **Biochim. Biophys, Acta,** 1183, 333-338.

Surewicz, W. K., Moscarello, M. A., Mantsch, H. H. (1987). "Secondary structure of the hydrophobic myelin protein in a lipid environment as determined by fourier-transform infrared spectrometry". **J. Biol. Chem.**, 262, 8598-8602.

Susi, H., Byler, D. M. (1986). "Resolution-enhanced Fourier transform infrared spectroscopy of enzyme". **Methods Enzymol.,** 130, 290-311.

Susi, H., Byler, D. M. (1983). "Protein structure by Fourier transform infrared spectroscopy: second derivative spectra". **Biochem. Biophys. Res. Commun.**, 115, 391-397.

Susi, H., (1972). "Infrared spectroscopy the sytrength of hydrogen bondiong". **Methods. Enzymol.,**26, 255.

Susi, H., Timasheff, S. N., Steven, L. (1967). "Infrared spectra and protein conformations in aqueous solutions". **J. Biol. Chem.**, 242, 5460-5466.

Susi, H. (1969). "Infrared spectra of biological Macromolecules and related systems. In: Structure and stability of Biological Macromolecules. (Timasheff, S. N., and Fasman, G. D., eds.) pp. 575-663, Marcel Dekker Inc.,New York.

Surewicz, W. K., Mantsch, H. H. (1988). "New insight into protein secondary structure from resolution-enhanced infrared spectra". **Biochim. Biophys. Acta.** 952, 115-130.

Syare, R., T., Andersson, B., Bograd, L. (1986). "The topology of membrane protein: the orintation of the 32 kDa Qb-binding chloroplast thylakoid membrane protein". **Cell**, 47, 601-608.

Tajmir-Riahi, H. A., Ahmed, A. (1993). "Complexation of Zn(II), and Cu(II), with proteins of light harvesting complex of chloroplast membranes". **J. Molec. Struc.,** 297, 103-108.

Tanaka, S., Wada, K. (1988). "The status of cysteine residues in the extrinsic 33 kDa protein of spinach photosystem II complexes". **Photosynth. Res.**, 17, 255-266.

Tang, D., Jankowiak, R., Yocum, C.F., Seibert, M., Small, G.J. (1990). "Excited state structure and energy transfer dynamics of two different preparations of the reaction center of photosystem II: A hole Burning study". **J. Phys. Chem.**, 94, 6519-6522.

Tavitian, B.A, Nabedryk, E., Mantele, W., Breton, J. (1986). "Light-induced Fourier Transform infrared (FTIR) spectroscopic investigation of primary reactions in photosystem I and photosystem II". **FEBS Lett.**, 201, 151-157.

Teeter, M. M,, Whitlow, M. (1988). "Test of circular dichroism (CD) methods for crambin and CD-assisted secondary structure prediction of its homologous toxins". **Proteins,** 4, 262-273.

Telfer, A., Barber, J. (1989). "Evidence for the photo-induced oxidation of the primary elctron donor P680 in the isolated photosystem II reaction center". **FEBS Lett.**, 246, 223-228.

Thornber, J. P., Peter, G.F., Chitnis, P.R., Nechustai, R. Vainstein, A. (1988). "Higher planyt and Bacterial Models". in : Light energy Transduction in Photosynthesis (Stevens, S., E. Jr. and Bryant, D. A. eds) pp 1327-154. American Chemical Society of Plant ohysiologists.

Trebst, A. (1986). "The topology of the plastoquinone and herbicide-binding polypeptides of photosystem II in the thylakoid membrane". **Z. Naturforsch**, 41c, 240-245

Tripathy, B. C., Mohanty, P. (1981). "Inactivation of Chloroplast Photosynthetic Electron Activity by Ni^{2+} ". **Biochim. Biophys. Acta**, 638, 217-234.

Tyagi, A., Hermans, j., Steppuhn, J., Jansson, C., Vater, F., Herrmann, R.G. (1987). "Nucleotide sequence of cDNA clones encoding the complete "33 kDa" precursor protein associated with the photosynthetic oxygen evolving complex from spinach". **Mol. Gen. Genet.**, 207, 288-293.

Van Gorkom, H.J. (1985). "Electron transfer in photosystem II". **Photosynth. Res.** 6, 97-112.

Van der Vos, R, Van Leeuwen, P.J., Braun, P., Hoff, A. (1992). "Analysis of the optical absorbance spectra of D1-D2 cytochrome b-559 complexes by absorbance-detected magnetic resonance structural properties of P680". **Biochim. Biophys. Acta,** 1140, 184-198.

Vincent, J. B., Christou, G. (1987). "A molecular double-pivot mechanism for water oxidation". **Inorg Chim. Acta,** 136: L41-L43.

Volger, H., Heber, U., Berzborn, R.j. (1978). "Loss of function of biomembranes and of membranes proteins during freezing" **Biochim. Biophys. Acta,** 511,455-469.

Volger, H., Santarius, K. A. (1981). "Release of membrane proteins in relation to heat injury of spinach chloroplasts". **Physiol. Plant.**, 51, 195-200.

Walker, D. (1979). "Energy, Plants and Man. Readers in Plant Productivity".. Packard Publishing, Chichester.

Wallach, D. F. H., Verma, S.P., Fookson, J. (1979). Application of laser raman and infrared spectroscopy to the analysis of membrane structure". **Biochim. Biophys. Acta,** 559, 153-208

Williams, R.S, Allen J. F, Brain, A.P.R., Ellis, R.J. (1987). "Effects of Mg^{2+} on excitation energy transfer between LHC II and LHC I in a chlorophyll-protein complex". **FEBS Lett.**, 225, 59-66.

Williams, W. P., Gounaris, K. (1992). Stabilization of PSII mediated electron transport in oxygen evolving PSII core preparations by the addition of compatible co-solutes". **Biochim. Biophys. Acta,** 1100, 92-97.

Wydrznski, T., Baumgart, F., MacMillian, F., Renger, G. (1990). "Is there a direct chloride cofactor requirement in oxygen evolving reactions of photosynthesis?". **Photosynth. Res.**, 25, 59-72.

Wyn Jones, R. G., Storey, R. (1981). "Physiology and Biochemistry of Drought Resistance". (Paleg, L.g., Aspinal, D., eds.) pp 171-204, Academic Press. New York.

Xu, Q., Bricker, T. M. (1992). "Structural Organization of Protein on the Oxidizing Side of Photosystem II". **J. Biol. Chem.**, 267, 25816-25821.

Xu, Q., Nelson, J., Bricker, T. B. (1994). "Secondary structure of the 33 kDa extrinsic protein of photosystem II: a far-UV circular dichroism study". **Biochim. Biophys. Acta,** 1188, 427-431.

Yang, P.W., Mantsch, H. H., Arrondo, J. L. R., Saint-Girons, I., Guillou, Y., Cohen, G. N., and Barzu, O. (1987). Fourier transform infrared investiigation of the Escherichia coli methionine aprorepressor **Biochemistry,** 26, 2706-2711.

Yang, J. W., Griffith, P. R., Byler, D. M., Susi, H. (1985). "Protein conformation by infrared spectroscopy: resolution enhancement by fourier self-deconvolution". **Appl. Spectrosc.**, 39, 282-287.

Yocum, C. F., Yerkes, C.T. Blankenship, R. E., Sharp, R. R., and Babcook G.T. (1981). "Stoichiometry, inhibitor sensitivity, and organization of manganese associated with photosynthetic oxygen evolution". **Proc. Natl. Acad. Sci. USA**, 78, 7507-7511.

Yocum, C. F. (1991). "Calcium activities of photosynthetic water oxidation" **Biochem. Biophys. Acta,** 1058. 1-15.

Youvan, D.C., Marrs, B. L. (1987). "Molecular Mechanisms of Photosynthesis". **Sci. Amer.**, 256, 42-48.